EGG-PHYS-5406

April 1981

INEL INTEGRAL DATA-TESTING REPORT FOR ENDF/B-V FISSION-PRODUCT AND ACTINIDE CROSS SECTIONS

MASTER

R. A. Anderl

U.S. Department of Energy
Idaho Operations Office • Idaho National Engineering Laboratory

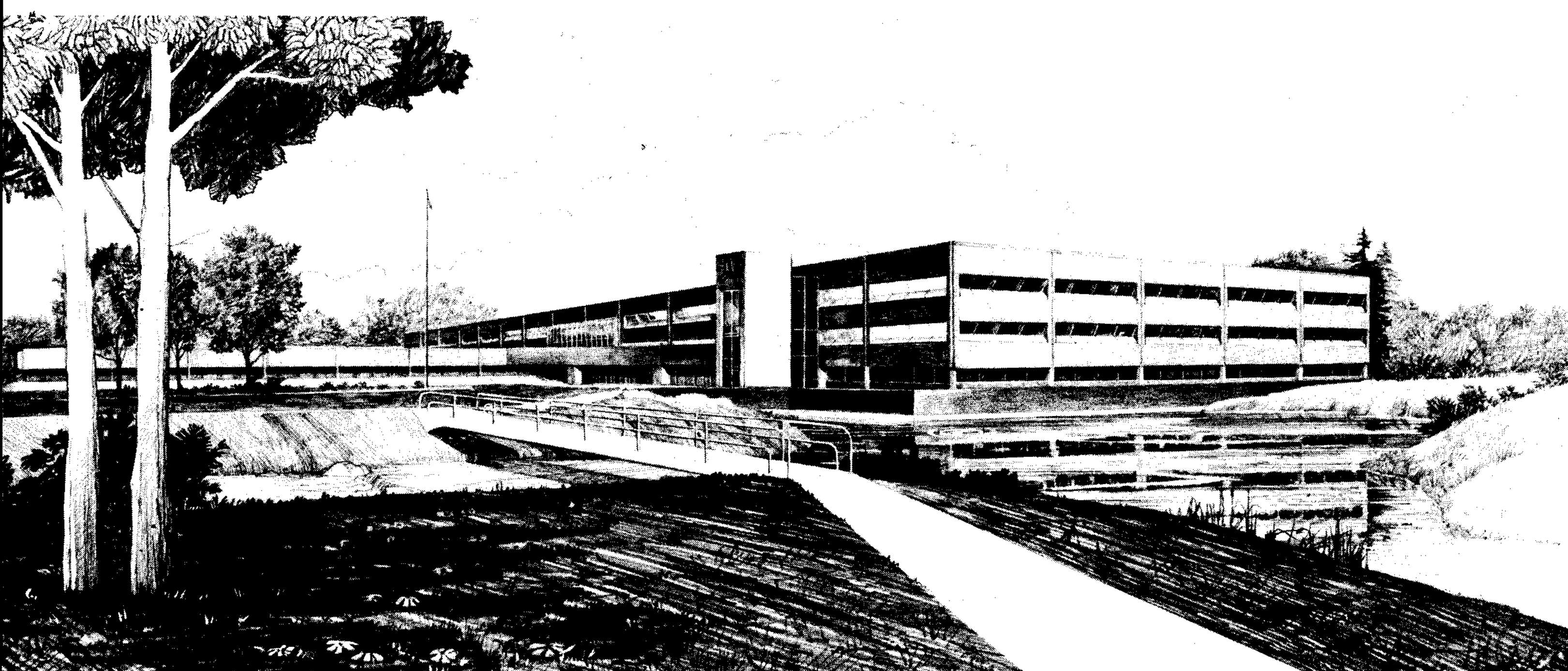

This is an informal report intended for use as a preliminary or working document

Prepared for the
U. S. Department of Energy
Idaho Operations Office
Under DOE Contract No. DE-AC07-76ID01570

EG&G Idaho

EGG-PHYS-5406

INEL INTEGRAL DATA-TESTING REPORT FOR ENDF/B-V FISSION-PRODUCT AND ACTINIDE CROSS SECTIONS

R. A. Anderl

Published April 1981

EG&G Idaho, Inc.
Idaho Falls, Idaho 83415

Prepared for the
U. S. Department of Energy
Idaho Operations Office
Under DOE Contract No. DE-AC07-76ID01570

JHS

ABSTRACT

This report documents an integral-testing study done at the Idaho National Engineering Laboratory for ENDF/B-V fission-product and actinide cross sections. The integral data base used comprises 52 measured spectrum-averaged cross sections for 34 fission-product neutron capture reactions and for 7 higher actinide fission and capture reactions. Included in this data base are integral data from both CFRMF and EBR-II irradiations. Neutron spectra for the irradiation fields are specified and characterized. For the CFRMF related data testing, multigroup flux representations based on transport calculations with both ENDF/B-IV and ENDF/B-V cross sections were used in the calculation of spectrum-averaged cross sections. Neutron spectra used for the EBR-II related data testing are based on multigroup flux representations obtained from spectrum-unfolding analyses. Calculated spectrum-averaged cross sections for the fission products and actinides were obtained using both ENDF/B-IV and ENDF/B-V data. Where possible, calculations were made to estimate the uncertainty in the calculated spectrum-averaged cross sections because of uncertainties and correlations in the input fluxes. Sources of discrepancies in integral testing were examined. These included inaccuracies due to changes in the spectrum shape and the use of incorrect weighting functions for the generation of collapsed cross sections. The results of this study indicate that the changes made in the fission-product and actinide cross sections in going from ENDF/B-IV to ENDF/B-V resulted in more consistency for 28 of the integral data, less consistency for 14 of the integral data and no change for 9 of the integral data.

ACKNOWLEDGEMENTS

The author wishes to acknowledge R. E. Schenter for generation of the 42 group cross-section libraries and for computational results based on those libraries. Several discussions with Y. D. Harker concerning the contents of this report were helpful and are appreciated. The efforts of J. K. Robinson in typing the manuscript and preparing the figures are appreciated.

CONTENTS

INEL INTEGRAL DATA-TESTING REPORT FOR ENDF/B-V FISSION-PRODUCT AND ACTINIDE CROSS SECTIONS*

R. A. Anderl

1. INTRODUCTION

The purpose of this document is to summarize the results of Idaho National Engineering Laboratory (INEL) integral testing of ENDF/B-V fission-product and actinide cross sections. This integral testing is based on the use of integral cross sections derived from measured reaction rates for samples of fission-product class and actinide class materials irradiated in the fast neutron fields of the Coupled Fast Reactivity Measurements Facility (CFRMF)[1] and in the Experimental Breeder Reactor-II (EBR-II).[2] Included in this document are a specification of the integral data base used, a specification of the spectra for the CFRMF and EBR-II, a presentation of integral-testing results, and a discussion of those results.

2. INTEGRAL-DATA BASE

2.1 CFRMF Data

Integral cross sections were reported originally for 38 fission-product class materials.[3] These data are based exclusively on the activation method for measuring integral cross sections. A more recent reference of this integral data is Ref. 4. In this reference, the fission-product integral data reported have been updated from the original results[3] by inclusion of current decay data and use of a more consistent flux normalization scheme. In the reanalysis effort, upon which Ref. 4 is based, some of the earlier measurements were judged suspect and were eliminated as useful data for integral testing. Fission-product integral data used for the present integral testing of ENDF/B-V

* Work supported by the U. S. Department of Energy under DOE Contract No. DE-AC07-76ID01570.

capture cross sections are those reported in Ref. 4. Although some partial cross sections (capture to isomeric states) were reported in Ref. 4, only total reaction cross sections are used in the present study. These measured values with estimated uncertainties are tabulated in column 3 of Table 3.

Capture and/or fission integral cross sections have been measured for 9 actinides ranging from ^{232}Th to ^{243}Am.[3,5,6,7] Five of these materials are included in the dosimetry file and the application of their integral data to testing the ENDF/B-V cross sections is given elsewhere. Integral testing results are included here for the higher actinides, ^{240}Pu, ^{242}Pu, ^{241}Am, and ^{243}Am. Measured integral cross sections were taken from Ref. 6 for ^{240}Pu and from Ref. 7 for the other actinides. They are given here in column 2 of Table 4. The ^{240}Pu fission integral cross section is based on measurements made with a double fission ionization chamber. The integral value used here is derived from the ratio data reported in Ref. 6 and uses a value of 1557 mb ($\pm$ 2.4%) for the ^{235}U fission integral cross section. The integral data reported for ^{242}Pu, ^{241}Am, and ^{243}Am are based on activation experiments which employed gamma-counting and alpha-counting techniques. Although the analysis of these experiments is not complete, the preliminary values are used here for integral testing purposes.

2.2 EBR-II Data

Integral-capture measurements have been reported for enriched isotopes of Nd, Sm and Eu irradiated in a row 8 position of EBR-II.[8] A final report of this work is being prepared.[9] In that experiment, isotopically-enriched samples were located both at midplane and in the reflector. The midplane spectrum is similar to that in CFRMF. In the reflector the neutron spectrum is significantly softer than at midplane. Integral reaction rates were obtained from mass-spectrometric analyses. The integral cross sections used for data testing were derived by dividing the measured integral reaction rates by the corresponding integral fluxes as determined from spectrum-unfolding analyses. These cross-section data are tabulated in column 3 of Table 5. The quoted uncertainties were obtained by adding in quadrature the uncertainty for the reaction-rate determination and the uncertainty in the integral flux as determined from the flux covariance matrices generated in the spectrum-unfolding analyses.

3. SPECTRA CHARACTERIZATION AND SPECIFICATION

3.1 CFRMF

3.1.1 Scope of Effort

In an effort to characterize the neutron spectrum in the fast neutron irradiation location of the CFRMF, an extensive series of measurements and neutronics calculations has been done. Both active and passive techniques have been employed to measure the central neutron spectrum. Active neutron spectrometry was done with proton-recoil detectors and ^{6}Li-semiconductor sandwich detectors. Passive neutron spectrometry was used to characterize the neutron spectrum by means of spectrum-unfolding analyses based on integral reaction rates measured for selected dosimetry materials. From a neutronics calculational standpoint, transport, Monte Carlo and resonance theory techniques have been applied. Early calculations have been made with ENDF/B-III and -IV cross sections. Details of most of the spectrum measurements and a comparison of those measurements to the earlier calculations are given in Refs. 1 and 10. In general the agreement between the measured and calculated spectra is good.

3.1.2 Base Calculations

More recent transport calculations have been made using ENDF/B-IV and preliminary ENDF/B-V cross sections. The calculations were made in 65 energy groups with 0.25 lethargy spacing from 10 MeV to 1.125 eV and with one broad thermal group. Macroscopic shielded cross section

65 group libraries were generated with the SCRABL[11] and PHROG[12] codes. One library contained only cross sections derived from ENDF/B-IV. A partial "Version-V" library was prepared by replacing the "Version-IV" macroscopic cross-section sets for the fast filter assembly (uranium block, uranium sleeve, boral liner and boron-10 sleeve) with cross sections derived from preliminary ENDF/B-V data for ^{235}U, ^{238}U, and ^{10}B.

The calculational model used was a full core, 24 region, 193 mesh point, one dimensional cylindrical representation of the CFRMF reactor. This model is consistent with the specifications in the benchmark description for the CFRMF.[10] Fluxes were obtained from eigenvalue calculations with SCAMP,[13] a one dimensional P1 transport code, using an S-6 approximation. Several SCAMP calculations were made using both the "Version-IV" 65 group library and the partial "Version-V" library. The calculations with the partial "Version-V" library included ENDF/B-V thermal fission spectrum data in all regions where fission occurs whereas the calculations with the "Version-IV" library included the ENDF/B-IV fission spectrum representation.

Summarized in Table 1 and illustrated in Figure 1 are the results of two of these SCAMP calculations. The area of each flux histogram was normalized to 1.0 prior to plotting as flux per unit lethargy. The group flux values tabulated are for the calculation with the partial "Version-V" library and the ENDF/B-V fission spectrum. The flux values are averaged over region 1 (sample region) of the model. The first three group values (21 MeV to 10 MeV) were generated by a fission-function extrapolation based on the values of groups 4 and 5. The ratio column in Table 1 contains the ratio of the "Version-V" calculation to the "Version-IV" calculation. The influence on the spectrum of the changes in fission-spectrum representation and in the cross sections is evidenced by the ratio values. The 68 group fluxes as given in Table 1 provided the base flux data for all integral-testing computations. An interpolation scheme applied to these base data was used to generate group fluxes in other energy structure representations for some integral computations.

TABLE 1. "VERSION-V" GROUP FLUXES FOR CENTRAL NEUTRON FIELD OF CFRMF

Group Number	Lower Energy (eV)	Lower Lethargy	Group Flux	Flux Ratio (V/IV)[a]	Group Number	Lower Energy (eV)	Lower Lethargy	Group Flux	Flux Ratio (V/IV)
1	16.49+6[b]	-0.50	3.840-6	1.43	2	12.84+6	-0.25	5.108-5	1.27
3	10.00+6	0.00	3.549-4	1.15	4	7.79+6	0.25	1.474-3	1.064
5	6.07+6	0.50	4.111-3	1.003	6	4.72+6	0.75	8.975-3	1.039
7	3.68+6	1.00	1.506-2	1.059	8	2.87+6	1.25	2.217-2	1.050
9	2.23+6	1.50	2.927-2	1.025	10	1.74+6	1.75	3.216-2	0.9941
11	1.35+6	2.00	3.792-2	1.014	12	1.05+6	2.25	4.775-2	1.0222
13	8.21+5	2.50	6.221-2	1.041	14	6.39+5	2.75	7.894-2	1.039
15	4.98+5	3.00	8.452-2	1.001	16	3.88+5	3.25	7.886-2	0.9809
17	3.02+5	3.50	7.847-2	0.9630	18	2.35+5	3.75	6.814-2	0.9528
19	1.83+5	4.00	5.812-2	0.9524	20	1.43+5	4.25	4.664-2	0.9489
21	1.11+5	4.50	4.383-2	0.9437	22	8.65+4	4.75	3.334-2	0.9744
23	6.74+4	5.00	3.337-2	0.9752	24	5.25+4	5.25	2.359-2	0.9385
25	4.09+4	5.50	2.037-2	1.076	26	3.18+4	5.75	1.322-2	0.8810
27	2.48+4	6.00	1.371-2	0.9283	28	1.93+4	6.25	9.811-3	0.9011
29	1.50+4	6.50	6.585-3	0.9095	30	1.17+4	6.75	6.382-3	0.8918
31	9.12+3	7.00	5.260-3	0.9008	32	7.10+3	7.25	3.998-3	0.9232
33	5.53+3	7.50	3.832-3	0.9334	34	4.31+3	7.75	3.670-3	0.9569
35	3.36+3	8.00	3.732-3	0.9116	36	2.61+3	8.25	2.918-3	0.8911
37	2.04+3	8.50	2.674-3	0.9028	38	1.59+3	8.75	2.795-3	0.9027
39	1.23+3	9.00	2.247-3	0.8768	40	961.1	9.25	1.671-3	0.9162
41	748.5	9.50	1.732-3	0.9110	42	582.9	9.75	1.343-3	0.9045
43	454.0	10.0	1.200-3	0.8690	44	353.6	10.25	7.920-4	0.8779

TABLE 1. (continued)

Group Number	Lower Energy (eV)	Lower Lethargy	Group Flux	Flux Ratio (V/IV)[a]	Group Number	Lower Energy (eV)	Lower Lethargy	Group Flux	Flux Ratio (V/IV)
45	275.4	10.50	7.306-4	0.9029	46	214.5	10.75	5.368-4	0.8644
47	167.0	11.0	4.235-4	0.8479	48	130.1	11.25	3.648-4	0.8212
49	101.3	11.50	1.720-4	0.8660	50	78.9	11.75	1.976-4	0.8564
51	61.4	12.00	9.153-5	0.8261	52	47.9	12.25	9.530-4	0.8727
53	37.3	12.50	4.815-5	0.9116	54	29.0	12.75	3.009-5	0.8634
55	22.6	13.00	2.329-5	0.9273	56	17.6	13.25	5.577-6	0.9147
57	13.7	13.50	8.797-6	0.9855	58	10.68	13.75	4.321-6	0.9681
59	8.32	14.00	1.547-6	1.0036	60	6.48	14.25	2.621-7	1.060
61	5.04	14.50	1.004-7	1.116	62	3.93	14.75	7.486-8	1.019
63	3.06	15.00	2.473-8	1.012	64	2.38	15.25	7.091-9	1.002
65	1.86	15.50	1.414-9	1.026	66	1.44	15.75	2.538-10	1.027
67	1.125	16.00	3.806-11	1.008	68	∞	0.0	6.139-12	0.9044

a. Flux Ratio: Ratio of group fluxes from "Version-V" calculation to those from calculation with "Version-IV" data.

b. 16.49+6 is equivalent to 16.49×10^6. Upper energy of group 1 is 21.117×10^6 eV.

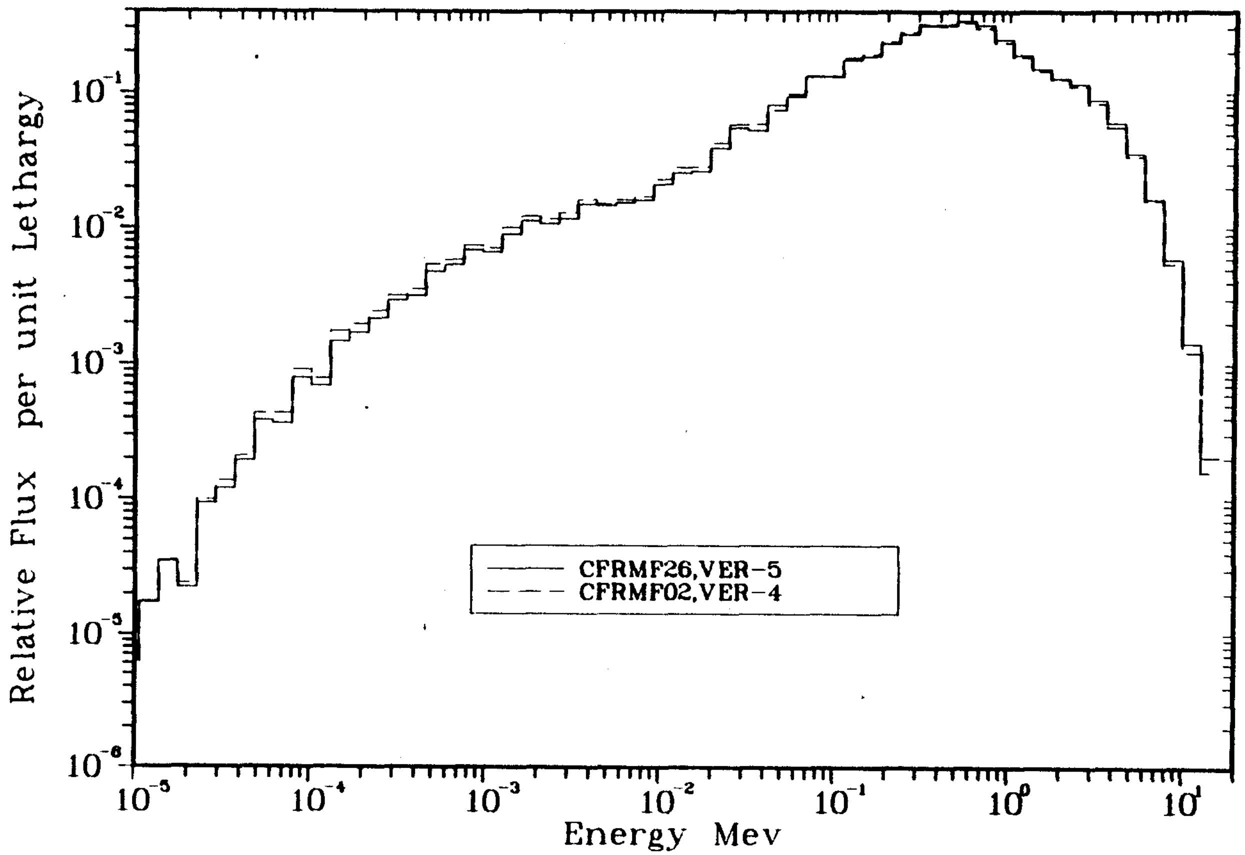

Figure 1. Comparison of CFRMF group fluxes from "Version-IV" and "Version-V" transport calculations.

3.1.3 Sensitivity and Uncertainty Analysis

Recently the AMPX[14] and FORSS[15] code systems were applied to a sensitivity and uncertainty analysis for the CFRMF.[16] The primary objective of this work was to determine, for the central neutron spectrum, a flux covariance matrix related to uncertainties and correlations in the nuclear data for the materials which comprise the facility. The calculational model used in this analysis was a simplified version of the cylindrical 24 region model in that 15 regions were used and more homogenization of the driver zone was done. The starting cross-section data base was a preliminary 100 group ENDF/B-V library which has been used extensively at ORNL for fast-reactor data testing. A 100 group self-shielded library was generated based on an approach which utilized Bondarenko factors. Detailed transport calculations (S_8, P_3) were made with XSDRNPM.[14] The 100 group fluxes generated by the XSDRNPM calculation agreed reasonably well with the ENDF/B-IV SCAMP calculation. Twenty-six-group cross sections were obtained for each region by collapsing the 100 group cross sections. The 26 group cross sections were used in the FANISN[15] calculations for generation of the fluxes and adjoints important to the sensitivity analysis.

Approximately 2500 energy dependent sensitivity profiles were generated in the sensitivity analysis. Dominant sensitivities included those for B-10 capture, U-238 elastic and inelastic scattering, U-238 capture, H total, Fe total, U-238 χ and ν, and ^{235}U χ and ν.

A flux covariance matrix was generated by combining the sensitivity coefficients with cross-section and fission-spectrum covariances. The cross-section covariance matrices used were based on the covariance information as given in ENDF/B-V and as processed with the PUFF2[17] code. Uncertainties in the U-238 inelastic-scattering cross sections and in the ^{235}U fission spectrum were found to contribute most to the standard deviations in the central flux spectrum. The flux-spectrum covariance matrix contained strong correlations.

Where possible, the 26 x 26-group flux covariance matrix was used to estimate the uncertainty in a calculated integral cross section in the following integral testing analyses. This uncertainty estimates the contribution due to relative flux spectrum uncertainties only.

3.1.4 Generation of 620-Group Fluxes

Both 620-point and 620-group-average fluxes (in the SAND-II energy structure) were generated for the CFRMF central neutron spectrum. These representations are important to accurate computations of spectrum-averaged cross sections. They can be used as weighting functions in the generation of broad group processed cross sections or directly in the computation of spectrum-averaged-cross sections if 620 group-average cross sections are available. Discrepancies between measured and calculated spectrum-averaged cross sections can, in some cases, be attributed to the use of different weighting functions in the generation of processed cross sections. Examples of this will be given in section 5.2.

In the past, a spline interpolation program was used in the generation of the 620-point/group representations of the CFRMF spectrum.[3] Input data to this program were a 71 group flux representation. This approach was suitable for most integral testing applications. However, in the integral testing effort for dosimetry reactions, significant discrepancies were noted between some calculated and measured integral cross sections for reactions with strong resonance response, especially in the regions of structure in the flux spectrum, e.g., $^{59}Co(n,\gamma)$. Because the spline interpolation approach applied directly to the 71 group fluxes could not treat accurately the regions of structure in the flux spectrum, a different approach was taken for the integral-testing analyses here.

The approach taken here for the generation of a 620-point/group representation of the CFRMF spectrum entailed the merging of fine-group spectral information from other neutronics calculations with the "base" broad group (68 group) fluxes. The sources of the fine-group information used were a very fine-group resonance calcuation with the RABBLE[18] code and the XSDRNPM calculation made as part of the sensitivity analysis. Output from the ultrafine RABBLE calculation, based on ENDF/B-IV cross sections, was collapsed to the SAND-II energy structure and provided fine group information on the CFRMF spectrum from 1.0 x 10^{-6} MeV to 2.7 x 10^{-3} MeV. Output from the XSDRNPM calculation provided high-resolution information in the regions of structure in the neutron spectrum above 3.5 x 10^{-3} MeV. The merging approach preserved the "broad-group" flux values between the energy bounds of each broad group in the 68-group flux spectrum. Both the 620-point/group flux representations were subsequently generated with the spline interpolation program using as input the "merged" fluxes. Shown in Fig. 2 is a comparison of the 620-group and 68-group fluxes for the CFRMF. A tabulation of the 620-group fluxes is given in Appendix A.

3.2 EBR-II

Characterization of the neutron spectra for the samples irradiated in EBR-II is based on passive neutron dosimetry and spectrum unfolding analyses with the FERRET code.[19,20] Details of this analysis are found in Ref. 9. Shown here in Fig. 3 is a comparison of the relative fluxes per unit lethargy for representative row 8 EBR-II midplane and reflector locations and the CFRMF central neutron field. The area of each flux histogram was normalized to 1 before it was plotted as flux per unit lethargy. As indicated by the figure, the midplane spectrum is similar to the CFRMF spectrum. However, the midplane spectrum does have a larger component of low-energy neutrons. Included in Table 2 are parameters which characterize the neutron spectra for the EBR-II experiment as compared to the CFRMF. A tabulation of representative midplane and reflector fluxes is given in Appendix A.

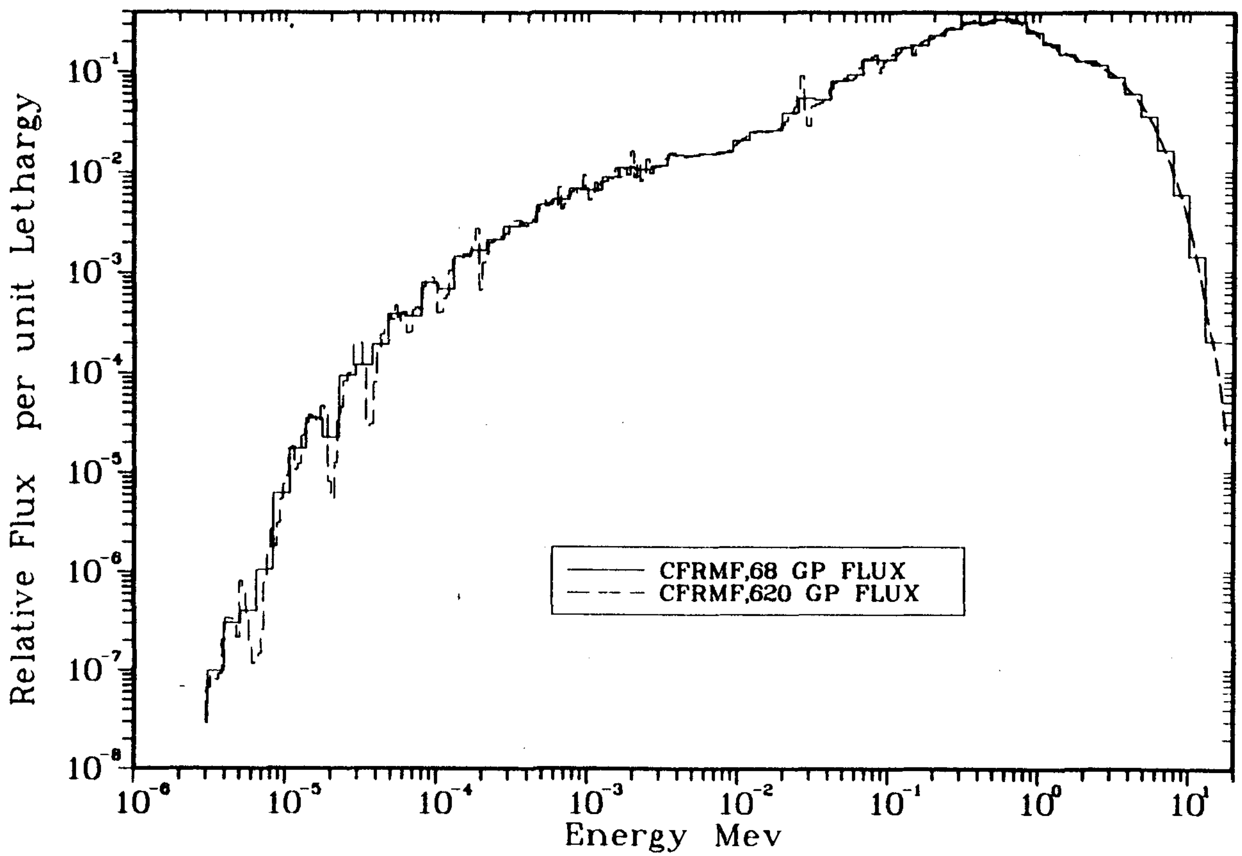

Figure 2. Comparison of 620-group and 68-group fluxes for CFRMF "Version-V" spectrum.

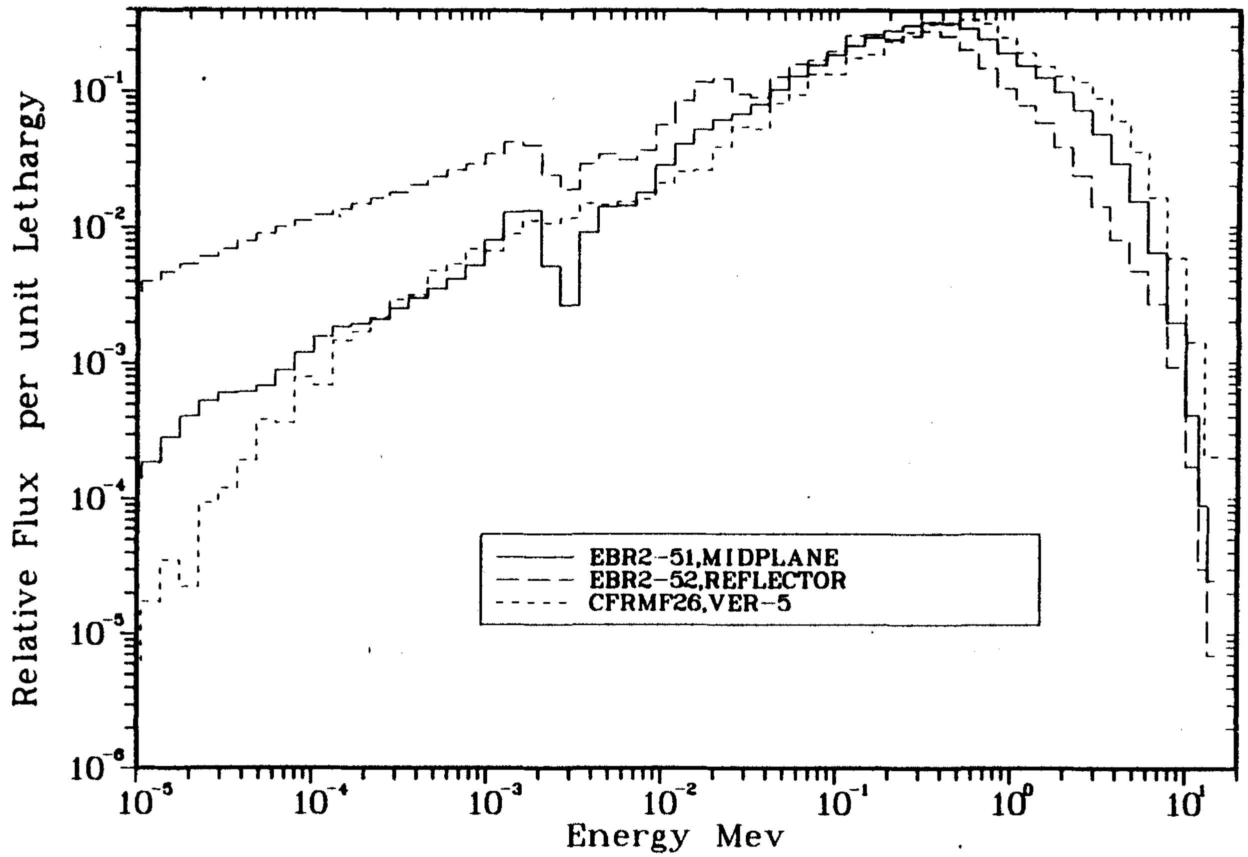

Figure 3. Comparison of adjusted group fluxes for EBR-II midplane and reflector locations with the CFRMF "Version-V" spectrum.

TABLE 2. CHARACTERIZATION OF CFRMF AND EBR-II NEUTRON SPECTRA

Field	Flux Level (n/cm^2-s)	Mean Energy (keV)	Median Energy (keV)	90% Range[a] E_L (keV)	90% Range[a] E_H (keV)
CFRMF (100 kW)	8.70 E+11 (1.9%)[b]	750	370	16	3000
EBR-II Midplane[c]	1.50 E+15 (5%)	550	220	12	2600
EBR-II Reflector[d]	7.60 E+14 (14%)	310	110	0.5	1500

a. 90% Range: 90% of the neutrons in the spectrum are between the lower and upper energy bounds, E_L and E_H.

b. Number in parentheses is the estimate of the uncertainty in the flux level.

c. Midplane: midplane location for subassembly position 8A4 in EBR-II.

d. Reflector: reflector location 31 cm above the midplane for subassembly position 8A4 in EBR-II.

4. INTEGRAL TEST RESULTS

4.1 Processed Cross-Section Libraries

Cross sections processed into different energy structures were used for various phases of this integral testing study. A fine-group library in the 620-group SAND-II energy structure, was obtained from the Nuclear Data Center at Brookhaven National Laboratory (BNL) for 20 fission-product and 2 actinide cross sections in ENDF/B-V. To complement these ENDF/B-V cross sections, a 72 group library for all ENDF/B-V fission-product and actinide cross sections of interest to this study was generated at the INEL. A power reactor weighting spectrum[21] was used in the processing of the 72 group library. Where possible, "Version-5" calculated spectrum-averaged cross sections reported here for the CFRMF were generated using the 620 group cross sections. Integral cross sections computed with 72 group cross sections and fluxes were used to fill the gaps.

A complete set of processed cross sections for ENDF/B-IV and ENDF/B-V fission products and actinides was available in the Hanford Engineering Development Laboratory (HEDL) 42-group energy structure. The weighting function used in the processing of these libraries was 1/E plus fission spectrum. The 42 group library was used in computations for comparing Version-IV and Version-V spectrum-averaged cross sections for fission products and actinides in the CFRMF.

Integral test results for the fission products irradiated in EBR-II are based on the use of the 72-group INEL library for the "Version-V" cross sections and on a 47-group library, generated at HEDL, for "Version-IV" cross sections. Cross sections processed into the 47-group energy structure were based on the use of fast reactor spectrum weighting.

4.2 Integral-Test Computations

The results of our integral-test computations are summarized in Tables 3, 4 and 5. Table 3 and Table 4, respectively, include the results for fission-product and actinide materials irradiated in the CFRMF. Table 5 includes the results for fission-product materials irradiated in EBR-II. All calculated spectrum-averaged cross sections in Tables 3 and 4, for which uncertainty estimates are given, are based on the use of 620-group cross sections and fluxes. Those spectrum-averaged cross sections with a dash in the uncertainty column were based on the use of 72-group cross sections and fluxes. The calculated spectrum-averaged cross sections in Table 5 are based on the use of 72-group cross sections and fluxes.

Some attempt was made to estimate the uncertainty in the calculated spectrum-averaged cross sections due to flux spectrum uncertainties and correlations. Where such calculations were done, values of the uncertainty component are reported under the column $\Delta\sigma_C$ in the tables. For the CFRMF data, this uncertainty calculation utilized the flux spectrum covariance matrix obtained from the sensitivity and uncertainty analysis. For the EBR-II data, the uncertainty calculations utilized the adjusted flux covariance matrices obtained from the spectrum unfolding analysis.

The measure of consistency between measured and calculated integral data is given by the C/E ratio. In Table 3, two columns are given for the C/E ratios. The first C/E column contains ratios of the calculated cross sections to the measured values tabulated. The second C/E column contains ratios of the calculated cross sections to the tabulated measured values corrected for self-shielding effects. Estimates of the integral self-shielding adjustment factors were taken from Refs. 22 and 23. Corrections for self-shielding effects for the actinide samples in CFRMF and for the fission-product samples in EBR-II were estimated to be negligible.

TABLE 3. INTEGRAL-TESTING SUMMARY FOR FISSION PRODUCTS IRRADIATED IN THE CFRMF

										90% Response[i]	
Isotope	Reaction	σ_m[a] (mb)	σ_c[b] (mb)	$\Delta\sigma_c$[c] (%)	C/E[d]	C/E[e]	(V/IV)[f]	$\bar{E}$[g] (keV)	E_M[h] (keV)	E_L (keV)	E_H (keV)
37 Rb 87	C[j]	12(10)	12.65	2.0	1.05	----	1.17	168	8.8	0.21	987
42 Mo 98	C	56.4(6.4)	65.71	1.8	1.17	1.09	0.97	223	21.4	0.35	1204
42 Mo 100	C	55(17)	48.84	1.8	0.89	0.86	1.03	214	24.8	0.33	1116
43 Tc 99	C	267(15)	319.9	2.0	1.20	1.15	1.21	165	30.7	0.34	952
44 Ru 102	C	88.9(6.6)	100.5	1.1	1.13	1.12	0.87	421	106.	1.1	2457
44 Ru 104	C	82.6(6.3)	86.44	1.6	1.05	1.04	1.02	268	41.0	0.21	1516
46 Pd 108	C	144(6.7)	198.5	1.8	1.38	1.20	1.37	246	16.6	0.03	1473
47 Ag 107	C	380(19)	384.9	1.9	1.01	0.97	0.94	193	40.4	0.16	1049
47 Ag 109	C	507(9.7)	450.2	2.0	0.89	0.86	1.53	177	34.6	0.11	974
51 Sb 121	C	251(8.3)	273.4	1.5	1.09	----	0.91	277	44.0	0.11	1571
51 Sb 123	C	154(7.0)	140.0	1.6	0.91	----	0.88	247	34.9	0.19	1409
53 I 127	C	298(10)	345.5	---	1.16	1.16	1.02	158	17.7	0.06	926
53 I 129	C	184(6.6)	196.3	1.8	1.07	----	1.15	190	16.0	0.13	1110
54 Xe 132	C	43.9(7.7)	48.28	---	1.10	----	1.00	350	131.	0.56	1633
54 Xe 134	C	14.6(6.9)	24.90	---	1.70	----	1.04	373	135.	0.95	1708
55 Cs 133	C	276(6.6)	285.1	1.9	1.03	1.02	0.97	163	15.2	0.08	1010
55 Cs 137	C	90(25)	7.33	---	0.081	----	1.00	177	2.5	1.35	1116
57 La 139	C	17.6(5.2)	21.77	1.9	1.24	1.10	0.90	214	13.3	0.06	1425
58 Ce 142	C	18.4(7.4)	24.61	1.0	1.34	----	1.00	458	165.	2.45	2399
59 Pr 141	C	73(15)	79.62	2.0	1.09	1.01	0.82	152	2.3	0.17	1120

TABLE 3. (continued)

Isotope	Reaction	σ_m[a] (mb)	σ_c[b] (mb)	$\Delta\sigma_c$[c] (%)	C/E[d]	C/E[e]	(V/IV)[f]	$\bar{E}$[g] (keV)	E_M[h] (keV)	90% Response[i] E_L (keV)	E_H (keV)
60 Nd 146	C	58(6.5)	72.52	1.0	1.25	1.24	0.81	457	127.	0.61	2780
60 Nd 148	C	89(14)	118.9	---	1.34	1.30	0.75	344	64.5	0.12	1917
60 Nd 150	C	66.6(12)	98.0	1.7	1.47	1.45	0.70	233	41.2	0.23	1343
61 Pm 147	C	641(13)	730.1	2.0	1.14	1.12	0.97	157	5.0	0.08	1060
62 Sm 152	C	277(6.4)	342.3	1.8	1.24	1.18	1.17	225	29.5	0.07	1297
63 Eu 151	C	2390(5.8)	2306	---	0.96	----	1.05	147	10.1	0.10	929
63 Eu 153	C	1450(7.0)	1444	---	1.00	----	1.06	142	16.9	0.10	860

a. σ_m: measured integral cross section in mb. Number in parentheses is the fractional uncertainty x 100% in the measured quantity.

b. σ_c: calculated integral cross section using ENDF/B-V reaction cross section and "Version-5" spectrum for CFRMF.

c. $\Delta\sigma_c$: estimate of fractional uncertainty x 100% in calculated integral cross section due to flux spectrum uncertainties defined by covariance matrix.

d. C/E: ratio of calculated cross section to experimental (measured) cross section.

e. C/E: ratio of calculated cross section to experimental (measured) cross section, experimental value corrected for self shielding.

f. V/IV: ratio of cross section calculated with ENDF/B-V reaction data to cross section calculated with ENDF/B-IV reaction data.

g. $\bar{E}$: average energy of the reaction response in CFRMF.

h. E_M: median energy of the reaction response in CFRMF.

i. 90% Response: 90% of the reaction response is between the energy bounds E_L and E_H.

j. C: radiative neutron capture reaction.

TABLE 4. INTEGRAL-TESTING SUMMARY FOR ACTINIDES IRRADIATED IN THE CFRMF

									90% Response[h]	
Isotope	Reaction	σ_m[a] (mb)	σ_c[b] (mb)	$\Delta\sigma_c$[c] (%)	C/E[d]	(V/IV)[e]	$\bar{E}$[f] (keV)	E_M[g] (keV)	E_L (keV)	E_H (keV)
94 Pu 240	F[i]	573.(3.8)	620.3	---	1.08	1.01	1606	869	191	5619
94 Pu 242	C[j]	146(15)	269.1	---	1.84	1.18	202	32.4	0.11	1147
94 Pu 242	F	557(10)	474.4	---	0.85	0.96	1733	967.	343.	5871
95 Am 241	C	1530(10)	1109	---	0.72	1.69	190	56.6	0.17	913
95 Am 241	F	504(10)	522.6	---	1.04	1.07	2032	1212.	439	6391
95 Am 243	C	1000(15)	594.0	2.2	0.59	1.30	99.2	10.5	0.10	605
95 Am 243	F	352(10)	418.1	5.3	1.19	1.21	2108	1235	489.	6842

a. σ_m: measured integral cross section in mb. Number in parentheses is the fractional uncertainty x 100% in the measured quantity.

b. σ_c: calculated integral cross section using ENDF/B-V reaction cross section and "Version-5" spectrum for CFRMF.

c. $\Delta\sigma_c$: estimate of fractional uncertainty x 100% in calculated integral cross section due to flux spectrum uncertainties defined by covariance matrix.

d. C/E: ratio of calculated cross section to experimental (measured) cross section.

e. V/IV: ratio of cross section calculated with ENDF/B-V reaction data to cross section calculated with ENDF/B-IV reaction data.

f. $\bar{E}$: average energy of the reaction response in CFRMF.

g. E_M: median energy of the reaction response in CFRMF.

h. 90% Response: 90% of the reaction response is between the energy bounds E_L and E_H.

i. F: neutron-induced fission reaction.

j. C: radiative neutron capture reaction.

TABLE 5. INTEGRAL-TESTING SUMMARY FOR FISSION PRODUCTS IRRADIATED IN EBR-II

									90% Response[h]	
Isotope	Reaction	σ_m[a] (mb)	σ_c[b] (mb)	$\Delta\sigma_c$[c] (%)	C/E[d]	(V/IV)[e]	$\bar{E}$[f] (keV)	E_M[g] (keV)	E_L (keV)	E_H (keV)
60 Nd 143	C[i]	400.(5.8)	341.3	5.4	0.85	0.99	110.	0.76	0.04	760
		1403(13.8)	1204.	7.6	0.86	0.96	18.4	0.14	0.04	102
60 Nd 144	C	73.6(5.6)	58.1	4.2	0.79	0.78	302.	64.6	0.31	1765
		158.(13.6)	147.6	9.8	0.93	0.89	61.	0.55	0.24	455
60 Nd 145	C	607(5.7)	468.0	6.0	0.77	1.20	112.	0.89	0.004	807
		2330(13.8)	1873.	9.9	0.80	1.12	15.8	0.08	0.004	70.6
62 Sm 147	C	1840(5.7)	1606.	7.3	0.87	1.31	84.9	0.36	0.02	627.
		6020(13.2)	6384.	14.7	1.06	1.20	15.1	0.03	0.01	67.5
62 Sm 149	C	3250(6.1)	2517.	6.2	0.77	1.31	58.8	0.70	0.007	406.
		10960(13.5)	9162.	12.9	0.84	1.12	13.6	0.07	0.003	85.9
63 Eu 151	C	3750(7.9)	2842.	5.3	0.76	1.05	111.	9.16	0.006	702.
		17800(14.8)	13630.	9.1	0.76	1.02	16.7	0.12	0.002	100.
63 Eu 152	C	3610(11.2)	3346.	4.9	0.93	1.00	100	14.2	0.01	555.
		10090(16.1)	12810	7.8	1.27	1.01	22.5	0.02	0.002	179.
63 Eu 153	C	2060(7.2)	1832.	5.3	0.89	1.08	106	12.2	0.007	648
		9830(14.1)	8850.	9.6	0.90	1.02	16.7	0.09	0.006	112
63 Eu 154	C	2660(9.6)	2006.	5.2	0.76	0.99	87.9	9.80	0.009	500
		8390(15.1)	8329.	8.9	0.99	0.98	18.7	0.01	0.002	149

a. σ_m: measured integral cross section in mb. Number in parentheses is the fractional uncertainty x 100% in the measured quantity. First value given for a specific reaction is the midplane value, second value corresponds to reflector position.

TABLE 5. (continued)

b. σ_c: calculated integral cross section using ENDF/B-V reaction cross section and "Version-5" spectrum for CFRMF.

c. $\Delta\sigma_c$: estimate of fractional uncertainty x 100% in calculated integral cross section due to flux spectrum uncertainties defined by covariance matrix.

d. C/E: ratio of calculated cross section to experimental (measured) cross section.

e. V/IV: ratio of cross section calculated with ENDF/B-V reaction data to cross section calculated with ENDF/B-IV reaction data.

f. $\overline{E}$: average energy of the reaction response in CFRMF.

g. E_M: median energy of the reaction response in CFRMF.

h. 90% Response: 90% of the reaction response is between the energy bounds E_L and E_H.

i. C: radiative neutron capture reaction.

To give some idea of the cross-section changes in going from ENDF/B-IV to ENDF/B-V, ratios of "Version-V" to "Version-IV" calculated spectrum-averaged cross sections are given in the column labeled (V/IV). These computations are based on the use of 42-group cross sections and a 42-group flux representation for the "Version-V" CFRMF neutron spectrum.

An attempt was made to characterize the reaction response for the materials irradiated in CFRMF and EBR-II. This characterization is specified by the mean energy, $\overline{E}$, the median energy, E_M, and the energies E_L and E_H which give the energy range over which 90% of the response occurs. These parameters indicate, in a qualitative sense, the region of the cross section that is "tested" by the neutron flux spectrum.

4.3 Reaction Energy Response

A graphic display of the energy response for a selected set of reactions is illustrated by Figures 4 to 12. The top half of each figure shows a 72-group representation of a specific cross section and the bottom half shows the relative energy response of that reaction in the indicated spectrum, namely, CFRMF or EBR-II. The area under the response histogram is normalized to 1.0. Hence, one can readily note the fractional response from each group. A complete set of such cross-section and response figures for all reactions in the neutron fields used in this integral-testing study is given in Appendix B.

The primary purpose of showing the cross-section/response plots is to illustrate the variability and complexity of the reaction response, especially when resolved resonances contribute substantially to the total response. In many cases the complexity of the response makes it difficult to interpret an integral consistency check for a cross section. As illustrated in Fig. 4, the response for ^{142}Ce in the CFRMF is relatively smooth, and the range of its response corresponds closely to the 90% range for the CFRMF neutron spectrum. The case for ^{102}Ru, Fig. 5,

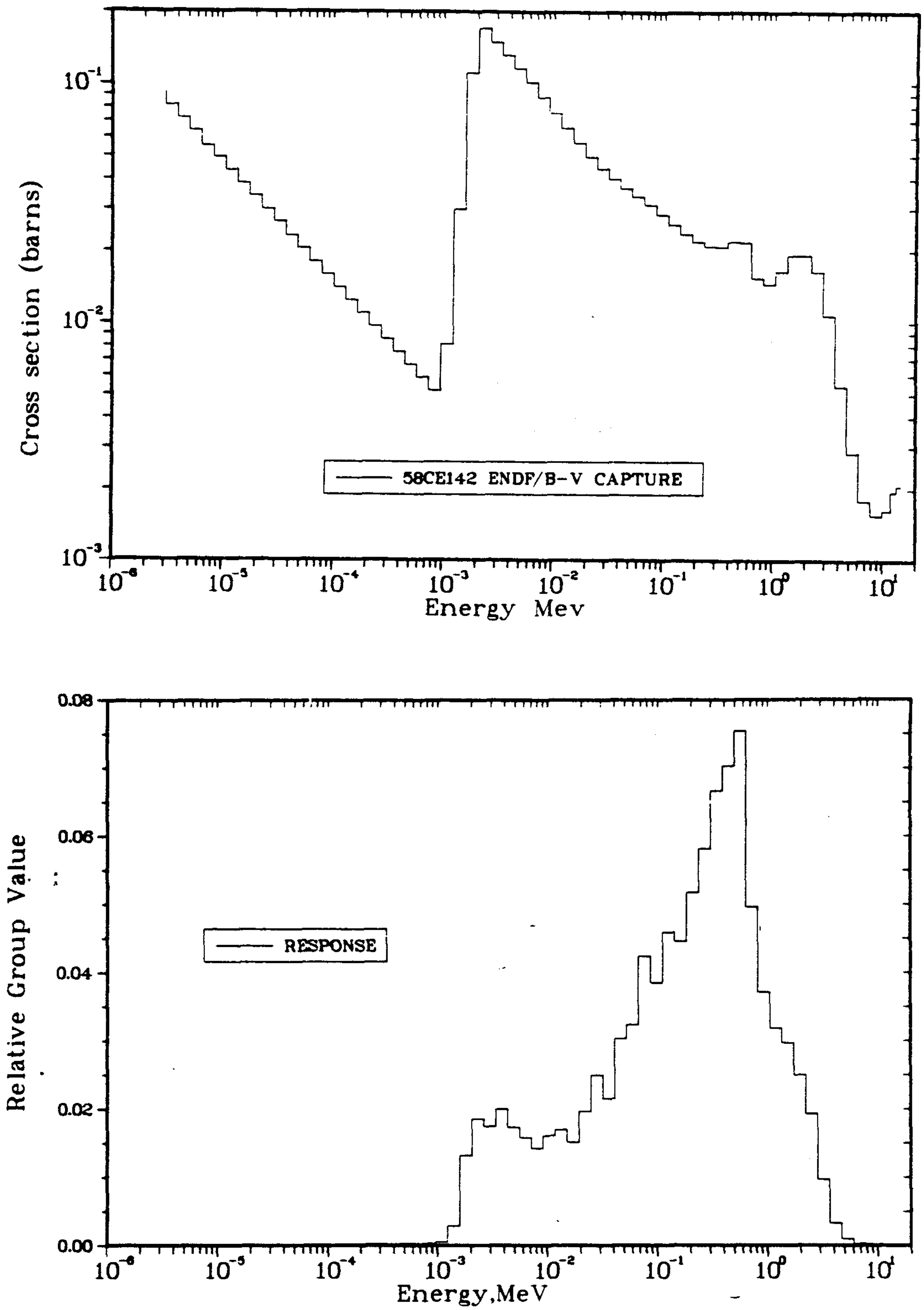

Figure 4. ENDF/B-V cross section and response in CFRMF for $^{142}Ce(n,\gamma)$.

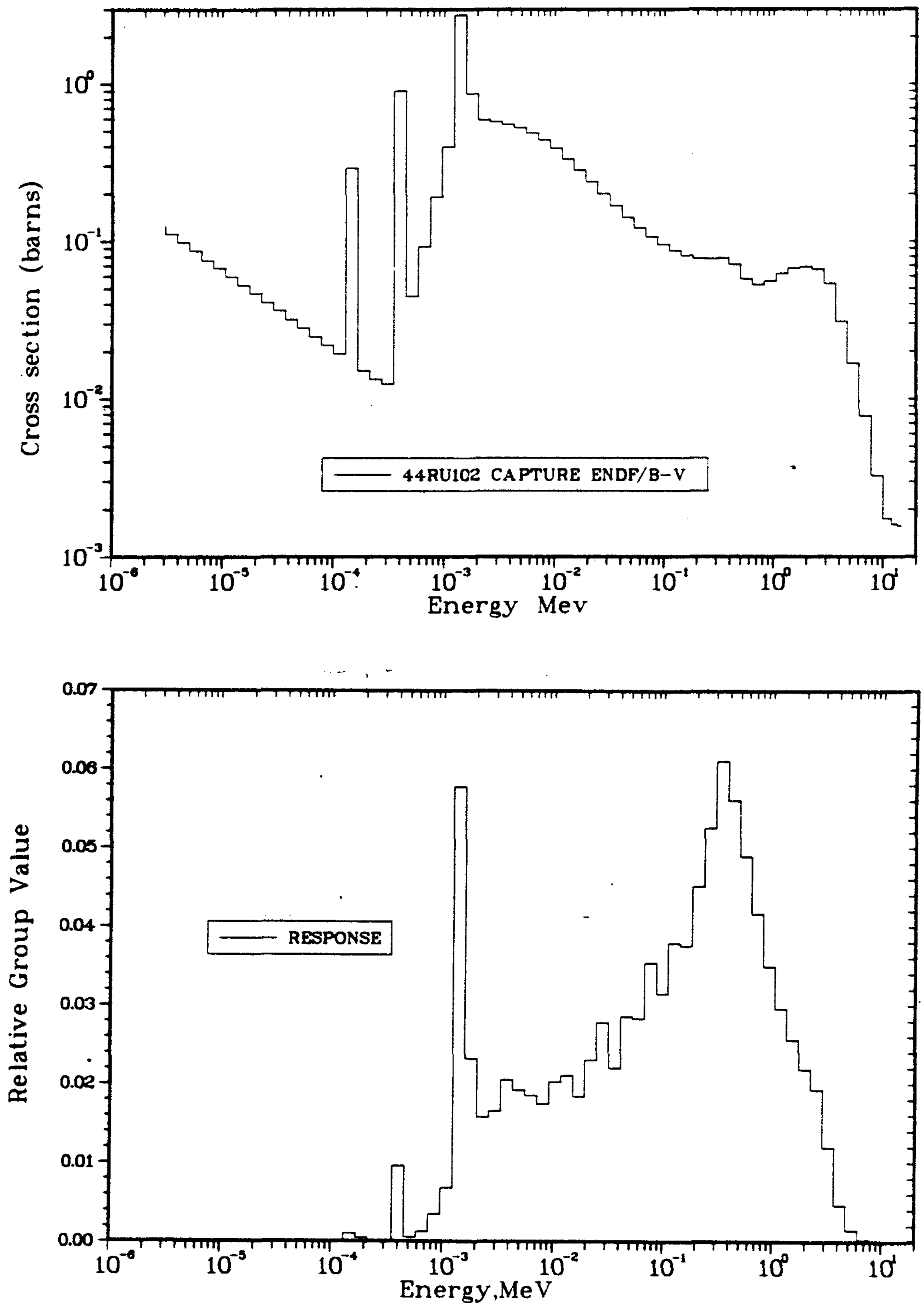

Figure 5. ENDF/B-V cross section and response in CFRMF for $^{102}Ru(n,\gamma)$.

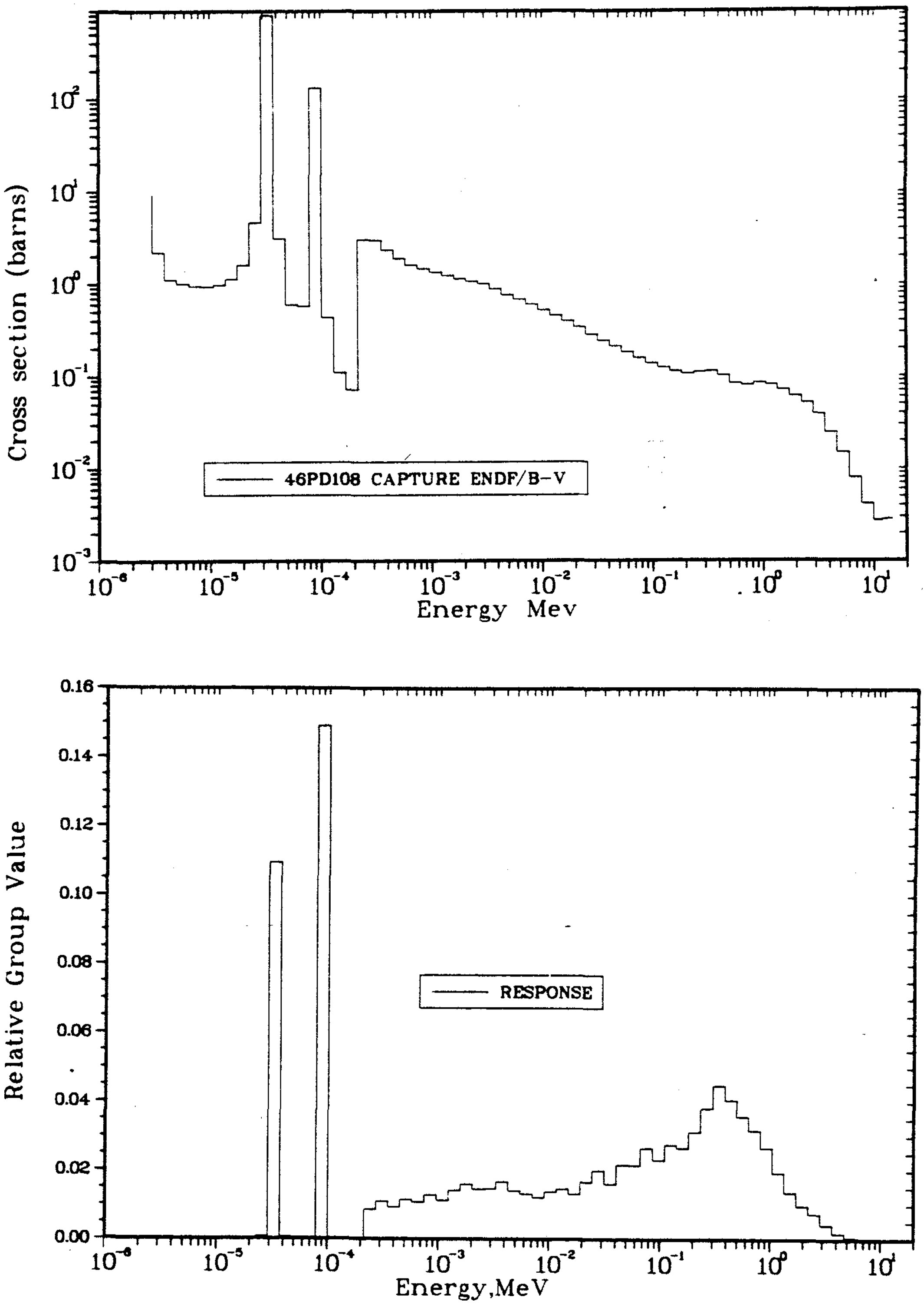

Figure 6. ENDF/B-V cross section and response in CFRMF for $^{108}Pd(n,\gamma)$.

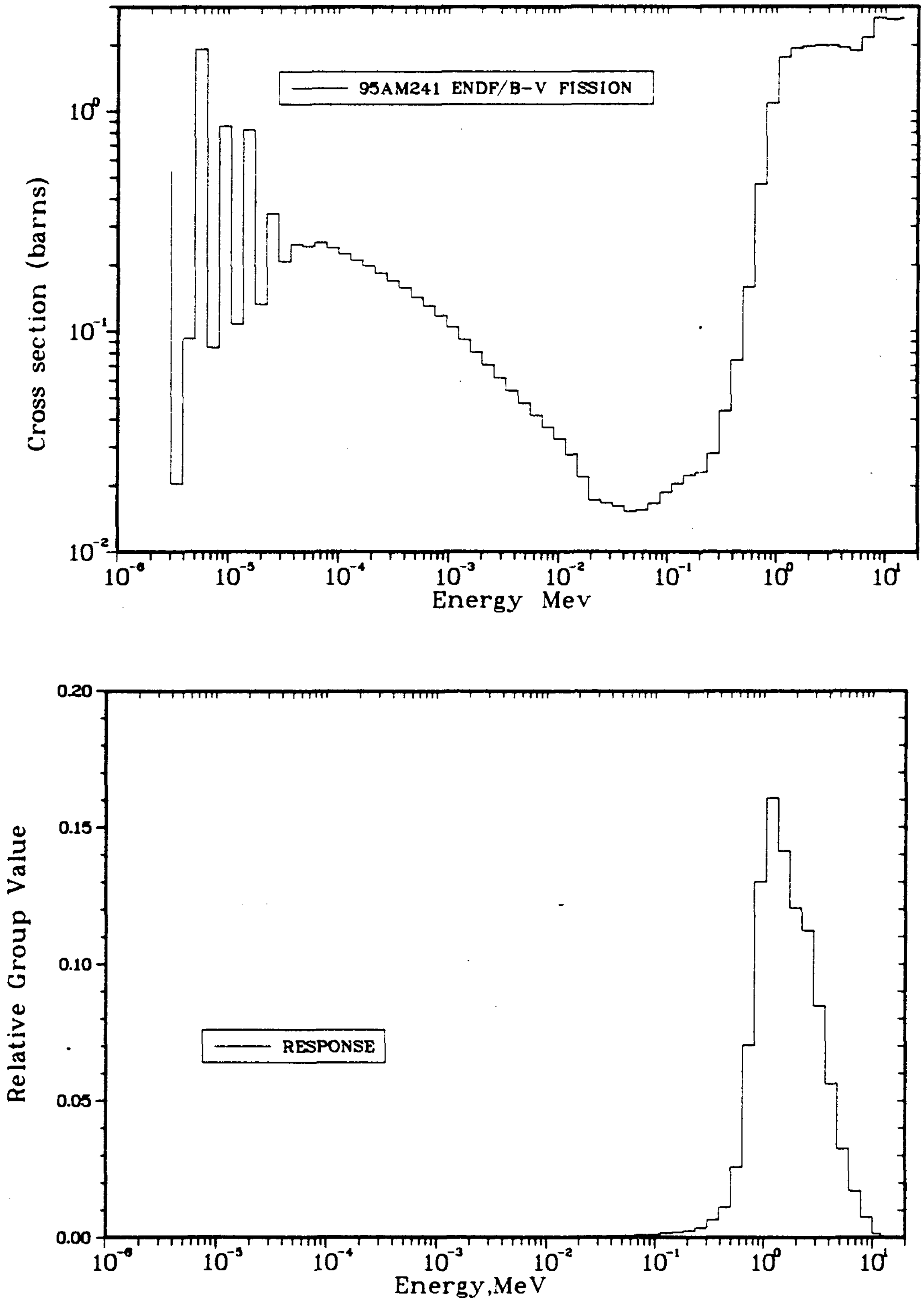

Figure 7. ENDF/B-V cross section and response in CFRMF for ^{241}Am(n,f).

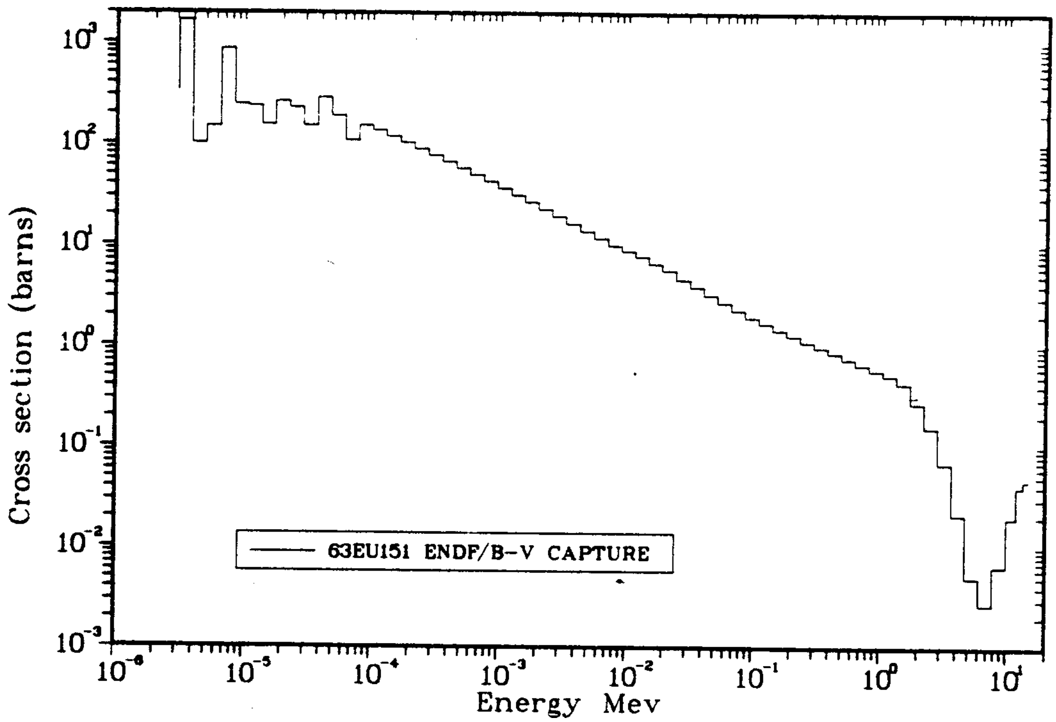

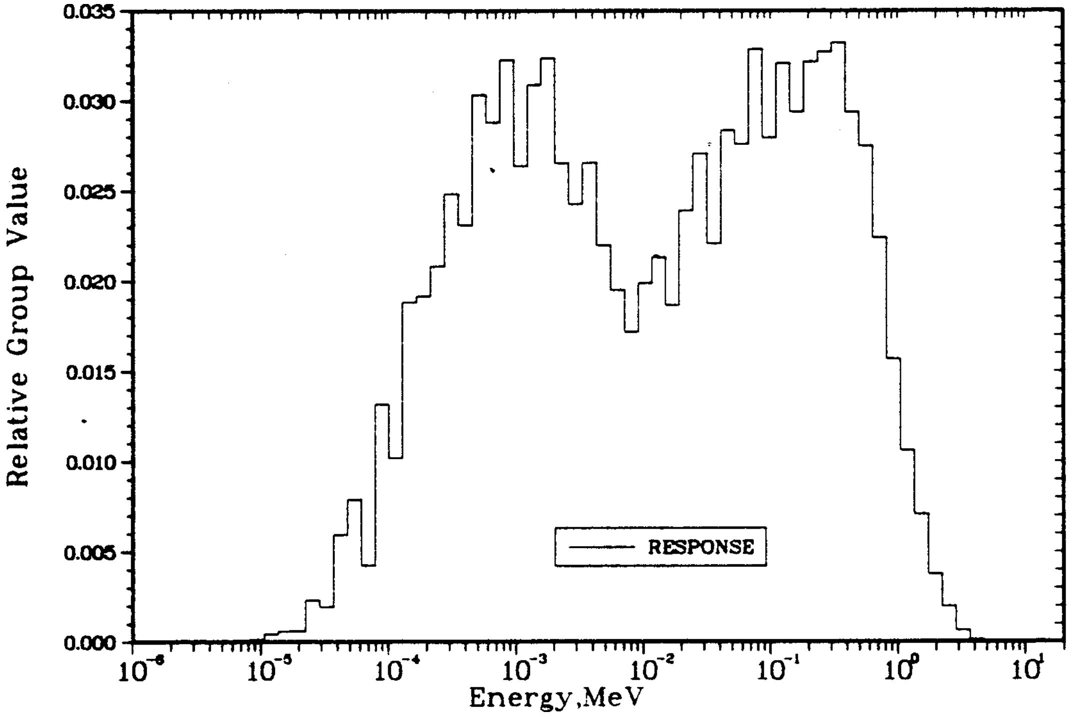

Figure 8. ENDF/B-V cross section and response in CFRMF for $^{151}Eu(n,\gamma)$.

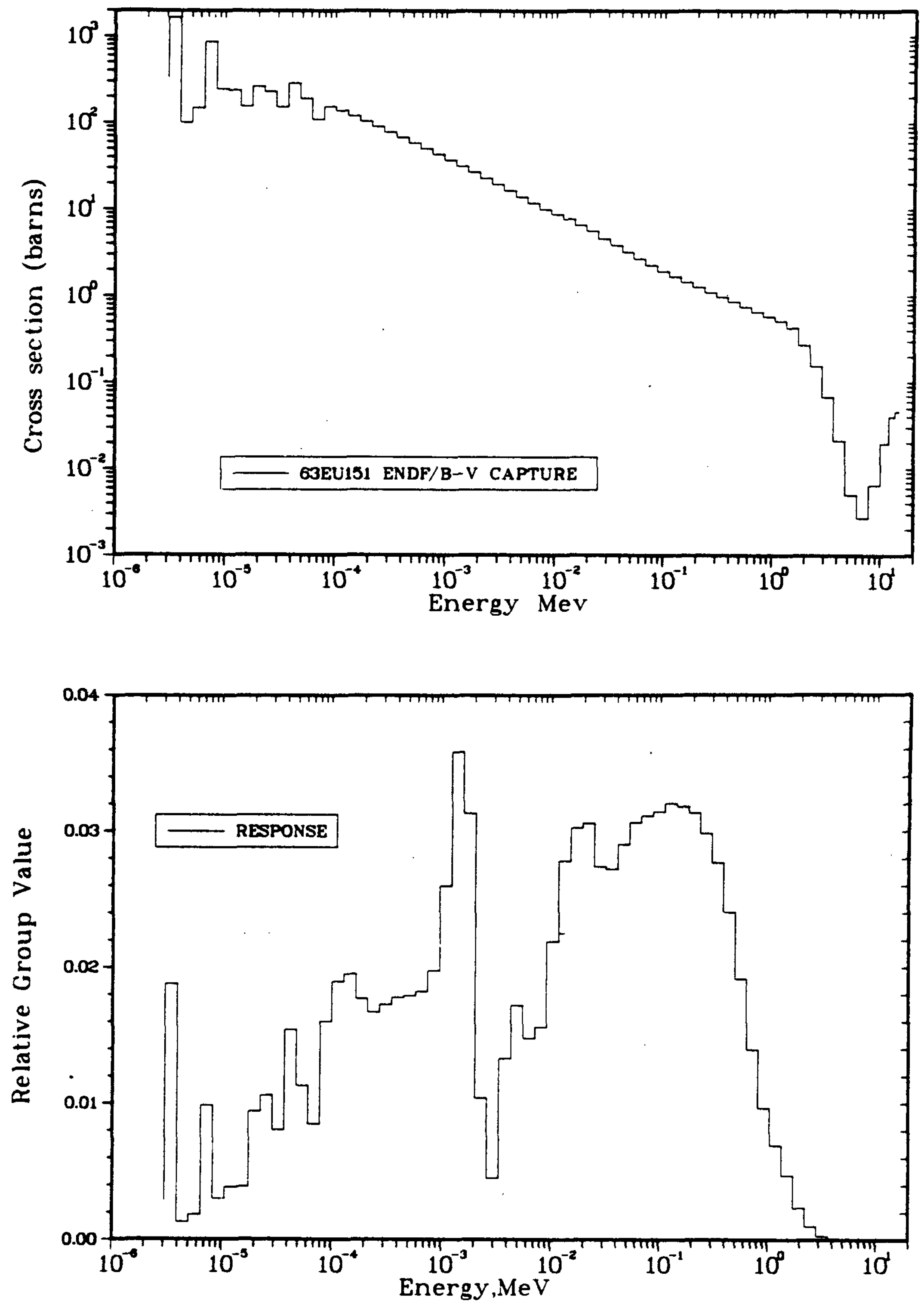

Figure 9. ENDF/B-V cross section and response in EBR-II midplane spectrum for ^{151}Eu.

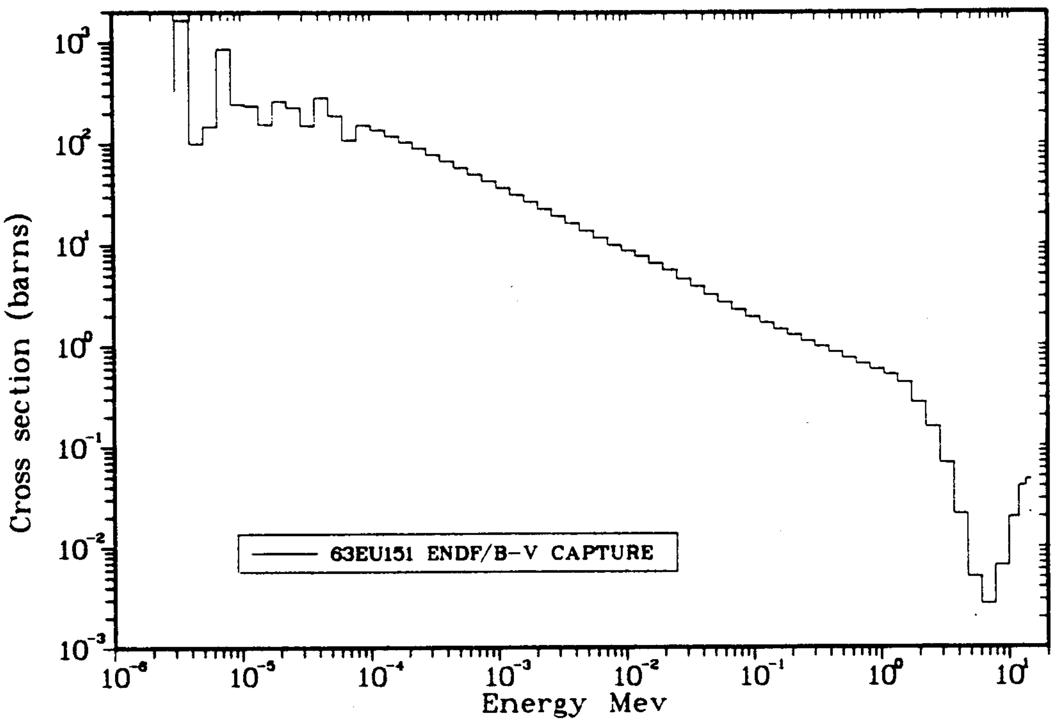

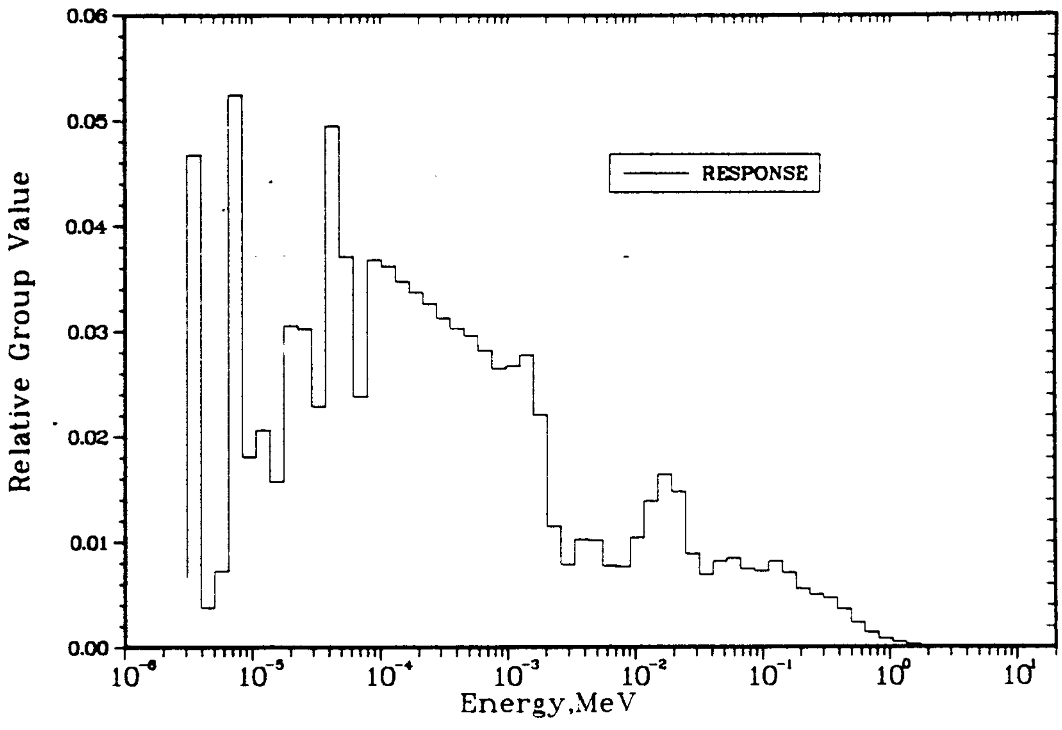

Figure 10. ENDF/B-V cross section and response in EBR-II reflector spectrum for ^{151}Eu.

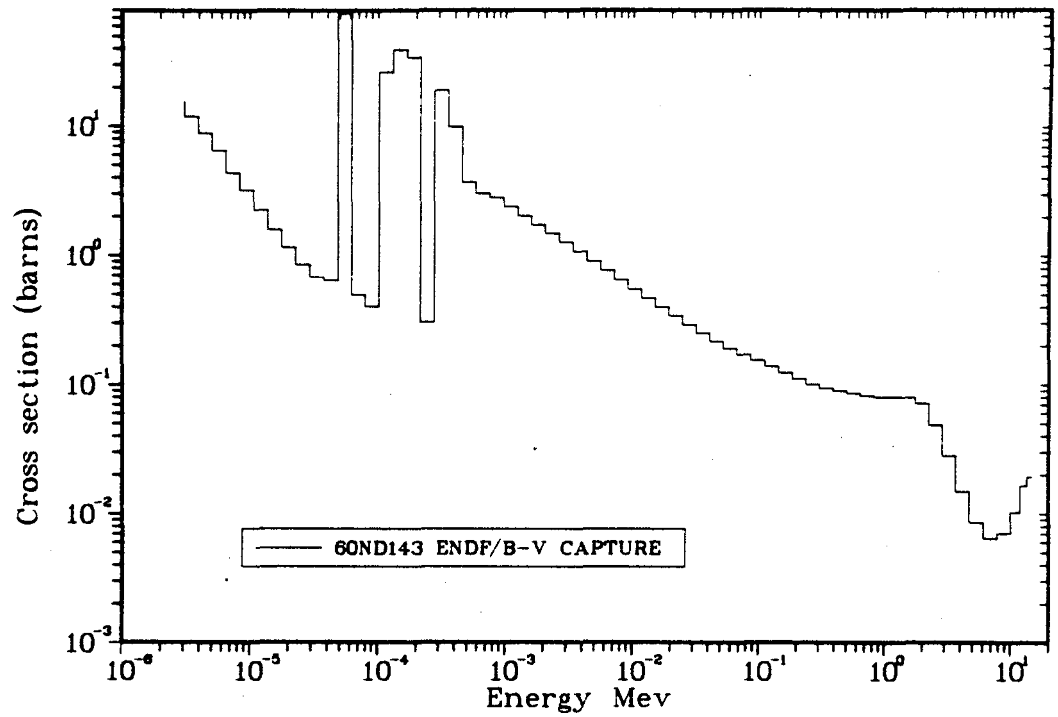

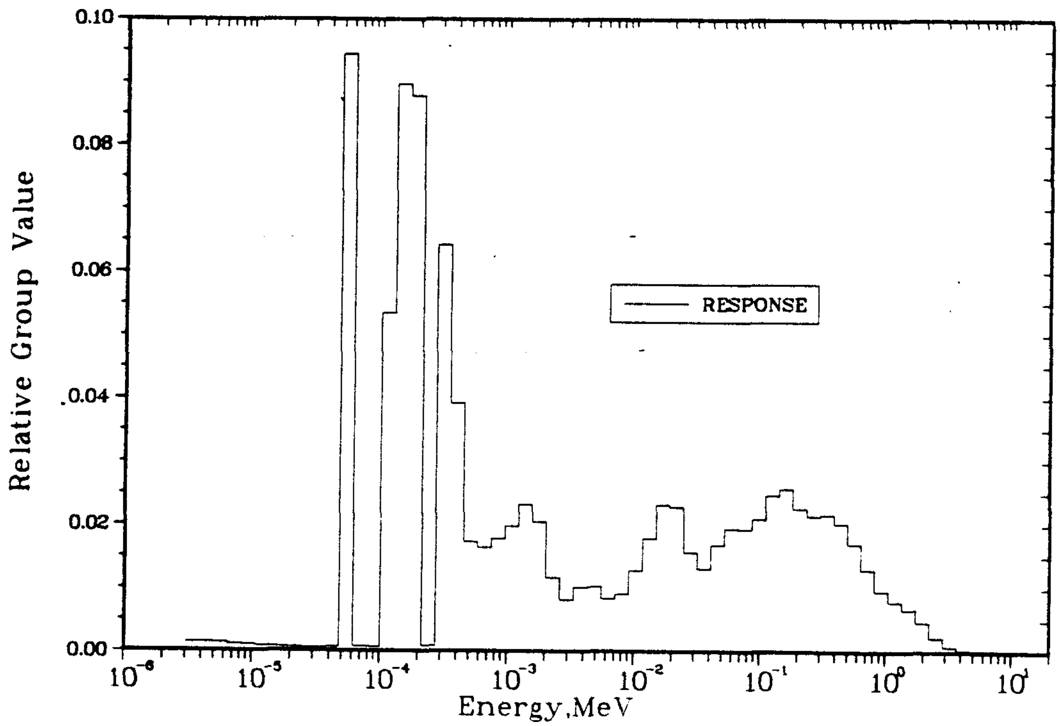

Figure 11. ENDF/B-V cross section and response in EBR-II midplane spectrum for ^{143}Nd.

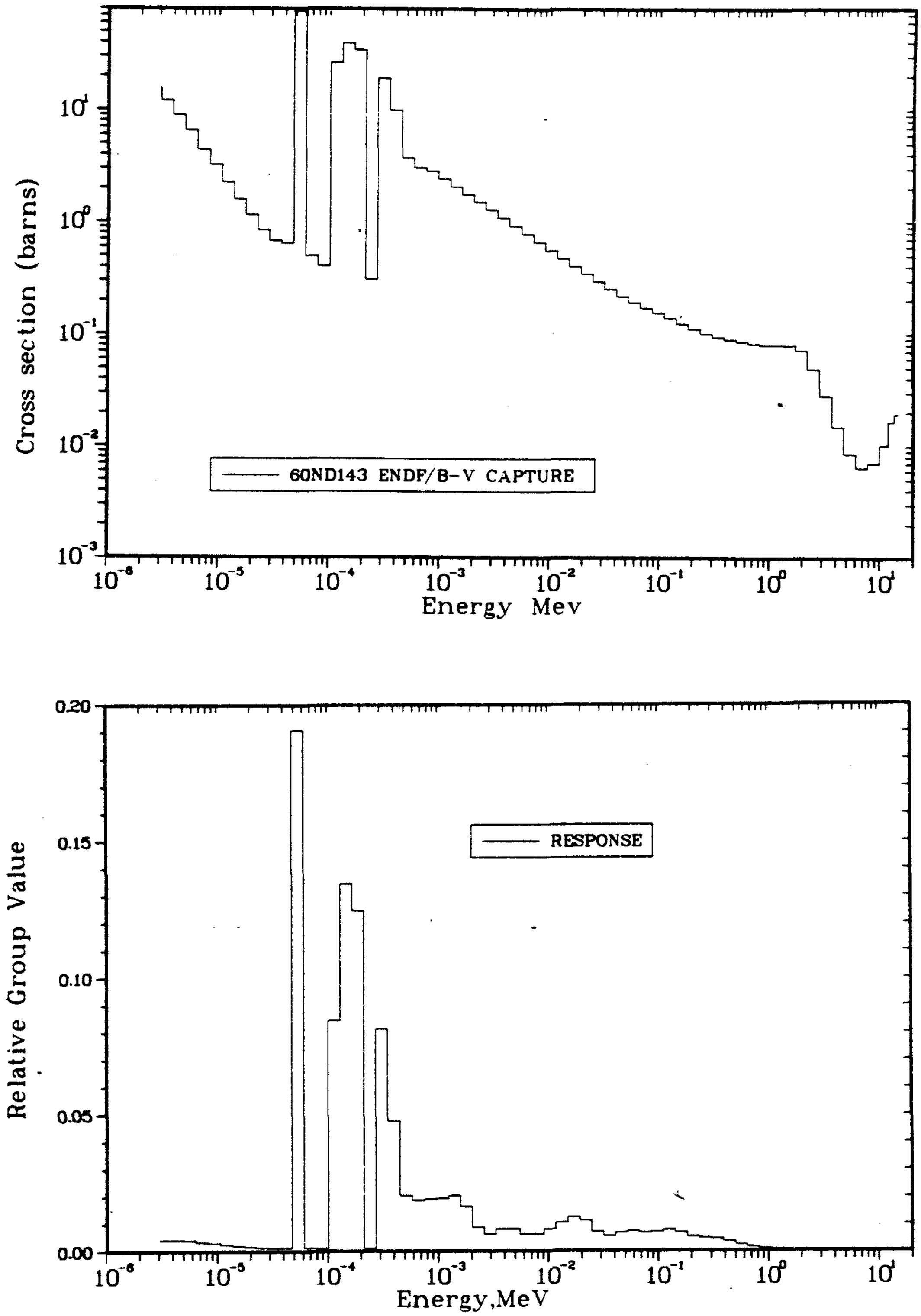

Figure 12. ENDF/B-V cross section and response in EBR-II reflector spectrum for ^{143}Nd.

shows the onset of resolved resonance response contributing approximately 6% to the total response. A more dramatic case of significant resolved-resonance response in the CFRMF spectrum is illustrated in Fig. 6 for the ^{108}Pd reaction. The two resonances at approximately 0.03 keV and 0.09 keV contribute 11% and 15%, respectively, to the total reaction response. This resonance response is in an energy range of the neutron spectrum where the flux is falling off rapidly and where significant structure is present in the flux spectrum (see Fig. 2). Hence an evaluation of integral tests for this reaction requires an evaluation of flux spectrum uncertainty in this energy range and an evaluation of resonance self-shielding corrections for the measured integral cross sections. A typical threshold response in the CFRMF spectrum looks like that for ^{241}Am fission as shown in Fig. 7. Clearly an accurate description of the high energy tail of the CFRMF central spectrum is necessary for a correct interpretation of the integral test for a threshold reaction. In Figs. 8, 9 and 10, energy responses are given for ^{151}Eu capture in three different neutron spectra, CFRMF, EBR-II midplane and EBR-II reflector. These plots show a rather broad response in all spectra. It is significant to note the change in the relative contributions from different energy regions. Integral tests for such reactions in different spectra allow for testing a cross section over different broad energy ranges. Finally Figs. 11 and 12 illustrate the response for ^{143}Nd capture in the EBR-II midplane and reflector neutron spectra. The role of significant resonance response is demonstrated, especially for the reflector location.

5. DISCUSSION

5.1 General Comments

It is instructive to examine Tables 3-5 and assess the results of this study in terms of the following points.

1. Are the discrepancies indicated by the C/E values outside the integral test uncertainty bounds?

2. Is there more, less or no change in the consistency between the measured integral data in going from ENDF/B-IV to ENDF/B-V cross sections?

3. Does the integral test give some indication as to the energy range over which the cross section should be reevaluated?

The results of this assessment are given in Table 6. The column labeled discrepancy range indicates whether an integral test discrepancy is <1, 1-2, 2-3, 3-4 or >4 times the uncertainty in the integral test. The integral test uncertainty is estimated by combining in quadrature the uncertainty of the measured and calculated spectrum-averaged cross sections. Obviously for some cases large uncertainties in the measured data mask any discrepancies which may be real. An assessment of the consistency between the measured integral data and the evaluated cross sections in going from ENDF/B-IV to ENDF/B-V is given by the three columns under the heading "Consistency (IV $\rightarrow$ V)." The appropriate column is marked by an X for each integral test.

In general, the evaluated cross sections are more uncertain above the resolved energy region than below. The generation of the cross section in this region is often based on model calculations and a limited differential and integral data base. For this reason the final two columns in Table 6 indicate the approximate energy, E_C, of the cutoff of the resolved resonance region and the percent response of the reaction above that energy. This information may be helpful in future evaluations for these cross sections.

5.2 Source of Discrepancies

Consistency checks between integral data and evaluated cross sections have been helpful in pointing to the need for improvement in evaluated cross sections. In general, assuming accurate integral data, such consistency checks can be reliably interpreted only if the differential

TABLE 6. ASSESSMENT OF INTEGRAL TEST RESULTS FOR FISSION PRODUCTS AND ACTINIDES

Isotope	Reaction	Neutron Field	C/E	Discrepancy Range	Consistency (IV → V)			E_C [a] (keV)	% Response
					More	Less	No Change		
37 Rb 87	(n,γ)	CFRMF	1.05(11) [b]	<1	X	-	-	15	50
42 Mo 98	(n,γ)	CFRMF	1.09(7)	1-2	-	X	-	4	66
42 Mo 100	(n,γ)	CFRMF	0.86(17)	<1	X	-	-	4	66
43 Tc 99	(n,γ)	CFRMF	1.15(15)	1-2	-	X	-	0.8	92
44 Ru 102	(n,γ)	CFRMF	1.12(7)	1-2	X	-	-	2	90
44 Ru 104	(n,γ)	CFRMF	1.04(7)	<1	-	X	-	0.5	80
46 Pd 108	(n,γ)	CFRMF	1.20(7)	2-3	-	X	-	0.2	74
47 Ag 107	(n,γ)	CFRMF	0.97(20)	<1	X	-	-	1	87
47 Ag 109	(n,γ)	CFRMF	0.86(10)	2-3	X	-	-	1	82
51 Sb 121	(n,γ)	CFRMF	1.09(8)	<1	X	-	-	1	84
51 Sb 123	(n,γ)	CFRMF	0.91(7)	1-2	-	X	-	1.5	81
53 I 127	(n,γ)	CFRMF	1.16(10)	1-2	X	-	-	5	60
53 I 129	(n,γ)	CFRMF	1.07(7)	1-2	-	X	-	0.1	99
54 Xe 132	(n,γ)	CFRMF	1.10(8)	1-2	-	-	X	2.5	89
54 Xe 134	(n,γ)	CFRMF	1.70(7)	>4	-	X	-	2	94
55 Cs 133	(n,γ)	CFRMF	1.02(7)	<1	X	-	-	2	68
55 Cs 137	(n,γ)	CFRMF	0.08(25)	>4	-	-	X	4	40
57 La 139	(n,γ)	CFRMF	1.10(6)	1-2	X	-	-	9	66
58 Ce 142	(n,γ)	CFRMF	1.34(8)	>4	-	-	X	1	99
59 Pr 141	(n,γ)	CFRMF	1.01(15)	<1	X	-	-	1	59
60 Nd 143	(n,γ)	EBR-II-M	0.85(8)	1-2	-	-	X	0.5	54
	(n,γ)	EBR-II-R	0.86(16)	<1	-	X	-	0.5	27

TABLE 6. (continued)

Isotope	Reaction	Neutron Field	C/E	Discrepancy Range	Consistency (IV → V) More	Less	No Change	E_C[a] (keV)	% Response
60 Nd 144	(n,γ)	EBR-II-M	0.79(7)	2-3	-	X	-	10	69
	(n,γ)	EBR-II-R	0.93(17)	<1	-	X	-	10	27
60 Nd 145	(n,γ)	EBR-II-M	0.77(8)	2-3	X	-	-	1	50
	(n,γ)	EBR-II-R	0.80(17)	1-2	X	-	-	1	20
60 Nd 146	(n,γ)	CFRMF	1.24(7)	3-4	X	-	-	4.5	84
60 Nd 148	(n,γ)	CFRMF	1.30(14)	2-3	X	-	-	1	70
60 Nd 150	(n,γ)	CFRMF	1.45(12)	3-4	X	-	-	2	71
61 Pm 147	(n,γ)	CFRMF	1.12(13)	<1	X	-	-	0.1	95
62 Sm 147	(n,γ)	EBR-II-M	0.87(9)	1-2	X	-	-	5	36
	(n,γ)	EBR-II-R	1.06(20)	<1	X	-	-	0.1	11
62 Sm 149	(n,γ)	EBR-II-M	0.77(9)	2-3	X	-	-	0.1	72
	(n,γ)	EBR-II-R	0.84(19)	<1	X	-	-	0.1	48
62 Sm 152	(n,γ)	CFRMF	1.18(7)	2-3	-	X	-	3	67
63 Eu 151	(n,γ)	CFRMF	0.96(6)	<1	X	-	-	0.1	96
	(n,γ)	EBR-II-M	0.76(10)	2-3	X	-	-	0.1	86
	(n,γ)	EBR-II-R	0.76(17)	1-2	X	-	-	0.1	56
63 Eu 152	(n,γ)	EBR-II-M	0.93(12)	<1	-	-	X	0.06	89
	(n,γ)	EBR-II-R	1.27(18)	1-2	-	-	X	0.06	64
63 Eu 153	(n,γ)	CFRMF	1.00(7)	<1	X	-	-	0.1	96
	(n,γ)	EBR-II-M	0.89(9)	1-2	X	-	-	0.1	84
	(n,γ)	EBR-II-R	0.90(17)	<1	X	-	-	0.1	51

TABLE 6. (continued)

Isotope	Reaction	Neutron Field	C/E	Discrepancy Range	Consistency (IV → V) More	Less	No Change	E_C[a] (keV)	% Response
63 Eu 154	(n,γ)	EBR-II-M	0.76(11)	2-3	-	-	X	0.06	88
	(n,γ)	EBR-II-R	0.99(18)	<1	-	-	X	0.06	62
94 Pu 240	(n,f)	CFRMF	1.08(4)	1-2	-	-	X	100	97
94 Pu 242	(n,γ)	CFRMF	1.84(15)	>4	-	X	-	1	80
94 Pu 242	(n,f)	CFRMF	0.85(10)	1-2	-	X	-	100	99
95 Am 241	(n,γ)	CFRMF	0.72(10)	2-3	X	-	-	0.07	98
95 Am 241	(n,f)	CFRMF	1.04(10)	<1	-	X	-	300	98
95 Am 243	(n,γ)	CFRMF	0.59(15)	2-3	X	-	-	0.2	91
95 Am 243	(n,f)	CFRMF	1.19(10)	1-2	-	-	X	200	99

a. E_C: approximate upper energy for the resolved resonance region. The % response is the percentage of the total reaction response above this energy.

b. The number in parentheses is the estimated % uncertainty in the C/E ratio as determined by adding in quadrature the uncertainties in the measured and calculated cross sections.

cross section curve shape and the shape of the neutron spectrum of the irradiation field are accurately known. Also, the interpretation of discrepancies betweeen integral data and evaluated cross section curves can be clouded further because of inaccuracies introduced by the use of multigroup-flux and cross-section representations in the calculation of spectrum-averaged cross sections. In this integral-testing study, the influence of such inaccuracies was examined.

The integral test results reported here for the CFRMF data are based on a preliminary "Version-V" representation of the central neutron field. Spectrum-averaged cross sections were also calculated with a "Version-IV" flux representation and the "Version-V" cross sections for the fission products and actinides. The integral data computed with the "Version-IV" fluxes were, on the average, approximately 3.6% higher than those calculated with the "Version-V" fluxes. In general the use of the "Version-V fluxes" resulted in a reduction in the discrepancies between measured and calculated integral data.

The CFRMF flux representation used for most of the calculations of spectrum-averaged cross sections was a 620-group histogram which included fine group structure (see section 3.1). Cross sections processed into such a large number of groups are not affected significantly by the use different weighting functions. However, integral cross-section calculations in a reduced energy structure, e.g., 42 groups, can generate discrepancies if the weighting function used in the cross-section processing is not representative of the irradiation neutron field. In a comparison of integral cross sections calculated using Vitamin-E[24] weighted and CFRMF spectrum weighted 42-group fission-product cross sections, discrepancies greater than 1% were observed for ^{102}Ru, ^{108}Pd, ^{123}Sb, ^{139}La, ^{141}Pr, ^{147}Pm, ^{150}Nd and ^{152}Sm. For ^{108}Pd and ^{139}La the discrepancies were 6.7% and 4.2%, respectively. These discrepancies could be accounted for by differences in the group cross sections for the large resolved resonances which were significant contributors to the total reaction response in the CFRMF spectrum. The most notable discrepancies were observed for those reactions with strong resonances in the vicinity of the structure in the CFRMF weighting function.

The identification of significant resolved resonance response for several of the fission-product reactions in the CFRMF points to another potential source of discrepancy, namely, self-shielding corrections for the measured integral data. Such corrections were made for some of the samples irradiated in the CFRMF. The correction, in general, resulted in a reduction in the integral test discrepancy (see Table 3).

5.3 Conclusions and Future Work

As is indicated by Table 6, changes made in the cross sections in going from ENDF/B-IV to ENDF/B-V resulted in more consistency for 28 of the integral data and less consistency for 14 of the integral data. Clearly, additional work is required to improve the consistency. From an integral-data standpoint, new measurements made should emphasize reduction in the measurement errors and an accurate determination of self-shielding effects. Such measurements are planned for some key fission-product isotopes in the CFRMF. It should also be pointed out that the CFRMF actinide integral data used in this study was preliminary in nature and final results will be obtained when the analyses of recent experiments is completed.

Efforts to improve the characterization of the CFRMF spectrum would be helpful. These include a recalculation of the CFRMF central neutron spectrum using a complete set of ENDF/B-V cross sections throughout the facility and not only in the filter assembly. To more accurately define the high energy-spectrum tail, the calculation should be made up to 16.90 MeV. In addition a fine group calculation which accurately defines the spectral structure would aid in refining a weighting function representative of the CFRMF.

Improvements in the CFRMF spectrum characterization can be made by utilizing generalized least-squares techniques[19] in spectrum-unfolding analyses based on the accurate dosimeter reaction rates[3] measured in the field. These analyses would refine the spectrum shape defined by the neutronics calculation. The flux covariance matrix obtained from such an analysis could be used in realistic estimates of the uncertainties in calculated spectrum-averaged cross section.

The integral data measured in both CFRMF and EBR-II could be used more effectively than just providing an integral consistency check for an evaluated cross section. All of the data could be utilized in a least-squares adjustment analysis of the multigroup fluxes and cross sections. This analysis could serve to point out, in a more quantitative sense, in which energy regions the evaluated cross sections are consistent and in which regions changes are required. Such an analysis has been done for the EBR-II integral data.[9] This approach could be taken a step further to the adjustment of pointwise cross sections based on all experimental data available, integral and differential, as well as model descriptions of the cross sections. Such analyses have been initiated for some of the CFRMF integral data.[25]

6. REFERENCES

1. J W Rogers, D. A. Millsap, and Y. D. Harker, "CFRMF Neutron Field Flux Spectral Characterization," Nucl. Tech. 25, 330 (1975).

2. L. J. Koch, W. B. Loewenstein, and H. O. Monson, "Addendum to Hazard Summary Report, Experimental Breeder Reactor-II (EBR-II)," USAEC Report ANL-5719 (Addendum), Argonne National Laboratory (1964).

3. Y. D. Harker, J W Rogers and D. A. Millsap, "Fission-Product and Reactor Dosimetry Studies at Coupled Fast Reactivity Measurements Facility," USDOE Report TREE-1259, Idaho National Engineering Laboratory (1978).

4. Y. D. Harker and R. A. Anderl, "Integral Cross-Section Measurements on Fission Products in Fast Neutron Fields," in Proc. Specialists' Meeting on Neutron Cross Sections of Fission Product Nuclei, Bologna, Italy, December 12-14, 1979, NEANDC(E)-209"L", 5 (1980).

5. R. A. Anderl and Y. D. Harker, "Measurement of the Integral Capture and Fission Cross Sections for ^{232}Th in the CFRMF," in Proc. International Conference on Nuclear Cross Sections for Technology, Knoxville, Tennessee, October 22-26, 1979, NBS Special Publication 594 (September, 1980) 475.

6. D. M. Gilliam and J W Rogers, "Spectrum-Averaged Fission Cross Sections for ^{235}U, ^{232}Th and ^{240}Pu in the Coupled Fast Reactivity Measurements Facility (CFRMF)," in Reports to the DOE Nuclear Data Committee, USDOE Report DOE-NDC-19, 124 (May, 1979).

7. Y. D. Harker, R. A. Anderl, E. H. Turk, and N. C. Schroeder, "Integral Measurements for Higher Actinides in CFRMF," in Proc. International Conference on Nuclear Cross Sections for Technology, Knoxville, Tennessee, October 22-26, 1979, NBS Special Publication 594 (September, 1980) 548.

8. R. A. Anderl, Y. D. Harker and F. Schmittroth, "Neodymium, Samarium and Europium Capture Cross-Section Adjustments Based on EBR-II Integral Measurements," in Proc. International Conference on Nuclear Cross Sections for Technology, Knoxville, Tennessee, October 22-26, 1979, NBS Special Publication 594 (September, 1980) 557.

9. R. A. Anderl, F. Schmittroth and Y. D. Harker, "Integral Capture Measurements and Cross Section Adjustments for Nd, Sm and Eu," USDOE Report EGG-PHYS-5182, Idaho National Engineering Laboratory to be published in 1981.

10. J W Rogers, D. A. Millsap and Y. D. Harker, "The Coupled Fast Reactivity Measurements Facility (CFRMF)," in Proc. of IAEA Consultants Meeting on Integral Cross-Section Measurements for Reactor Dosimetry, IAEA, Vienna, Austria, November 15-19, 1976, IAEA-208, vol. II, 117 (1976).

11. D. A. Millsap, EG&G Idaho, Inc., Private Communication (1980).

12. R. L. Curtis, F. J. Wheeler, G. L. Singer and R. A. Grimesey, "PHROG - A Fortran IV Program to Generate Fast Neutron Spectra and Average Multigroup Constants," IN-1435, Idaho Nuclear Corporation (April, 1971).

13. C. L. Beck, Idaho Nuclear Corporation, Private Communication (February 1968).

14. N. M. Green, W. E. Ford, III, et al., "AMPX: A Modular Code System for Generating Coupled Neutron-Gamma Libraries from ENDF/B," USDOE Report ORNL/TM-3706, Oak Ridge National Laboratory (1976).

15. J. L. Lucius, C. R. Weisbin, J. H. Marable, J. D. Drischler, R. Q. Wright, and J. E. White, "A User's Manual for the FORSS Sensitivity and Uncertainty Analysis Code System," USDOE Report, ORNL-5316, Oak Ridge National Laboratory (1977).

16. J. M. Ryskamp, R. A. Anderl, B. L. Broadhead, W. E. Ford, III, J. L. Lucius, J. H. Marable, and J. J. Wagschal, "Sensitivity and a priori Uncertainty Analysis of the CFRMF Central Flux Spectrum," USDOE Report, EGG-PHYS-5243, Idaho National Engineering Laboratory (1980).

17. "PUFF2 Determination of Multigroup Covariance Matrices from ENDF/B-V Uncertainty Files," RSIC Computer Code Collection, PSR-157 (1980).

18. P. H. Kier and A. A. Robba, "RABBLE, A Program for Computation of Resonance Absorption in Multiregion Reactor Cells," USAEC Report ANL-7326, Argonne National Laboratory (1967).

19. F. Schmittroth, "A Method for Data Evaluations with Lognormal Distributions," Nucl. Sci. Eng. 72, 19 (1979).

20. F. Schmittroth, "FERRET Data Analysis Code," USDOE Report HEDL-TME 79-40, Hanford Engineering Development Laboratory (1979).

21. W. B. Wilson, T. R. England, R. J. LaBauve, "Multigroup and Few-Group Cross Sections for ENDF/B-IV Fission Products; the TOAFEW Collapsing Code and Data File of 154-Group Fission-Product Cross Sections," USNRC Report LA-7174-MS, Los Alamos Scientific Laboratory (1978).

22. J. W. M. Dekker and H. Ch. Rieffe, "Adjusted Capture Cross Sections of Fission Product Nuclides from STEK Reactivity Worths and CFRMF Activation Data, Volume II (Nd, Pm, Sm Isotopes)," ECN-55, Netherlands Energy Research Foundation (1979).

23. J. W. M. Dekker and H. Ch. Rieffe, "Adjusted Capture Cross Sections of Fission Product Nuclides from STEK Reactivity Worths and CFRMF Activation Data," ECN-28, Netherlands Energy Research Foundation (1977).

24. C. R. Weisbin, R. W. Roussin, J. J. Wagschal, J. E. White, R. Q. Wright, "Vitamin-E: An ENDF/B-V Multigroup Cross-Section Library for LMFBR Core and Shield, LWR Shield, Dosimetry and Fusion Blanket Technology," USDOE Report ORNL-5505, Oak Ridge National Laboratory (1979).

25. R. E. Schenter, D. L. Johnson, F. M. Mann and F. Schmittroth, "Evaluations of Fission-Product Capture Cross Sections for ENDF/B-V," in Proc. International Conference on Nuclear Cross Sections for Technology, Knoxville, Tennessee, October 22-26, 1979, NBS Special Publication 594 (September, 1980) 662.

APPENDIX A. TABULATION OF GROUP FLUXES

Included in this appendix are listings of the multigroup fluxes for the CFRMF and for EBR-II. The group fluxes given in Table A-1 correspond to the 620 group representation of the "Version-V" fluxes for the central neutron field of the CFRMF. This fine group representation was generated as described in section 3.1.4. The sum of all group fluxes in Table A-1 is equal to 1.0. The energy bounds are given in MeV and the upper energy bound for group 620 is 18.0 MeV. As indicated in section 4.2, these 620 group fluxes were used, where possible, in the computation of the calculated integral cross sections listed in Table 3 and in Table 4.

Listed in Table A-2 are the EBR-II group fluxes as generated by the spectrum-unfolding analysis. These fluxes are given according to the 47 group energy structure defined in the table. The energy bounds are given in MeV and the lower energy bound for group 47 is 2.53 E-8 MeV. Group fluxes are given for six spectra which correspond to six unique locations in the EBR-II irradiation experiment. The sum of the group fluxes for a given spectrum is equal to the integral flux in n/cm^2-sec for that spectrum. Each of the six spectra is related to the various dosimeter sets and rare-earth samples as detailed in Table A-3. The spline interpolation program was used to generate 72 group fluxes from these 47 group fluxes. The 72 group fluxes were used in the computation of the calculated integral cross sections listed in Table 5.

TABLE A-1. "VERSION-V" 620 GROUP FLUXES FOR CENTRAL NEUTRON FIELD OF CFRMF

GROUP NUMBER	LOWER ENERGY	GROUP FLUX	GROUP NUMBER	LOWER ENERGY	GROUP FLUX	GROUP NUMBER	LOWER ENERGY	GROUP FLUX
1	1.00E-10	0.	2	1.05E-10	0.	3	1.10E-10	0.
4	1.15E-10	0.	5	1.20E-10	0.	6	1.28E-10	0.
7	1.35E-10	0.	8	1.43E-10	0.	9	1.50E-10	0.
10	1.60E-10	0.	11	1.70E-10	0.	12	1.80E-10	0.
13	1.90E-10	0.	14	2.00E-10	0.	15	2.10E-10	0.
16	2.20E-10	0.	17	2.30E-10	0.	18	2.40E-10	0.
19	2.55E-10	0.	20	2.70E-10	0.	21	2.80E-10	0.
22	3.00E-10	0.	23	3.20E-10	0.	24	3.40E-10	0.
25	3.60E-10	0.	26	3.80E-10	0.	27	4.00E-10	0.
28	4.25E-10	0.	29	4.50E-10	0.	30	4.75E-10	0.
31	5.00E-10	0.	32	5.25E-10	0.	33	5.50E-10	0.
34	5.75E-10	0.	35	6.00E-10	0.	36	6.30E-10	0.
37	6.60E-10	0.	38	6.90E-10	0.	39	7.20E-10	0.
40	7.60E-10	0.	41	8.00E-10	0.	42	8.40E-10	0.
43	8.80E-10	0.	44	9.20E-10	0.	45	9.60E-10	0.
46	1.00E-09	0.	47	1.05E-09	0.	48	1.10E-09	0.
49	1.15E-09	0.	50	1.20E-09	0.	51	1.28E-09	0.
52	1.35E-09	0.	53	1.43E-09	0.	54	1.50E-09	0.
55	1.60E-09	0.	56	1.70E-09	0.	57	1.80E-09	0.
58	1.90E-09	0.	59	2.00E-09	0.	60	2.10E-09	0.
61	2.20E-09	0.	62	2.30E-09	0.	63	2.40E-09	0.
64	2.55E-09	0.	65	2.70E-09	0.	66	2.80E-09	0.
67	3.00E-09	0.	68	3.20E-09	0.	69	3.40E-09	0.
70	3.60E-09	0.	71	3.80E-09	0.	72	4.00E-09	0.
73	4.25E-09	0.	74	4.50E-09	0.	75	4.75E-09	0.
76	5.00E-09	0.	77	5.25E-09	0.	78	5.50E-09	0.
79	5.75E-09	0.	80	6.00E-09	0.	81	6.30E-09	0.
82	6.60E-09	0.	83	6.90E-09	0.	84	7.20E-09	0.
85	7.60E-09	0.	86	8.00E-09	0.	87	8.40E-09	0.
88	8.80E-09	0.	89	9.20E-09	0.	90	9.60E-09	0.
91	1.00E-08	0.	92	1.05E-08	0.	93	1.10E-08	0.
94	1.15E-08	0.	95	1.20E-08	0.	96	1.28E-08	0.

TABLE A-1. (CONTINUED)

GROUP NUMBER	LOWER ENERGY	GROUP FLUX	GROUP NUMBER	LOWER ENERGY	GROUP FLUX	GROUP NUMBER	LOWER ENERGY	GROUP FLUX
97	1.35E-08	0.	98	1.43E-08	0.	99	1.50E-08	0.
100	1.60E-08	0.	101	1.70E-08	0.	102	1.80E-08	0.
103	1.90E-08	0.	104	2.00E-08	0.	105	2.10E-08	0.
106	2.20E-08	0.	107	2.30E-08	0.	108	2.40E-08	0.
109	2.55E-08	0.	110	2.70E-08	0.	111	2.80E-08	0.
112	3.00E-08	0.	113	3.20E-08	0.	114	3.40E-08	0.
115	3.60E-08	0.	116	3.80E-08	0.	117	4.00E-08	0.
118	4.25E-08	0.	119	4.50E-08	0.	120	4.75E-08	0.
121	5.00E-08	0.	122	5.25E-08	0.	123	5.50E-08	0.
124	5.75E-08	0.	125	6.00E-08	0.	126	6.30E-08	0.
127	6.60E-08	0.	128	6.90E-08	0.	129	7.20E-08	0.
130	7.60E-08	0.	131	8.00E-08	0.	132	8.40E-08	0.
133	8.80E-08	0.	134	9.20E-08	0.	135	9.60E-08	0.
136	1.00E-07	0.	137	1.05E-07	2.031E-13	138	1.10E-07	1.952E-13
139	1.15E-07	1.880E-13	140	1.20E-07	2.698E-13	141	1.28E-07	2.565E-13
142	1.35E-07	2.447E-13	143	1.43E-07	2.342E-13	144	1.50E-07	2.975E-13
145	1.60E-07	2.826E-13	146	1.70E-07	2.694E-13	147	1.80E-07	2.575E-13
148	1.90E-07	2.465E-13	149	2.00E-07	2.365E-13	150	2.10E-07	2.273E-13
151	2.20E-07	2.188E-13	152	2.30E-07	2.109E-13	153	2.40E-07	3.026E-13
154	2.55E-07	2.877E-13	155	2.70E-07	1.842E-13	156	2.80E-07	3.517E-13
157	3.00E-07	3.316E-13	158	3.20E-07	3.135E-13	159	3.40E-07	2.973E-13
160	3.60E-07	2.826E-13	161	3.80E-07	2.692E-13	162	4.00E-07	3.194E-13
163	4.25E-07	3.025E-13	164	4.50E-07	2.877E-13	165	4.75E-07	2.746E-13
166	5.00E-07	2.630E-13	167	5.25E-07	2.527E-13	168	5.50E-07	2.434E-13
169	5.75E-07	2.351E-13	170	6.00E-07	2.722E-13	171	6.30E-07	2.626E-13
172	6.60E-07	2.539E-13	173	6.90E-07	2.461E-13	174	7.20E-07	3.173E-13
175	7.60E-07	3.062E-13	176	8.00E-07	2.964E-13	177	8.40E-07	2.877E-13
178	8.80E-07	2.799E-13	179	9.20E-07	2.729E-13	180	9.60E-07	2.665E-13
181	1.00E-06	3.002E-13	182	1.05E-06	4.140E-13	183	1.10E-06	1.637E-12
184	1.15E-06	3.595E-12	185	1.20E-06	6.632E-12	186	1.28E-06	8.524E-12
187	1.35E-06	1.241E-11	188	1.43E-06	2.698E-11	189	1.50E-06	4.241E-11
190	1.60E-06	4.794E-11	191	1.70E-06	6.230E-11	192	1.80E-06	1.405E-10

TABLE A-1. (CONTINUED)

GROUP NUMBER	LOWER ENERGY	GROUP FLUX	GROUP NUMBER	LOWER ENERGY	GROUP FLUX	GROUP NUMBER	LOWER ENERGY	GROUP FLUX
193	1.90E-06	2.099E-10	194	2.00E-06	2.017E-10	195	2.10E-06	2.474E-10
196	2.20E-06	2.986E-10	197	2.30E-06	4.903E-10	198	2.40E-06	1.379E-09
199	2.55E-06	1.362E-09	200	2.70E-06	9.159E-10	201	2.80E-06	2.009E-09
202	3.00E-06	4.266E-09	203	3.20E-06	5.419E-09	204	3.40E-06	4.589E-09
205	3.60E-06	4.957E-09	206	3.80E-06	1.051E-08	207	4.00E-06	2.054E-08
208	4.25E-06	1.909E-08	209	4.50E-06	1.640E-08	210	4.75E-06	1.100E-08
211	5.00E-06	3.944E-08	212	5.25E-06	3.048E-08	213	5.50E-06	1.638E-08
214	5.75E-06	7.528E-09	215	6.00E-06	5.685E-09	216	6.30E-06	6.417E-09
217	6.60E-06	6.552E-09	218	6.90E-06	1.095E-08	219	7.20E-06	4.206E-08
220	7.60E-06	8.960E-08	221	8.00E-06	1.304E-07	222	8.40E-06	8.389E-08
223	8.80E-06	1.374E-07	224	9.20E-06	2.292E-07	225	9.60E-06	3.134E-07
226	1.00E-05	4.511E-07	227	1.05E-05	7.995E-07	228	1.10E-05	8.076E-07
229	1.15E-05	4.512E-07	230	1.20E-05	7.391E-07	231	1.28E-05	1.341E-06
232	1.35E-05	1.587E-06	233	1.43E-05	1.932E-06	234	1.50E-05	2.321E-06
235	1.60E-05	1.893E-06	236	1.70E-05	2.645E-06	237	1.80E-05	2.055E-06
238	1.90E-05	4.155E-07	239	2.00E-05	2.611E-07	240	2.10E-05	5.832E-07
241	2.20E-05	1.680E-06	242	2.30E-05	1.899E-06	243	2.40E-05	4.959E-06
244	2.55E-05	5.680E-06	245	2.70E-05	4.067E-06	246	2.80E-05	1.313E-05
247	3.00E-05	1.285E-05	248	3.20E-05	7.436E-06	249	3.40E-05	1.647E-06
250	3.60E-05	1.650E-06	251	3.80E-05	4.067E-06	252	4.00E-05	1.034E-05
253	4.25E-05	1.377E-05	254	4.50E-05	1.628E-05	255	4.75E-05	1.972E-05
256	5.00E-05	1.649E-05	257	5.25E-05	2.188E-05	258	5.50E-05	1.354E-05
259	5.75E-05	1.705E-05	260	6.00E-05	1.969E-05	261	6.30E-05	1.167E-05
262	6.60E-05	1.144E-05	263	6.90E-05	1.798E-05	264	7.20E-05	2.443E-05
265	7.60E-05	2.210E-05	266	8.00E-05	3.515E-05	267	8.40E-05	4.083E-05
268	8.80E-05	3.895E-05	269	9.20E-05	3.822E-05	270	9.60E-05	3.220E-05
271	1.00E-04	1.929E-05	272	1.05E-04	1.875E-05	273	1.10E-04	2.413E-05
274	1.15E-04	2.534E-05	275	1.20E-04	6.395E-05	276	1.28E-04	7.777E-05
277	1.35E-04	7.345E-05	278	1.43E-04	7.258E-05	279	1.50E-04	1.003E-04
280	1.60E-04	9.334E-05	281	1.70E-04	1.195E-04	282	1.80E-04	1.509E-04
283	1.90E-04	3.435E-05	284	2.00E-04	6.153E-05	285	2.10E-04	7.207E-05
286	2.20E-04	8.892E-05	287	2.30E-04	8.644E-05	288	2.40E-04	1.401E-04

TABLE A-1. (CONTINUED)

GROUP NUMBER	LOWER ENERGY	GROUP FLUX	GROUP NUMBER	LOWER ENERGY	GROUP FLUX	GROUP NUMBER	LOWER ENERGY	GROUP FLUX
289	2.55E-04	1.317E-04	290	2.70E-04	8.175E-05	291	2.80E-04	1.694E-04
292	3.00E-04	1.940E-04	293	3.20E-04	2.008E-04	294	3.40E-04	1.924E-04
295	3.60E-04	1.609E-04	296	3.80E-04	1.509E-04	297	4.00E-04	1.956E-04
298	4.25E-04	1.931E-04	299	4.50E-04	2.212E-04	300	4.75E-04	2.487E-04
301	5.00E-04	2.547E-04	302	5.25E-04	2.149E-04	303	5.50E-04	2.229E-04
304	5.75E-04	2.280E-04	305	6.00E-04	2.296E-04	306	6.30E-04	3.328E-04
307	6.60E-04	1.935E-04	308	6.90E-04	2.047E-04	309	7.20E-04	3.116E-04
310	7.60E-04	3.267E-04	311	8.00E-04	3.324E-04	312	8.40E-04	2.789E-04
313	8.80E-04	2.970E-04	314	9.20E-04	4.011E-04	315	9.60E-04	2.865E-04
316	1.00E-03	2.598E-04	317	1.05E-03	2.821E-04	318	1.10E-03	3.537E-04
319	1.15E-03	2.764E-04	320	1.20E-03	4.809E-04	321	1.28E-03	4.628E-04
322	1.35E-03	4.815E-04	323	1.43E-03	4.399E-04	324	1.50E-03	7.169E-04
325	1.60E-03	5.440E-04	326	1.70E-03	6.178E-04	327	1.80E-03	5.111E-04
328	1.90E-03	8.397E-04	329	2.00E-03	4.332E-04	330	2.10E-03	5.962E-04
331	2.20E-03	3.615E-04	332	2.30E-03	3.992E-04	333	2.40E-03	8.226E-04
334	2.55E-03	5.583E-04	335	2.70E-03	4.066E-04	336	2.80E-03	7.863E-04
337	3.00E-03	7.640E-04	338	3.20E-03	8.267E-04	339	3.40E-03	8.958E-04
340	3.60E-03	8.475E-04	341	3.80E-03	7.522E-04	342	4.00E-03	8.544E-04
343	4.25E-03	8.093E-04	344	4.50E-03	7.810E-04	345	4.75E-03	7.536E-04
346	5.00E-03	7.270E-04	347	5.25E-03	7.012E-04	348	5.50E-03	6.761E-04
349	5.75E-03	6.515E-04	350	6.00E-03	7.499E-04	351	6.30E-03	7.158E-04
352	6.60E-03	6.826E-04	353	6.90E-03	6.503E-04	354	7.20E-03	8.242E-04
355	7.60E-03	7.924E-04	356	8.00E-03	7.765E-04	357	8.40E-03	7.737E-04
358	8.80E-03	7.817E-04	359	9.20E-03	7.952E-04	360	9.60E-03	8.060E-04
361	1.00E-02	1.018E-03	362	1.05E-02	1.024E-03	363	1.10E-02	1.026E-03
364	1.15E-02	1.025E-03	365	1.20E-02	1.519E-03	366	1.28E-02	1.475E-03
367	1.35E-02	1.411E-03	368	1.43E-02	1.331E-03	369	1.50E-02	1.643E-03
370	1.60E-02	1.541E-03	371	1.70E-02	1.494E-03	372	1.80E-02	1.491E-03
373	1.90E-02	1.524E-03	374	2.00E-02	1.588E-03	375	2.10E-02	1.677E-03
376	2.20E-02	1.789E-03	377	2.30E-02	1.923E-03	378	2.40E-02	4.069E-03
379	2.55E-02	5.292E-03	380	2.70E-02	1.418E-03	381	2.80E-02	2.017E-03
382	3.00E-02	2.946E-03	383	3.20E-02	2.881E-03	384	3.40E-02	2.802E-03

TABLE A-1. (CONTINUED)

GROUP NUMBER	LOWER ENERGY	GROUP FLUX	GROUP NUMBER	LOWER ENERGY	GROUP FLUX	GROUP NUMBER	LOWER ENERGY	GROUP FLUX
385	3.60E-02	2.859E-03	386	3.80E-02	3.029E-03	387	4.00E-02	4.150E-03
388	4.25E-02	4.459E-03	389	4.50E-02	4.550E-03	390	4.75E-02	4.451E-03
391	5.00E-02	4.188E-03	392	5.25E-02	3.844E-03	393	5.50E-02	3.658E-03
394	5.75E-02	3.665E-03	395	6.00E-02	4.642E-03	396	6.30E-02	5.148E-03
397	6.60E-02	5.839E-03	398	6.90E-02	5.889E-03	399	7.20E-02	6.681E-03
400	7.60E-02	7.328E-03	401	8.00E-02	7.323E-03	402	8.40E-02	4.602E-03
403	8.80E-02	4.958E-03	404	9.20E-02	5.380E-03	405	9.60E-02	5.626E-03
406	1.00E-01	7.148E-03	407	1.05E-01	7.033E-03	408	1.10E-01	6.739E-03
409	1.15E-01	6.672E-03	410	1.20E-01	1.060E-02	411	1.28E-01	1.105E-02
412	1.35E-01	1.017E-02	413	1.43E-01	7.611E-03	414	1.50E-01	1.113E-02
415	1.60E-01	1.220E-02	416	1.70E-01	1.207E-02	417	1.80E-01	1.148E-02
418	1.90E-01	1.115E-02	419	2.00E-01	1.133E-02	420	2.10E-01	1.135E-02
421	2.20E-01	1.096E-02	422	2.30E-01	1.080E-02	423	2.40E-01	1.649E-02
424	2.55E-01	1.595E-02	425	2.70E-01	9.627E-03	426	2.80E-01	1.892E-02
427	3.00E-01	1.940E-02	428	3.20E-01	1.859E-02	429	3.40E-01	1.793E-02
430	3.60E-01	1.789E-02	431	3.80E-01	1.642E-02	432	4.00E-01	1.820E-02
433	4.25E-01	1.747E-02	434	4.50E-01	1.759E-02	435	4.75E-01	1.722E-02
436	5.00E-01	1.644E-02	437	5.25E-01	1.573E-02	438	5.50E-01	1.510E-02
439	5.75E-01	1.451E-02	440	6.00E-01	1.664E-02	441	6.30E-01	1.581E-02
442	6.60E-01	1.497E-02	443	6.90E-01	1.399E-02	444	7.20E-01	1.681E-02
445	7.60E-01	1.487E-02	446	8.00E-01	1.344E-02	447	8.40E-01	1.242E-02
448	8.80E-01	1.171E-02	449	9.20E-01	1.080E-02	450	9.60E-01	9.459E-03
451	1.00E+00	2.080E-02	452	1.10E+00	1.719E-02	453	1.20E+00	1.448E-02
454	1.30E+00	1.246E-02	455	1.40E+00	1.087E-02	456	1.50E+00	9.660E-03
457	1.60E+00	8.812E-03	458	1.70E+00	8.005E-03	459	1.80E+00	7.102E-03
460	1.90E+00	6.453E-03	461	2.00E+00	6.079E-03	462	2.10E+00	5.743E-03
463	2.20E+00	5.445E-03	464	2.30E+00	5.555E-03	465	2.40E+00	5.033E-03
466	2.50E+00	4.548E-03	467	2.60E+00	4.169E-03	468	2.70E+00	3.858E-03
469	2.80E+00	3.598E-03	470	2.90E+00	3.366E-03	471	3.00E+00	3.145E-03
472	3.10E+00	2.935E-03	473	3.20E+00	2.735E-03	474	3.30E+00	2.547E-03
475	3.40E+00	2.371E-03	476	3.50E+00	2.205E-03	477	3.60E+00	2.051E-03
478	3.70E+00	1.909E-03	479	3.80E+00	1.780E-03	480	3.90E+00	1.662E-03

TABLE A-1. (CONTINUED)

GROUP NUMBER	LOWER ENERGY	GROUP FLUX	GROUP NUMBER	LOWER ENERGY	GROUP FLUX	GROUP NUMBER	LOWER ENERGY	GROUP FLUX
481	4.00E+00	1.555E-03	482	4.10E+00	1.456E-03	483	4.20E+00	1.365E-03
484	4.30E+00	1.280E-03	485	4.40E+00	1.202E-03	486	4.50E+00	1.128E-03
487	4.60E+00	1.060E-03	488	4.70E+00	9.950E-04	489	4.80E+00	9.335E-04
490	4.90E+00	8.749E-04	491	5.00E+00	8.192E-04	492	5.10E+00	7.664E-04
493	5.20E+00	7.164E-04	494	5.30E+00	6.693E-04	495	5.40E+00	6.249E-04
496	5.50E+00	5.833E-04	497	5.60E+00	5.442E-04	498	5.70E+00	5.075E-04
499	5.80E+00	4.732E-04	500	5.90E+00	4.412E-04	501	6.00E+00	4.112E-04
502	6.10E+00	3.834E-04	503	6.20E+00	3.575E-04	504	6.30E+00	3.336E-04
505	6.40E+00	3.114E-04	506	6.50E+00	2.907E-04	507	6.60E+00	2.715E-04
508	6.70E+00	2.536E-04	509	6.80E+00	2.370E-04	510	6.90E+00	2.215E-04
511	7.00E+00	2.071E-04	512	7.10E+00	1.936E-04	513	7.20E+00	1.810E-04
514	7.30E+00	1.693E-04	515	7.40E+00	1.583E-04	516	7.50E+00	1.481E-04
517	7.60E+00	1.385E-04	518	7.70E+00	1.295E-04	519	7.80E+00	1.212E-04
520	7.90E+00	1.134E-04	521	8.00E+00	1.062E-04	522	8.10E+00	9.943E-05
523	8.20E+00	9.314E-05	524	8.30E+00	8.725E-05	525	8.40E+00	8.175E-05
526	8.50E+00	7.660E-05	527	8.60E+00	7.178E-05	528	8.70E+00	6.726E-05
529	8.80E+00	6.303E-05	530	8.90E+00	5.905E-05	531	9.00E+00	5.533E-05
532	9.10E+00	5.183E-05	533	9.20E+00	4.854E-05	534	9.30E+00	4.546E-05
535	9.40E+00	4.256E-05	536	9.50E+00	3.984E-05	537	9.60E+00	3.728E-05
538	9.70E+00	3.488E-05	539	9.80E+00	3.262E-05	540	9.90E+00	3.051E-05
541	1.00E+01	2.851E-05	542	1.01E+01	2.662E-05	543	1.02E+01	2.483E-05
544	1.03E+01	2.314E-05	545	1.04E+01	2.155E-05	546	1.05E+01	2.005E-05
547	1.06E+01	1.864E-05	548	1.07E+01	1.733E-05	549	1.08E+01	1.609E-05
550	1.09E+01	1.494E-05	551	1.10E+01	1.387E-05	552	1.11E+01	1.286E-05
553	1.12E+01	1.193E-05	554	1.13E+01	1.107E-05	555	1.14E+01	1.026E-05
556	1.15E+01	9.511E-06	557	1.16E+01	8.817E-06	558	1.17E+01	8.173E-06
559	1.18E+01	7.577E-06	560	1.19E+01	7.024E-06	561	1.20E+01	6.512E-06
562	1.21E+01	6.038E-06	563	1.22E+01	5.599E-06	564	1.23E+01	5.193E-06
565	1.24E+01	4.817E-06	566	1.25E+01	4.470E-06	567	1.26E+01	4.148E-06
568	1.27E+01	3.851E-06	569	1.28E+01	3.576E-06	570	1.29E+01	3.326E-06
571	1.30E+01	3.099E-06	572	1.31E+01	2.893E-06	573	1.32E+01	2.705E-06
574	1.33E+01	2.533E-06	575	1.34E+01	2.376E-06	576	1.35E+01	2.232E-06

TABLE A-1. (CONTINUED)

GROUP NUMBER	LOWER ENERGY	GROUP FLUX	GROUP NUMBER	LOWER ENERGY	GROUP FLUX	GROUP NUMBER	LOWER ENERGY	GROUP FLUX
577	1.36E+01	2.098E-06	578	1.37E+01	1.975E-06	579	1.38E+01	1.860E-06
580	1.39E+01	1.753E-06	581	1.40E+01	1.654E-06	582	1.41E+01	1.560E-06
583	1.42E+01	1.473E-06	584	1.43E+01	1.390E-06	585	1.44E+01	1.313E-06
586	1.45E+01	1.239E-06	587	1.46E+01	1.170E-06	588	1.47E+01	1.104E-06
589	1.48E+01	1.041E-06	590	1.49E+01	9.818E-07	591	1.50E+01	9.251E-07
592	1.51E+01	8.712E-07	593	1.52E+01	8.198E-07	594	1.53E+01	7.709E-07
595	1.54E+01	7.242E-07	596	1.55E+01	6.797E-07	597	1.56E+01	6.373E-07
598	1.57E+01	5.969E-07	599	1.58E+01	5.584E-07	600	1.59E+01	5.218E-07
601	1.60E+01	4.870E-07	602	1.61E+01	4.539E-07	603	1.62E+01	4.225E-07
604	1.63E+01	3.927E-07	605	1.64E+01	3.645E-07	606	1.65E+01	3.378E-07
607	1.66E+01	3.123E-07	608	1.67E+01	2.881E-07	609	1.68E+01	2.652E-07
610	1.69E+01	2.436E-07	611	1.70E+01	2.233E-07	612	1.71E+01	2.044E-07
613	1.72E+01	1.868E-07	614	1.73E+01	1.704E-07	615	1.74E+01	1.552E-07
616	1.75E+01	1.411E-07	617	1.76E+01	1.282E-07	618	1.77E+01	1.163E-07
619	1.78E+01	1.054E-07	620	1.79E+01	9.538E-08			

TABLE A-2. EBR-II GROUP FLUXES FROM SPECTRUM UNFOLDING ANALYSIS

GROUP NUMBER	UPPER ENERGY	GROUP FLUXES FOR DESIGNATED SPECTRUM ID'S 51.	55	52	53	57	56
1	1.691E+01	1.244E+09	7.359E+08	1.465E+08	8.688E+07	1.283E+08	8.040E+07
2	1.492E+01	3.652E+09	2.266E+09	5.289E+08	2.997E+08	4.435E+08	2.728E+08
3	1.350E+01	2.332E+10	1.529E+10	4.217E+09	2.262E+09	3.429E+09	2.057E+09
4	1.162E+01	9.892E+10	6.800E+10	2.165E+10	1.098E+10	1.746E+10	1.019E+10
5	1.000E+01	3.052E+11	2.151E+11	7.475E+10	3.616E+10	6.155E+10	3.507E+10
6	8.607E+00	7.234E+11	5.128E+11	1.739E+11	8.184E+10	1.517E+11	8.497E+10
7	7.408E+00	2.081E+12	1.484E+12	4.440E+11	2.070E+11	4.124E+11	2.293E+11
8	6.065E+00	4.181E+12	3.017E+12	6.853E+11	3.257E+11	6.840E+11	3.823E+11
9	4.966E+00	1.216E+13	8.944E+12	1.756E+12	8.518E+11	1.697E+12	9.781E+11
10	3.679E+00	1.777E+13	1.320E+13	2.689E+12	1.348E+12	2.370E+12	1.445E+12
11	2.865E+00	2.663E+13	2.024E+13	4.531E+12	2.353E+12	3.774E+12	2.443E+12
12	2.231E+00	3.614E+13	2.879E+13	7.403E+12	3.939E+12	5.979E+12	4.096E+12
13	1.738E+00	4.589E+13	3.709E+13	1.116E+13	5.998E+12	8.892E+12	6.412E+12
14	1.353E+00	4.401E+13	3.431E+13	1.163E+13	6.255E+12	9.343E+12	7.002E+12
15	1.108E+00	8.170E+13	6.181E+13	2.317E+13	1.258E+13	1.915E+13	1.484E+13
16	8.209E-01	8.868E+13	6.921E+13	2.807E+13	1.570E+13	2.406E+13	1.907E+13
17	6.393E-01	1.069E+14	8.723E+13	3.849E+13	2.281E+13	3.417E+13	2.766E+13
18	4.979E-01	1.168E+14	9.896E+13	4.869E+13	3.157E+13	4.465E+13	3.703E+13
19	3.877E-01	1.185E+14	1.013E+14	5.304E+13	3.795E+13	5.009E+13	4.218E+13
20	3.020E-01	2.150E+14	1.802E+14	9.462E+13	7.441E+13	9.194E+13	7.786E+13
21	1.832E-01	1.706E+14	1.686E+14	9.936E+13	8.588E+13	9.948E+13	8.514E+13
22	1.111E-01	1.251E+14	1.084E+14	6.973E+13	6.467E+13	7.205E+13	6.159E+13
23	6.738E-02	8.517E+13	7.835E+13	5.455E+13	5.362E+13	5.835E+13	4.979E+13
24	4.087E-02	5.459E+13	4.627E+13	3.538E+13	3.576E+13	3.921E+13	3.278E+13
25	2.479E-02	4.751E+12	5.596E+12	4.429E+12	4.658E+12	5.048E+12	4.266E+12
26	2.358E-02	3.723E+13	4.877E+13	4.161E+13	4.448E+13	4.859E+13	4.078E+13
27	1.503E-02	2.555E+13	2.676E+13	2.717E+13	2.843E+13	3.194E+13	2.631E+13
28	9.119E-03	1.182E+13	1.077E+13	1.300E+13	1.351E+13	1.530E+13	1.256E+13
29	5.531E-03	8.569E+12	9.013E+12	1.219E+13	1.275E+13	1.391E+13	1.192E+13
30	3.355E-03	8.349E+11	2.247E+12	2.919E+12	3.060E+12	3.212E+12	2.895E+12
31	2.747E-03	3.198E+11	1.093E+12	1.409E+12	1.436E+12	1.483E+12	1.381E+12
32	2.485E-03	1.727E+12	2.846E+12	3.874E+12	3.778E+12	3.922E+12	3.720E+12

TABLE A-2. (CONTINUED)

GROUP NUMBER	UPPER ENERGY	GROUP FLUXES FOR DESIGNATED SPECTRUM ID'S 51.	55	52	53	57	56
33	2.035E-03	9.646E+12	1.003E+13	1.579E+13	1.483E+13	1.552E+13	1.501E+13
34	1.234E-03	4.882E+12	6.331E+12	1.219E+13	1.138E+13	1.188E+13	1.184E+13
35	7.485E-04	2.815E+12	4.398E+12	9.498E+12	8.956E+12	9.328E+12	9.452E+12
36	4.540E-04	2.030E+12	3.213E+12	7.330E+12	6.981E+12	7.325E+12	7.480E+12
37	2.754E-04	1.485E+12	2.414E+12	5.943E+12	5.832E+12	6.130E+12	6.030E+12
38	1.670E-04	1.256E+12	1.896E+12	4.953E+12	5.108E+12	5.405E+12	4.866E+12
39	1.013E-04	7.627E+11	1.442E+12	4.064E+12	4.412E+12	4.462E+12	4.040E+12
40	6.144E-05	4.742E+11	1.007E+12	3.226E+12	3.703E+12	3.588E+12	3.244E+12
41	3.727E-05	4.167E+11	6.865E+11	2.489E+12	2.922E+12	2.787E+12	2.499E+12
42	2.260E-05	2.549E+11	4.577E+11	1.913E+12	2.246E+12	2.146E+12	1.916E+12
43	1.371E-05	1.196E+11	3.003E+11	1.393E+12	1.639E+12	1.560E+12	1.417E+12
44	8.315E-06	9.912E+10	1.992E+11	8.961E+11	1.085E+12	1.001E+12	9.620E+11
45	5.044E-06	1.015E+11	1.211E+11	5.123E+11	6.375E+11	5.679E+11	5.803E+11
46	3.059E-06	9.274E+10	8.568E+10	3.887E+11	4.732E+11	4.258E+11	4.413E+11
47	1.125E-06	3.004E+10	2.123E+10	1.172E+11	1.346E+11	1.261E+11	1.281E+11

TABLE A-3. CROSS-REFERENCE TABLE FOR SPECTRA AND SAMPLES IN EBR-II EXPERIMENT

Spectrum ID	Applicable Dosimeter Set	Axial Location	Applicable Capsules	Rare-Earth Samples
51	XX-1	MID[a]	EC-1	^{152}Eu, ^{154}Eu
			EC-3	^{151}Eu, ^{153}Eu
55	XX-3	MID	EC-7	^{143}Nd, ^{145}Nd
			EC-5	^{147}Sm, ^{149}Sm
52	XX-2	REF[b]	EC-2	^{152}Eu, ^{154}Eu
53	XX-4	REF	EC-8	^{143}Nd, ^{145}Nd
56	XX-2E	REF	EC-4	^{151}Eu, ^{153}Eu
57	XX-4E	REF	EC-6	^{147}Sm, ^{149}Sm

a. MID: Samples at reactor midplane.

b. REF: Samples located in the axial reflector.

APPENDIX B. COMPILATION OF CROSS-SECTION AND RESPONSE PLOTS

This appendix compiles a visual display of the cross-section and energy response for all of the reactions included in the data-testing study. The top half of each figure shows a 72-group representation of a specific cross section and the bottom half shows the relative energy response of that reaction in the indicated spectrum, namely, CFRMF or EBR-II. The area under the response histogram is normalized to 1.0. Hence, one can readily note the fractional response from each group.

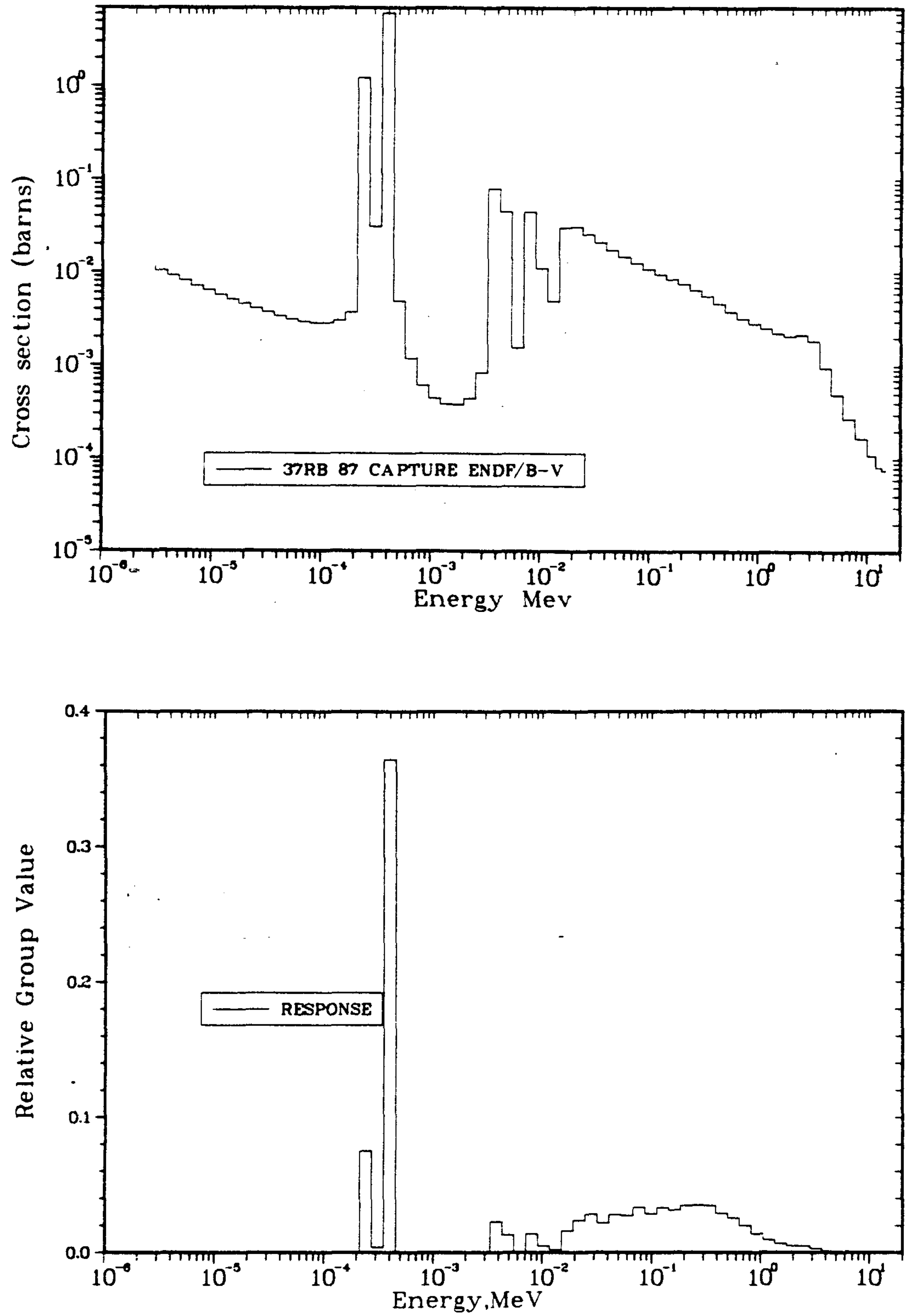

Figure B-1. ENDF/B-V cross section and response in CFRMF for $^{87}Rb(n,\gamma)$.

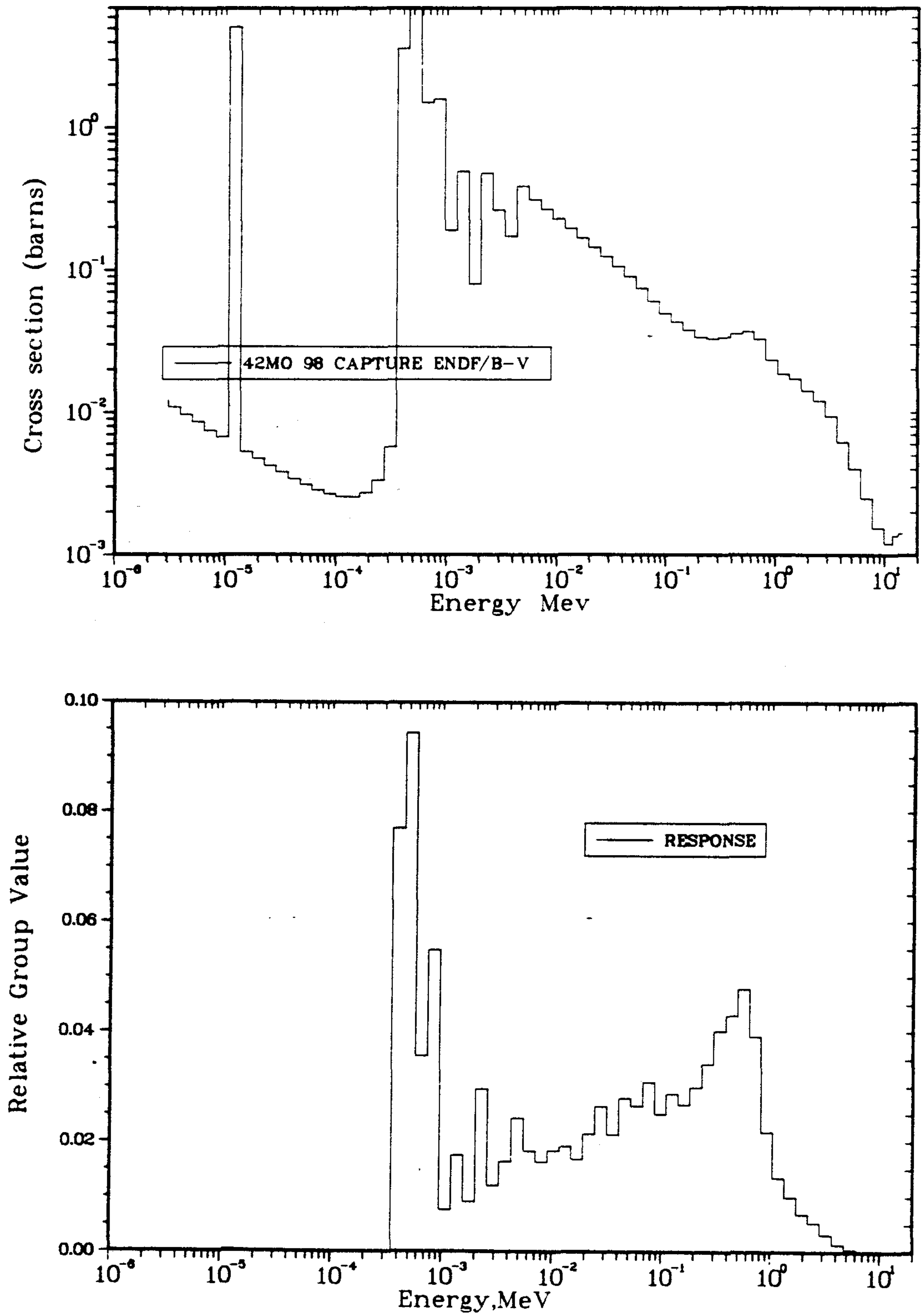

Figure B-2. ENDF/B-V cross section and response in CFRMF for ^{98}Mo(n,γ).

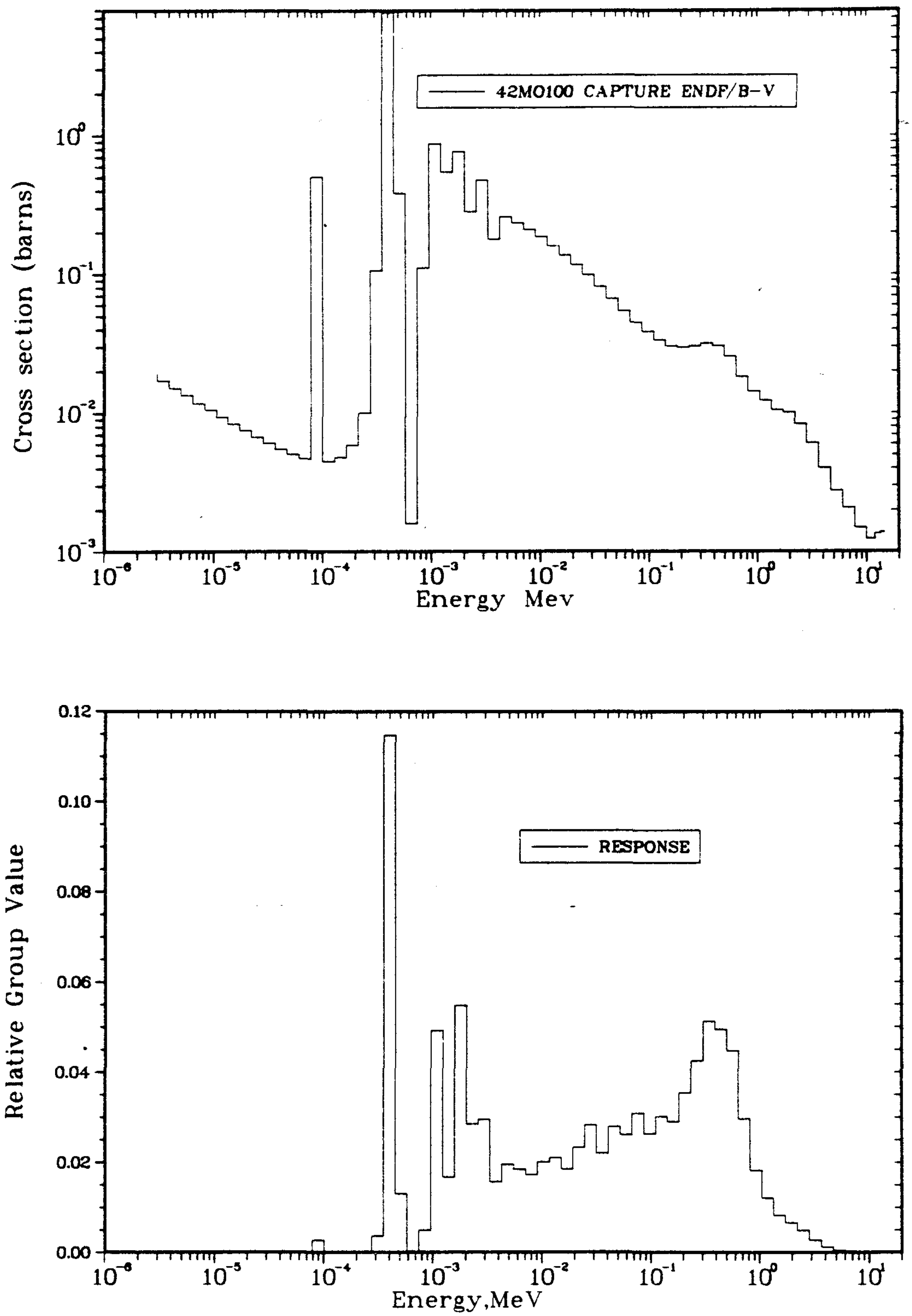

Figure B-3. ENDF/B-V cross section and response in CFRMF for $^{100}Mo(n,\gamma)$.

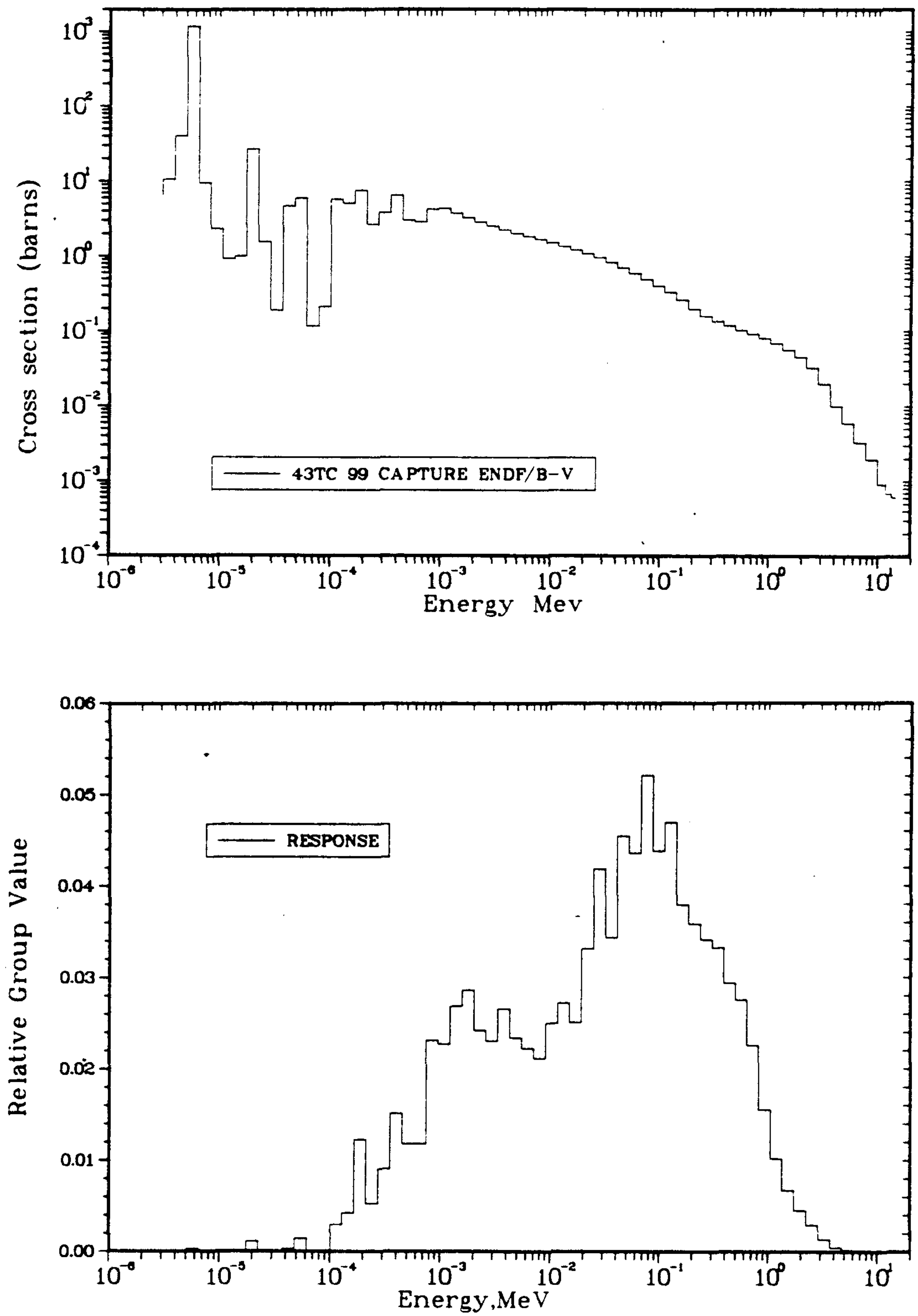

Figure B-4. ENDF/B-V cross section and response in CFRMF for $^{99}Tc(n,\gamma)$.

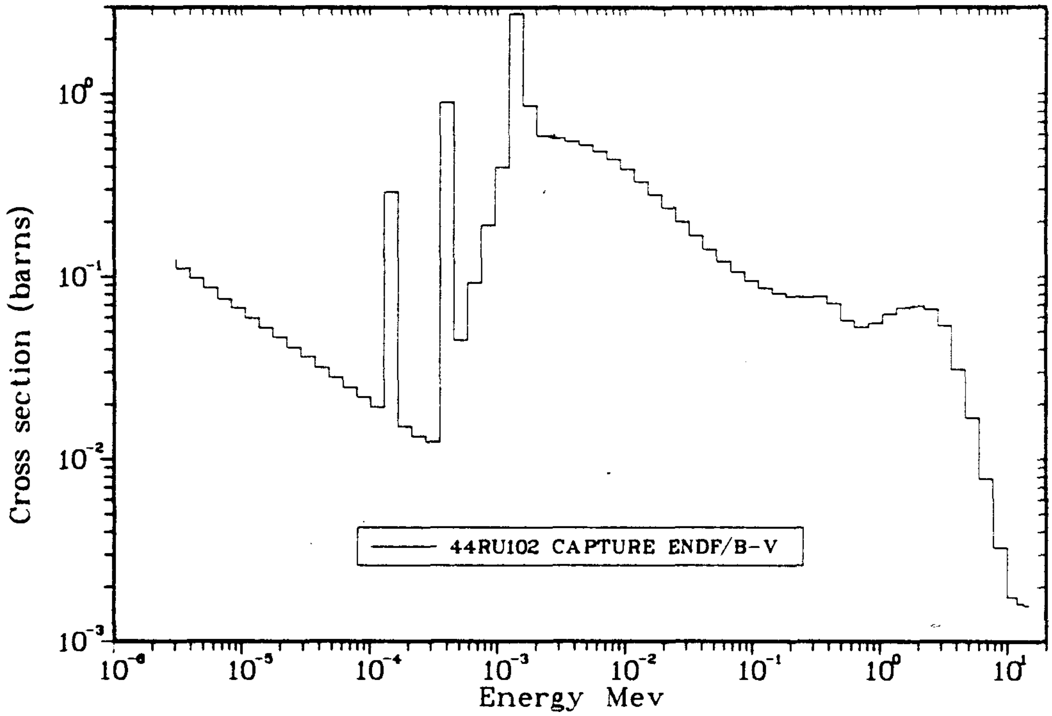

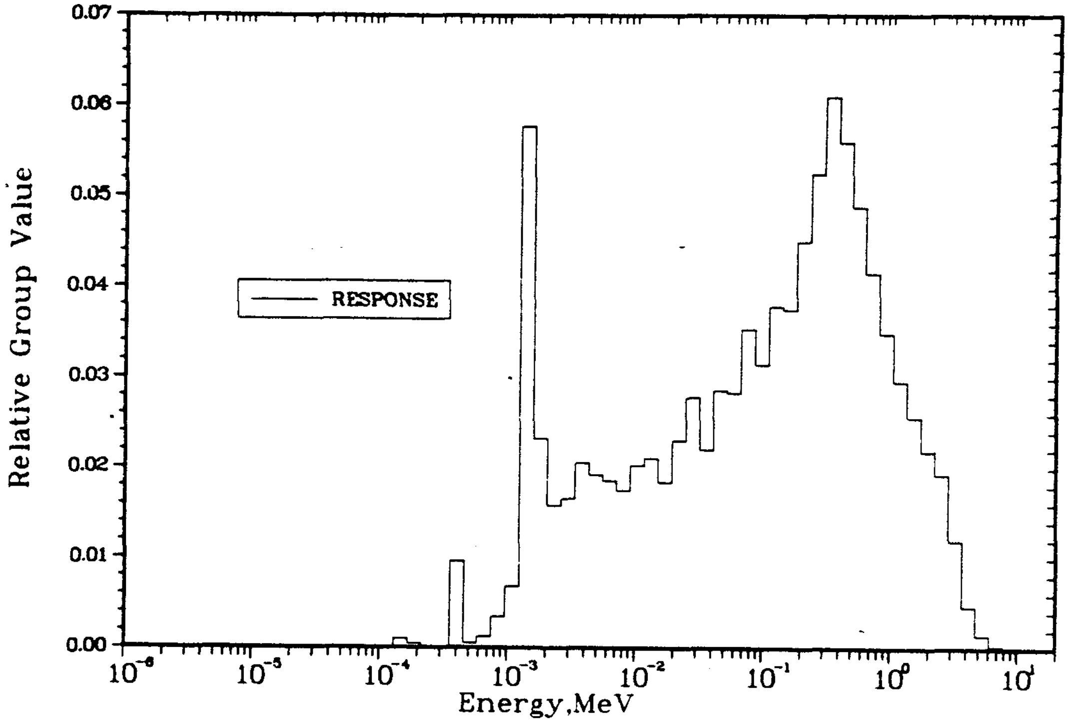

Figure B-5. ENDF/B-V cross section and response in CFRMF for $^{102}Ru(n,\gamma)$.

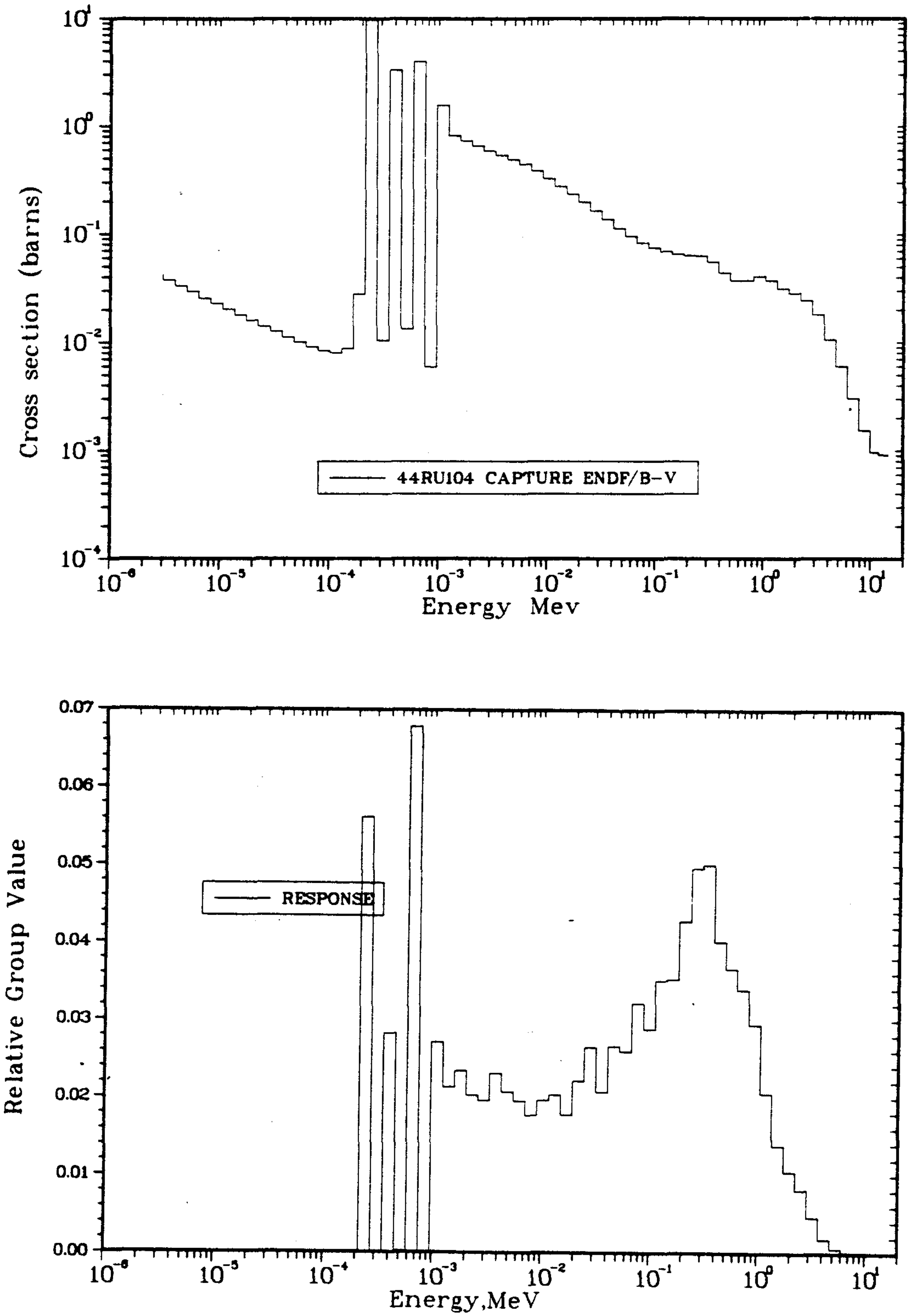

Figure B-6. ENDF/B-V cross section and response in CFRMF for $^{104}Ru(n,\gamma)$.

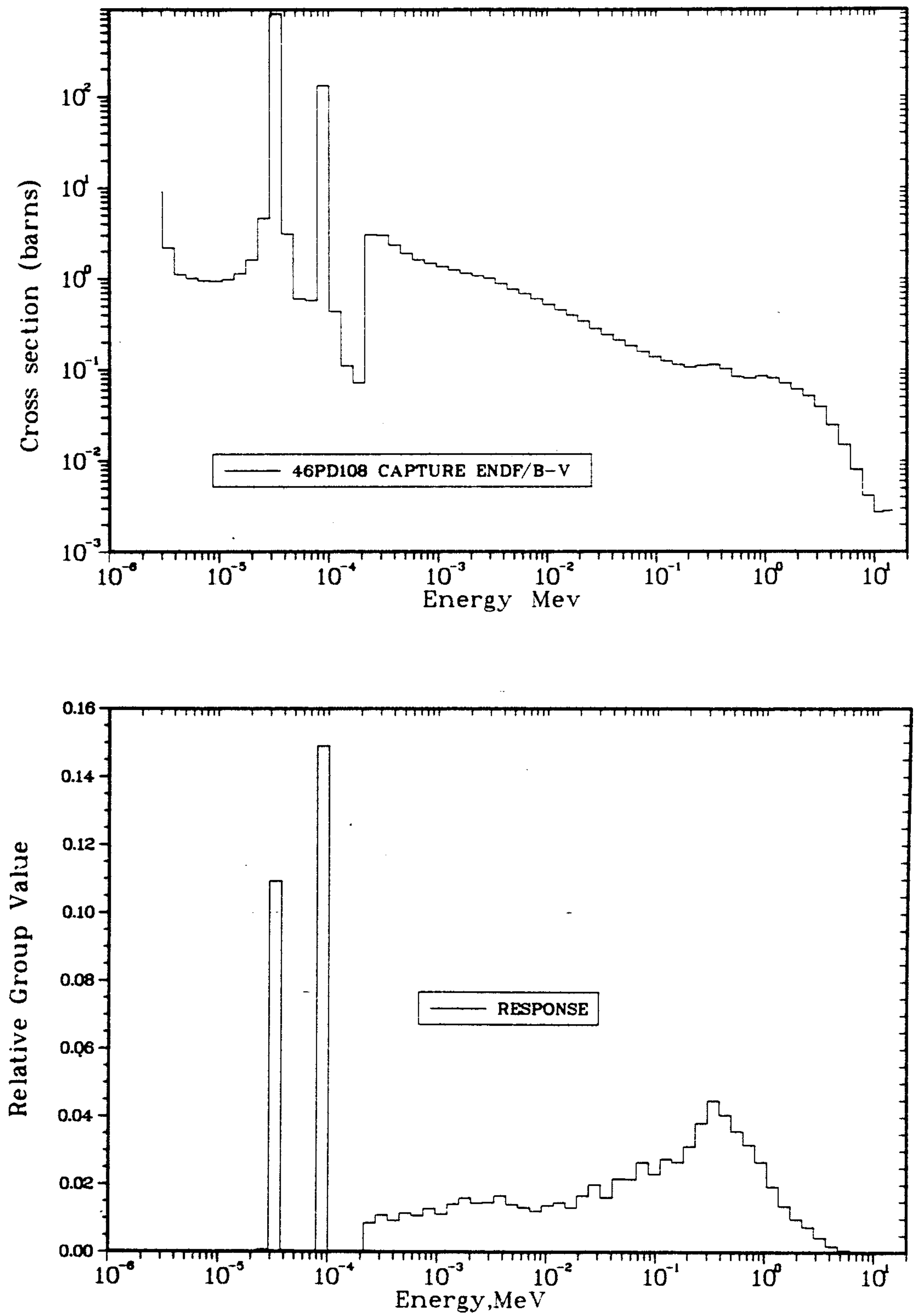

Figure B-7. ENDF/B-V cross section and response in CFRMF for $^{108}Pd(n,\gamma)$.

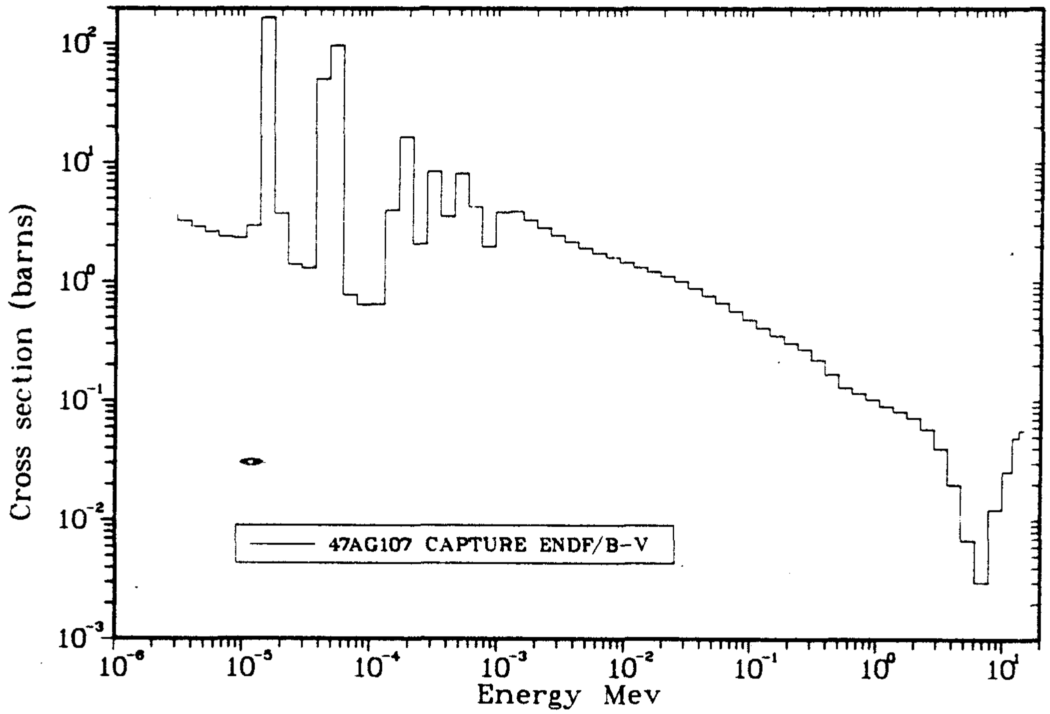

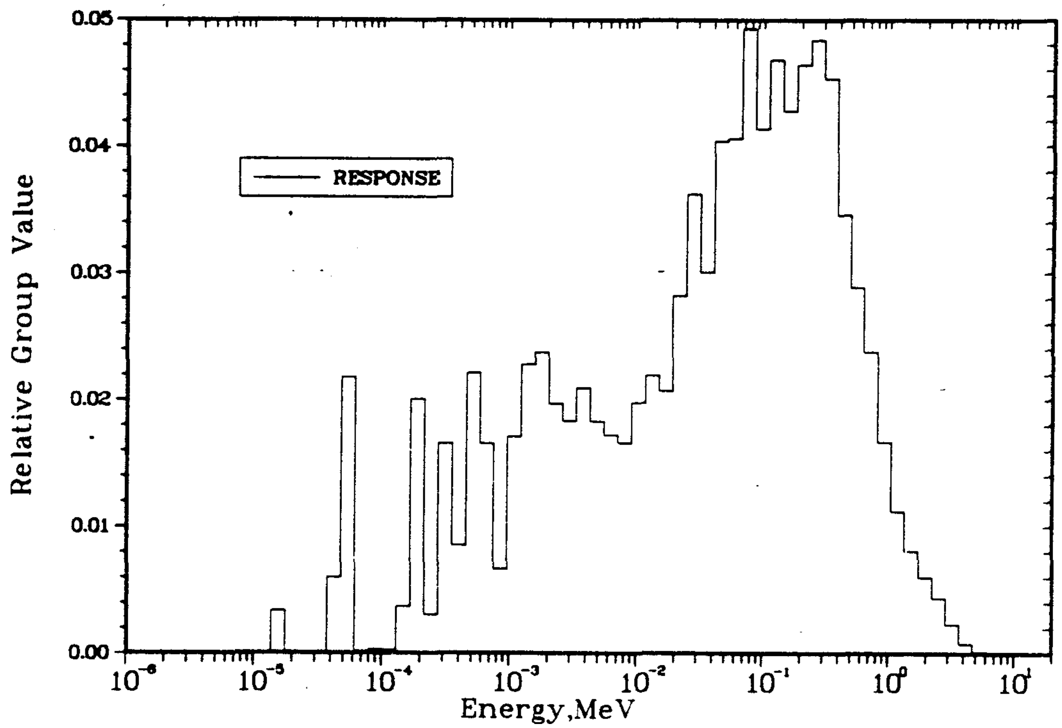

Figure B-8. ENDF/B-V cross section and response in CFRMF for $^{107}Ag(n,\gamma)$.

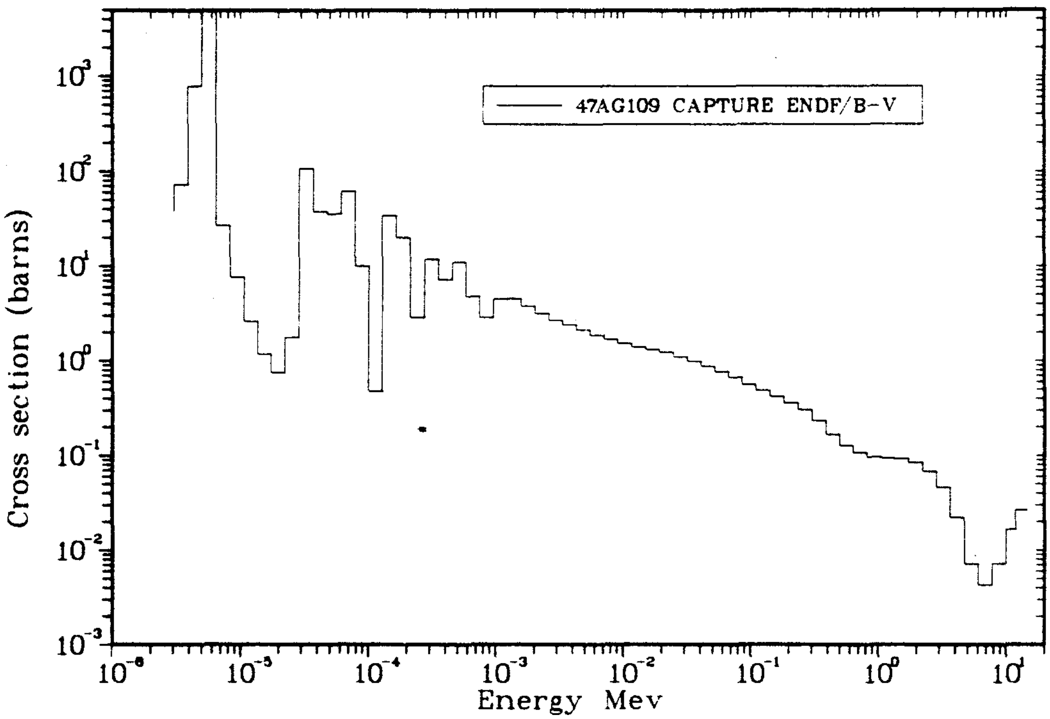

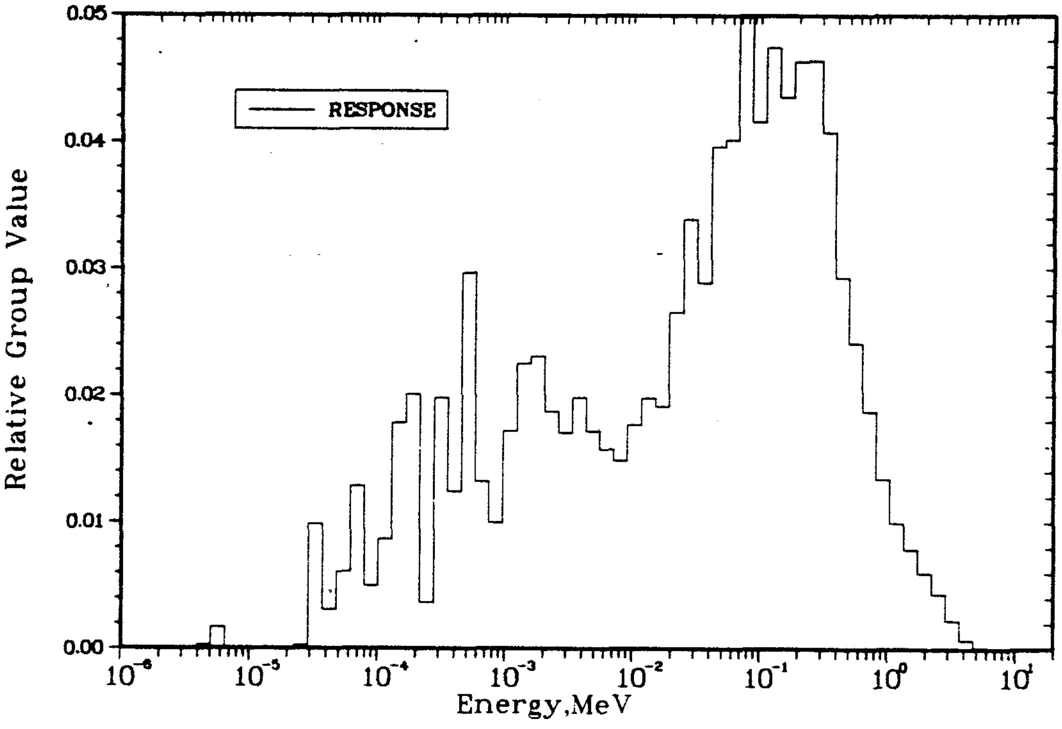

Figure B-9. ENDF/B-V cross section and response in CFRMF for $^{109}Ag(n,\gamma)$.

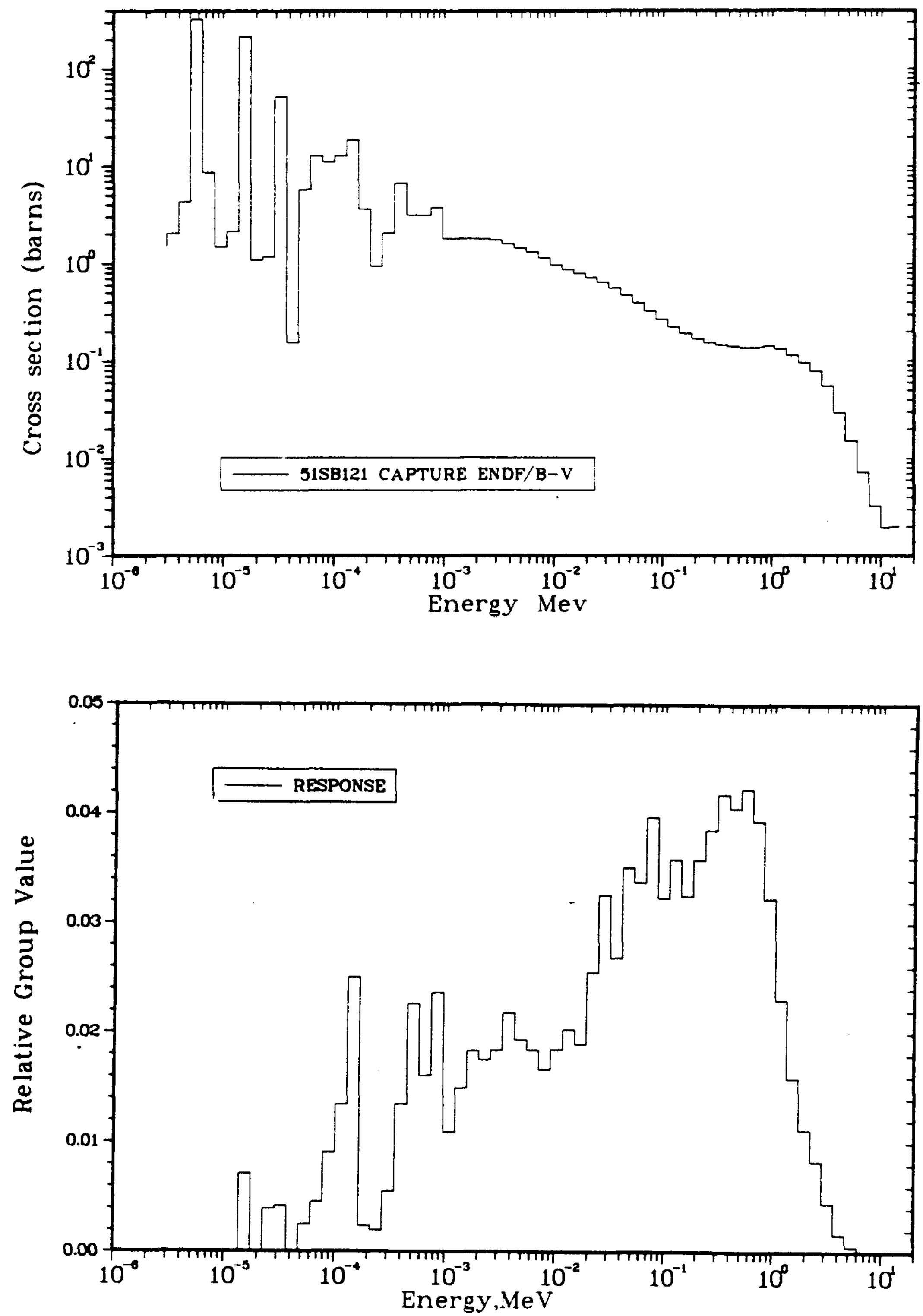

Figure B-10. ENDF/B-V cross section and response in CFRMF for $^{121}Sb(n,\gamma)$.

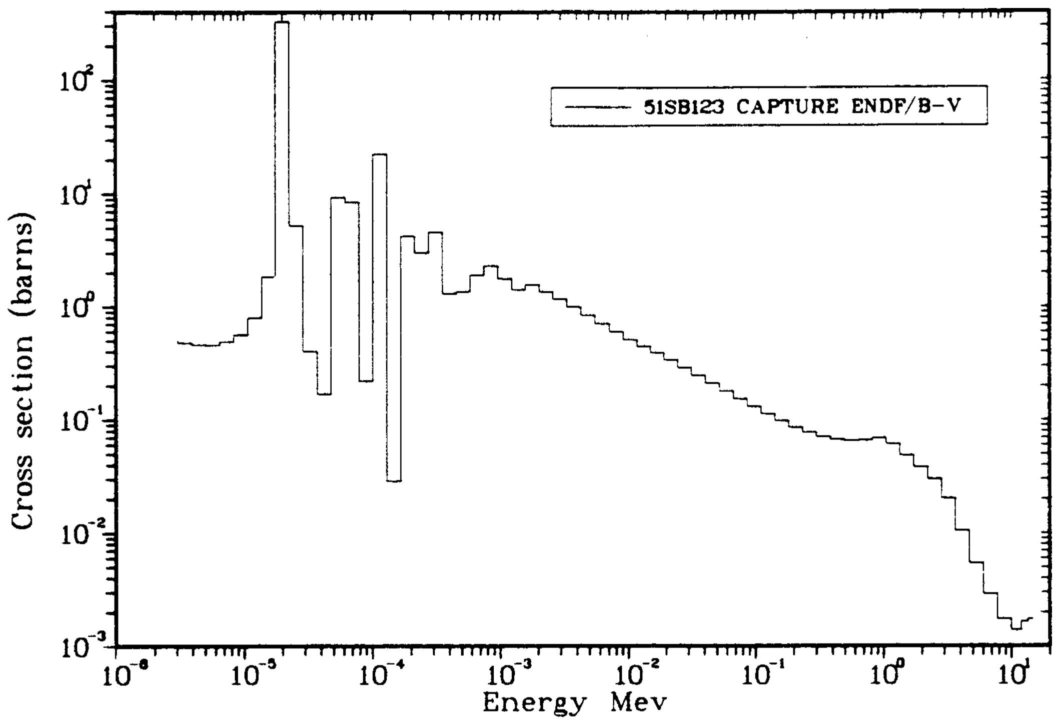

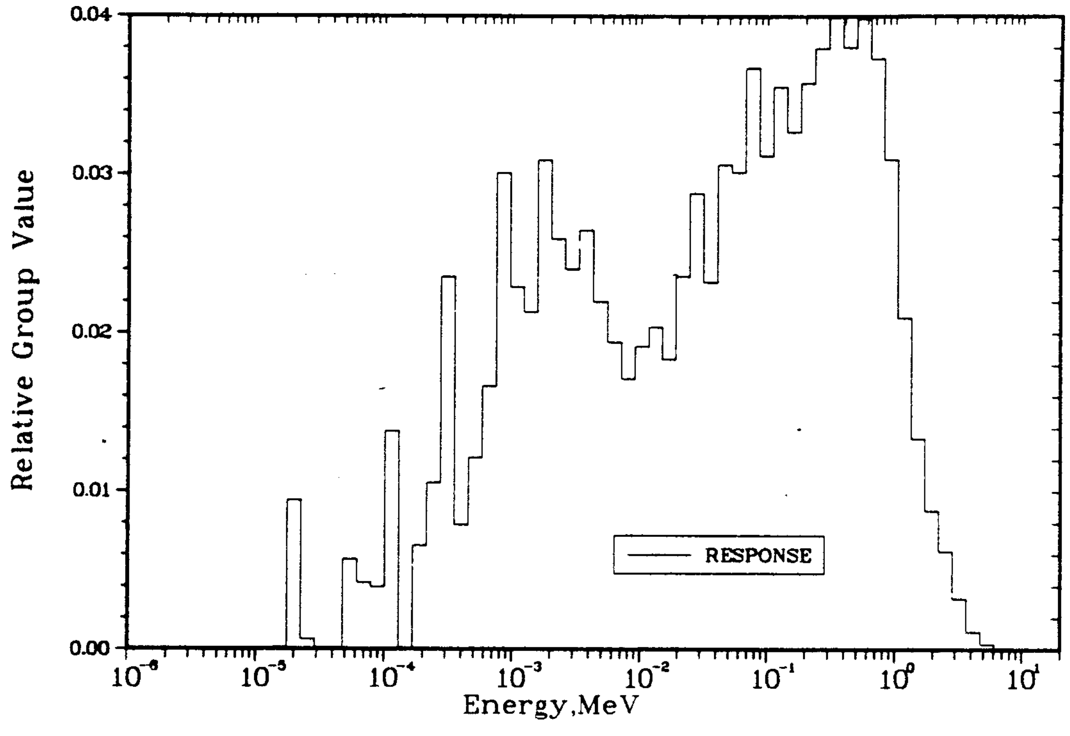

Figure B-11. ENDF/B-V cross section and response in CFRMF for $^{123}Sb(n,\gamma)$.

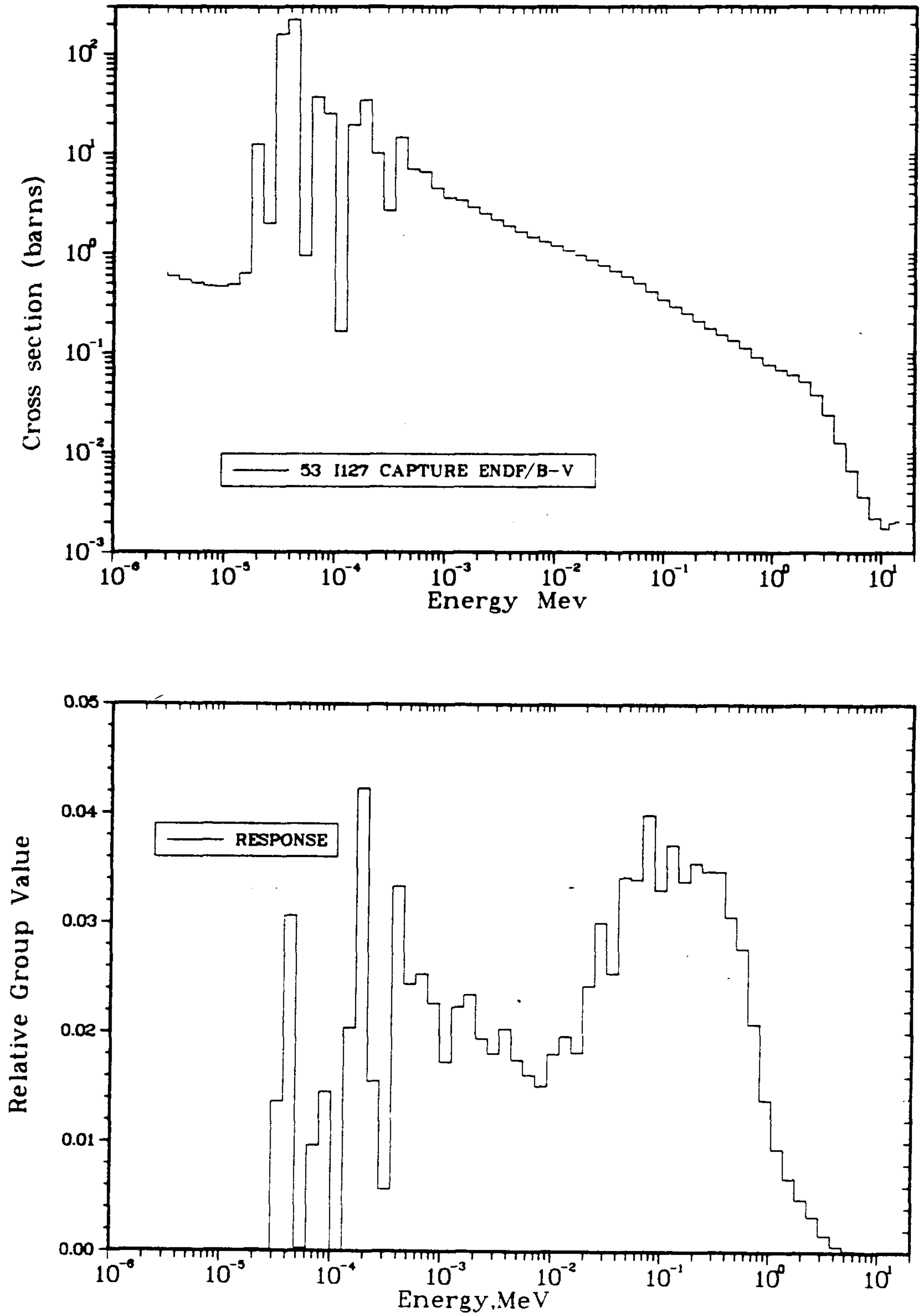

Figure B-12. ENDF/B-V cross section and response in CFRMF for $^{127}I(n,\gamma)$.

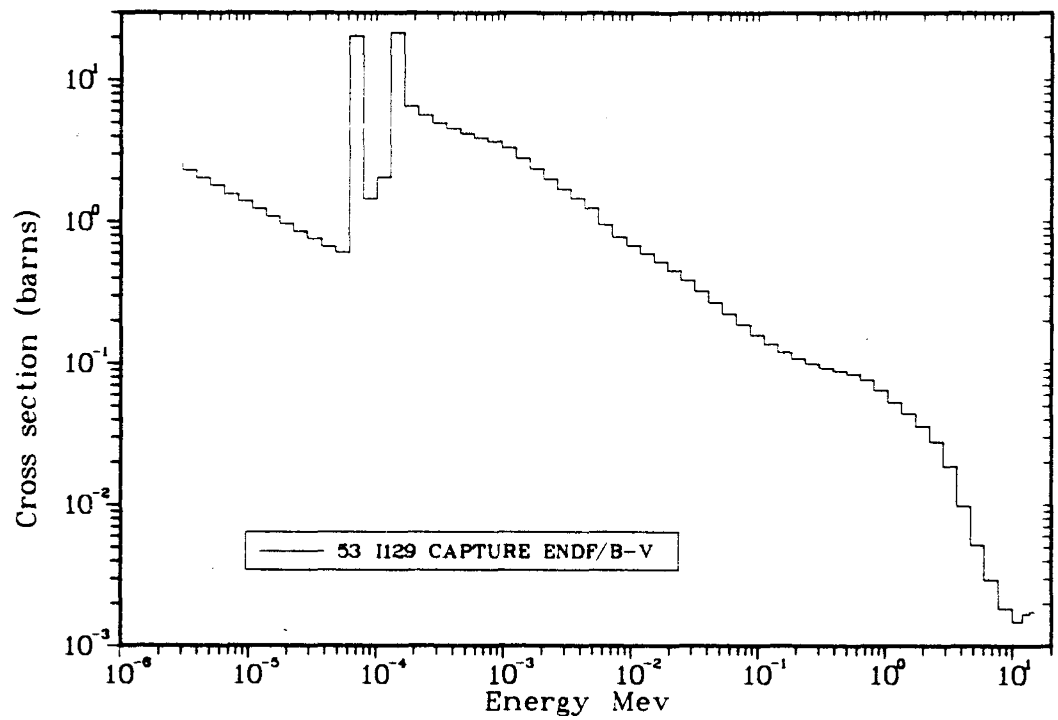

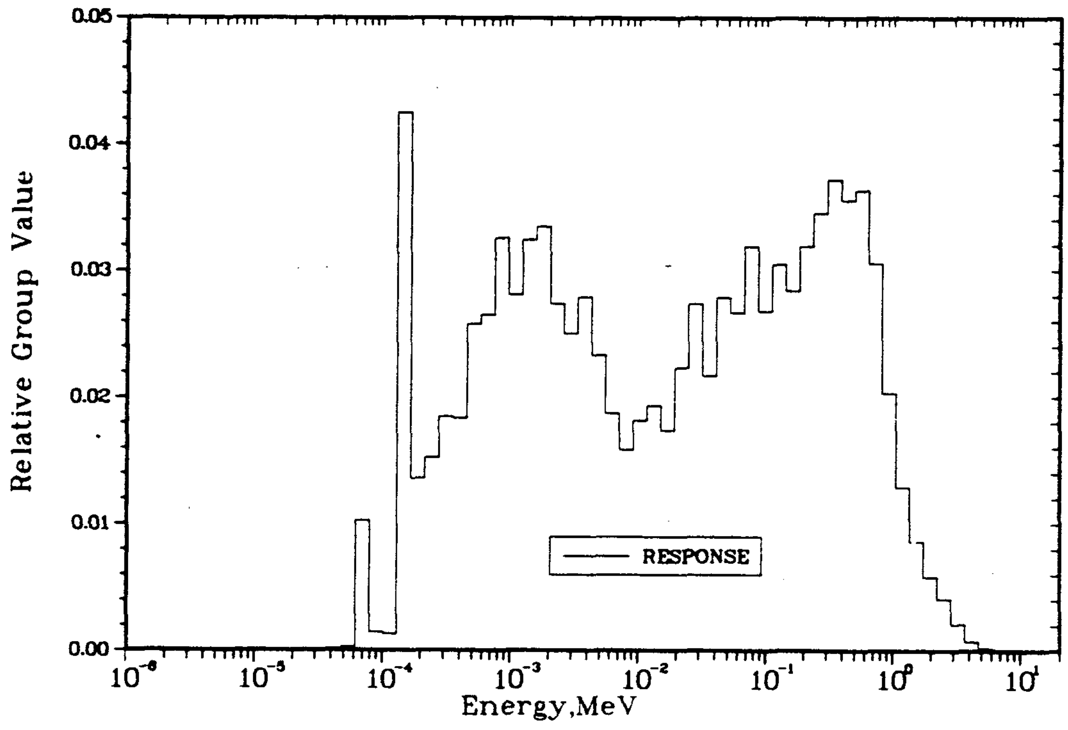

Figure B-13. ENDF/B-V cross section and response in CFRMF for $^{129}I(n,\gamma)$.

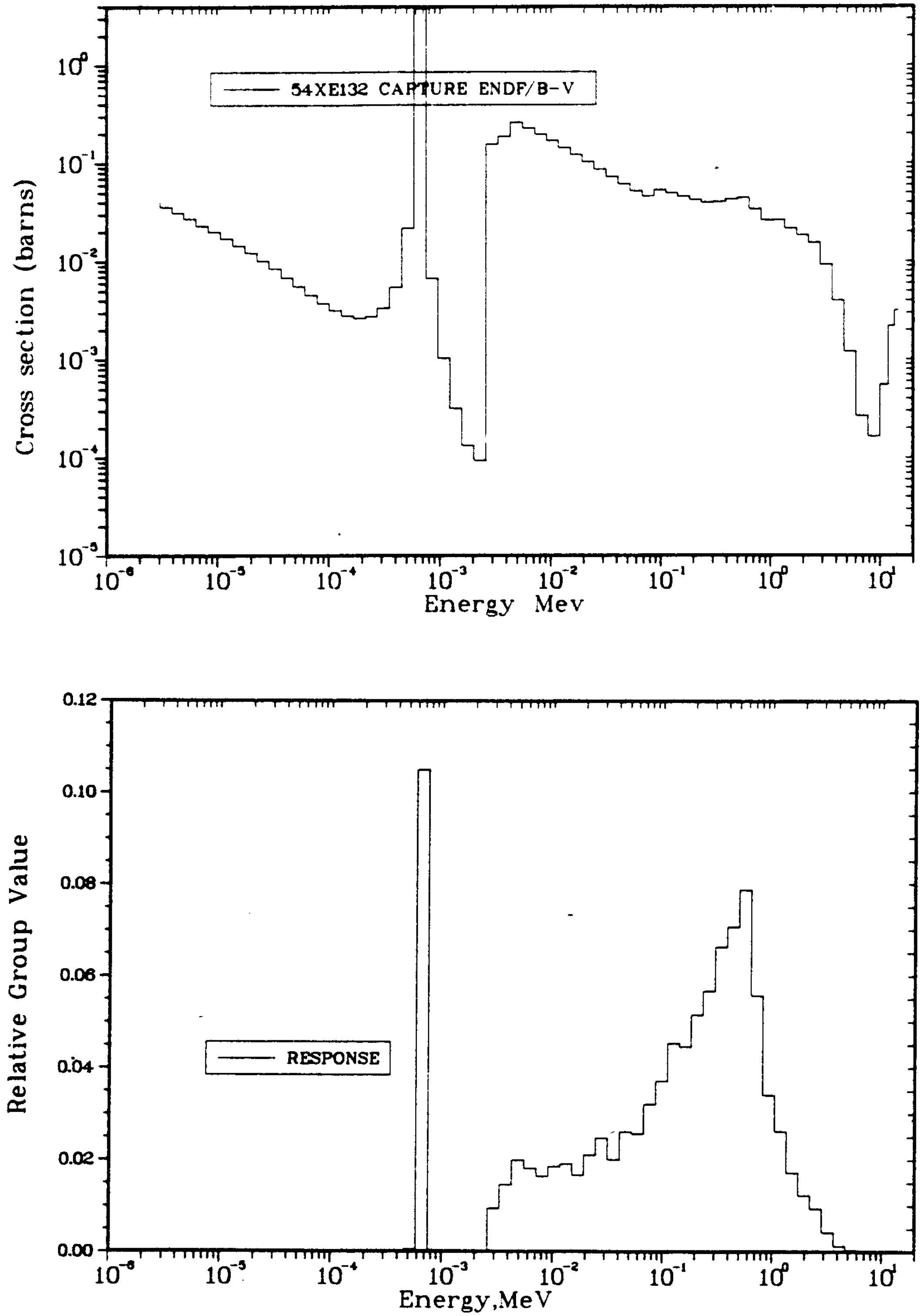

Figure B-14. ENDF/B-V cross section and response in CFRMF for $^{132}Xe(n,\gamma)$.

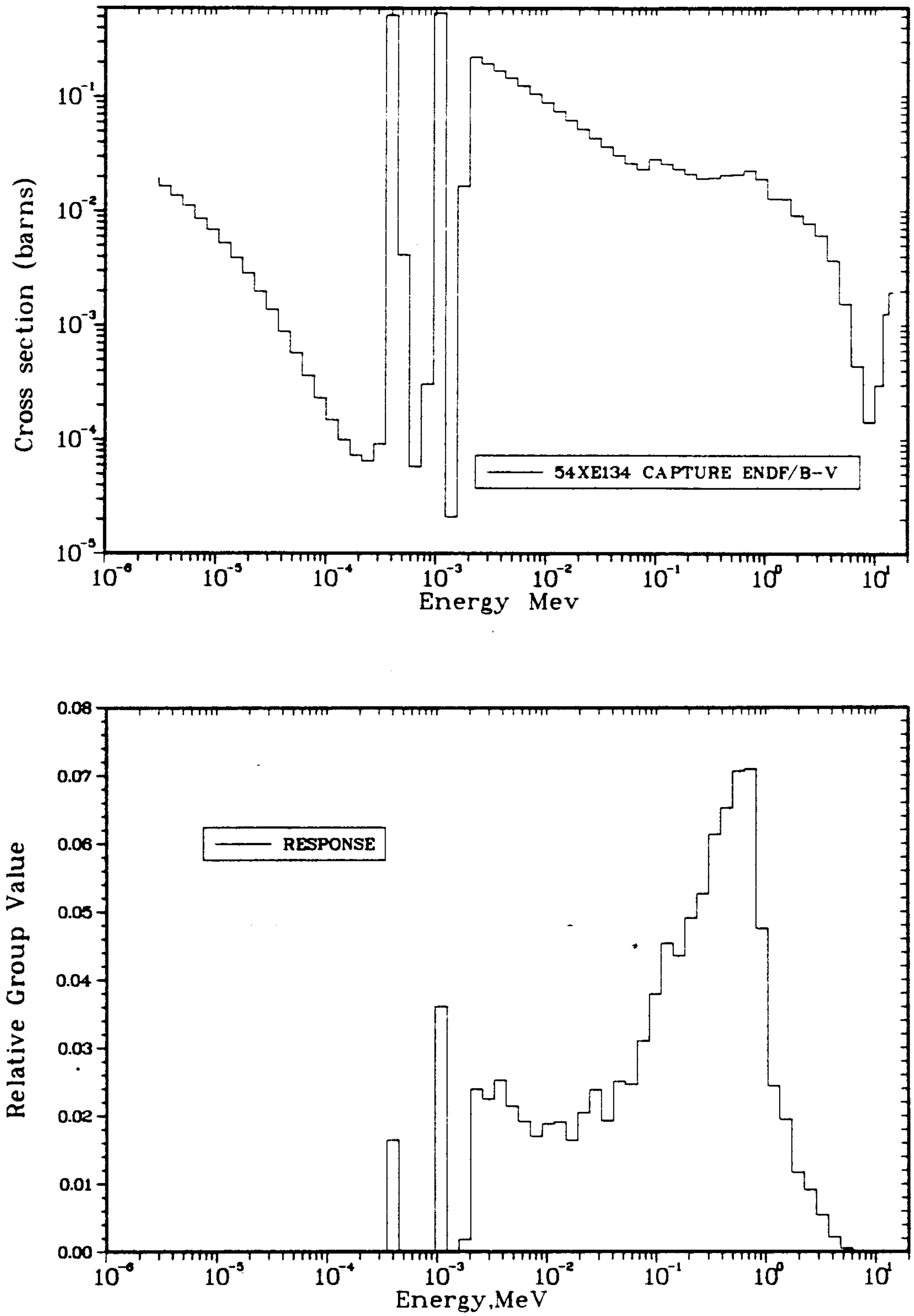

Figure B-15. ENDF/B-V cross section and response in CFRMF for $^{134}Xe(n,\gamma)$.

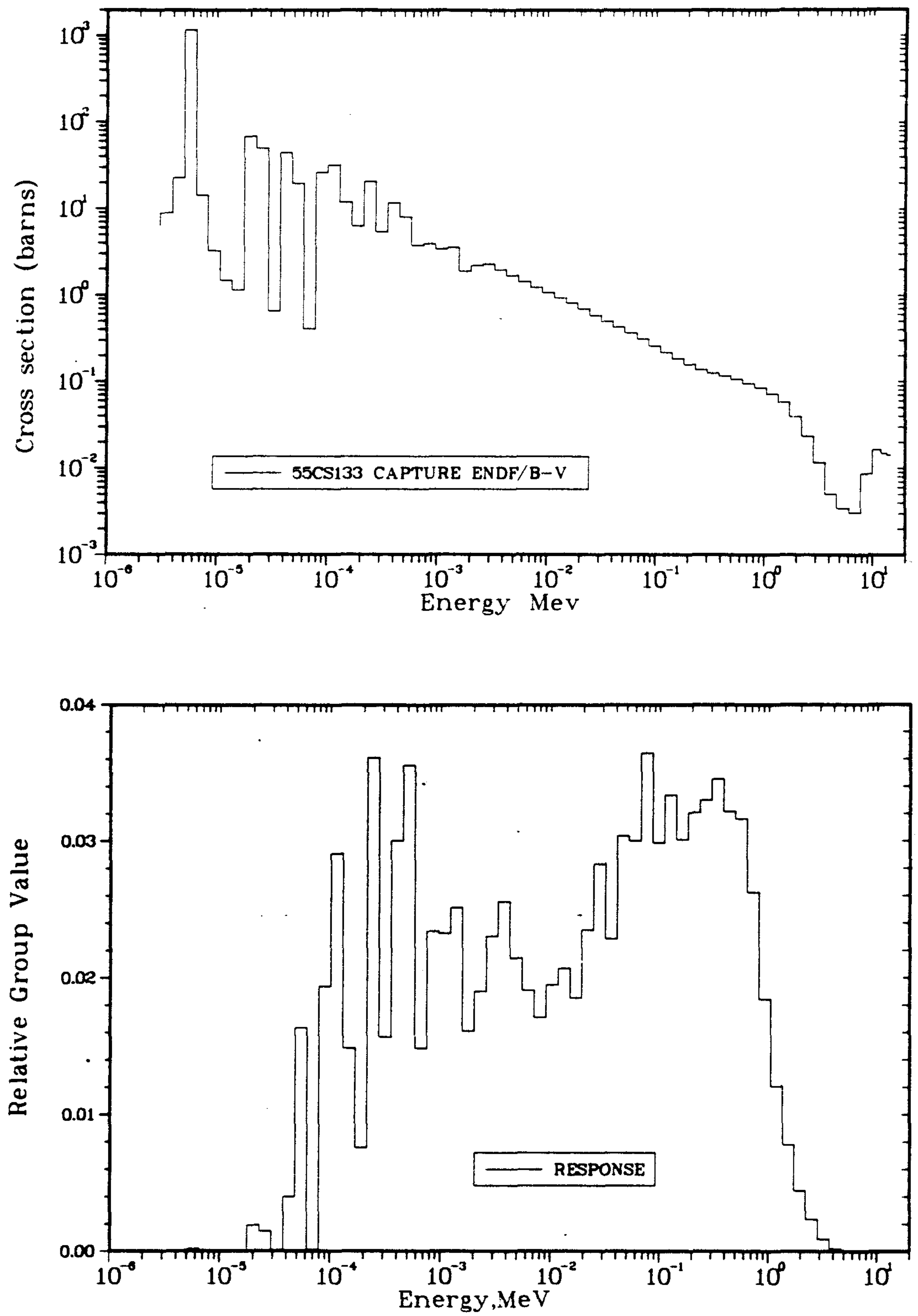

Figure B-16. ENDF/B-V cross section and response in CFRMF for $^{133}Cs(n,\gamma)$.

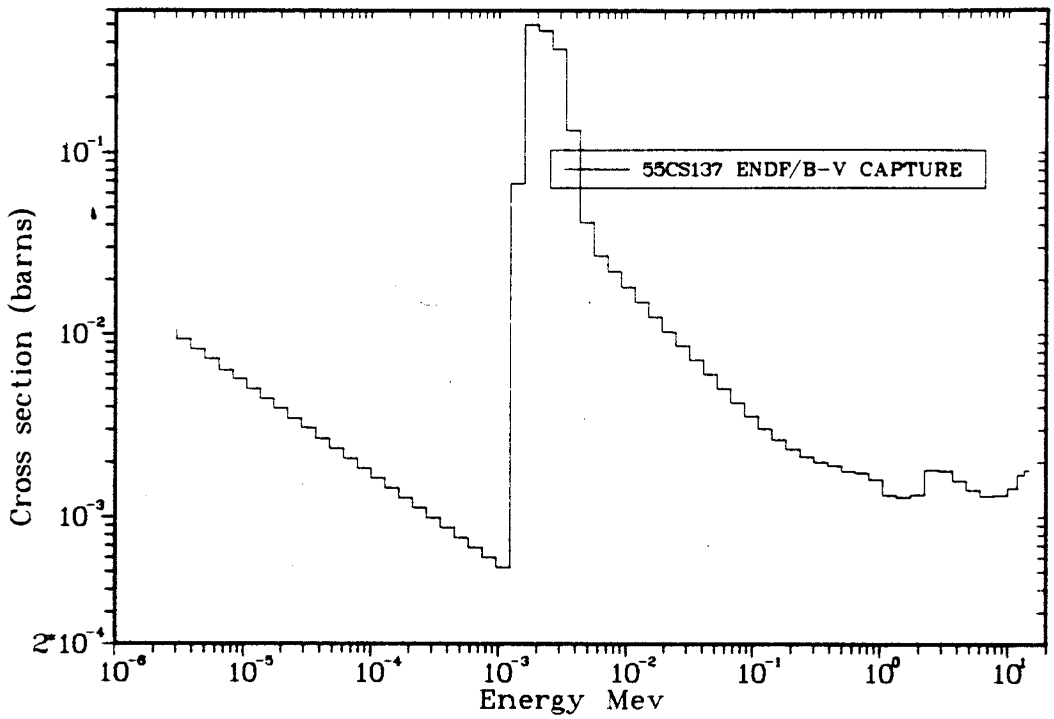

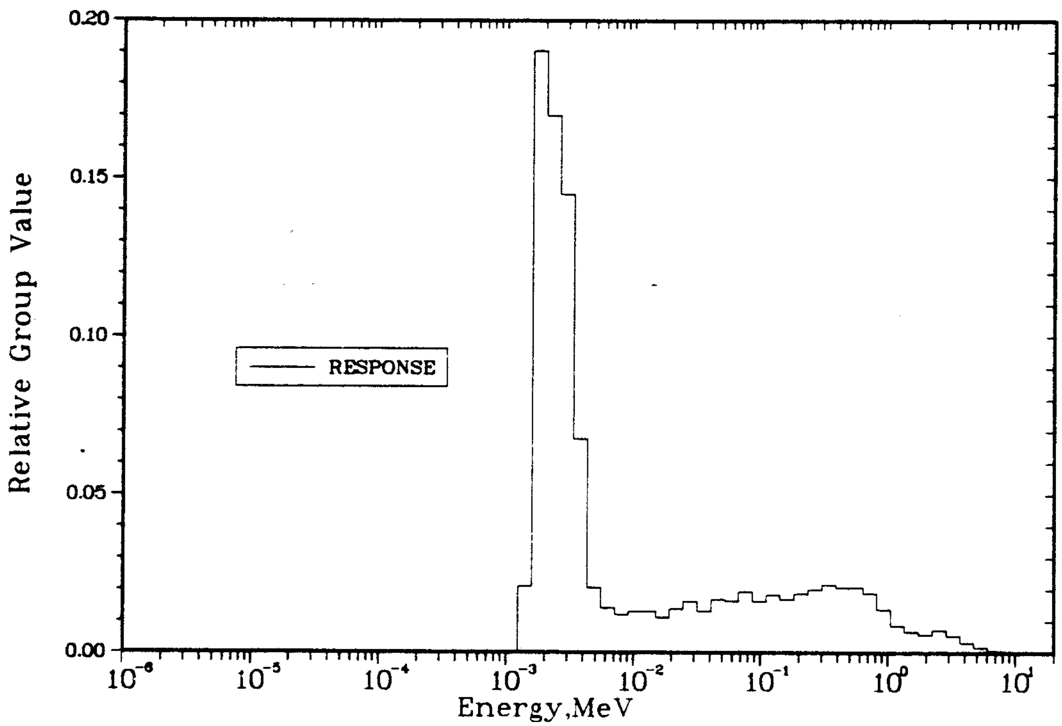

Figure B-17. ENDF/B-V cross section and response in CFRMF for $^{137}Cs(n,\gamma)$.

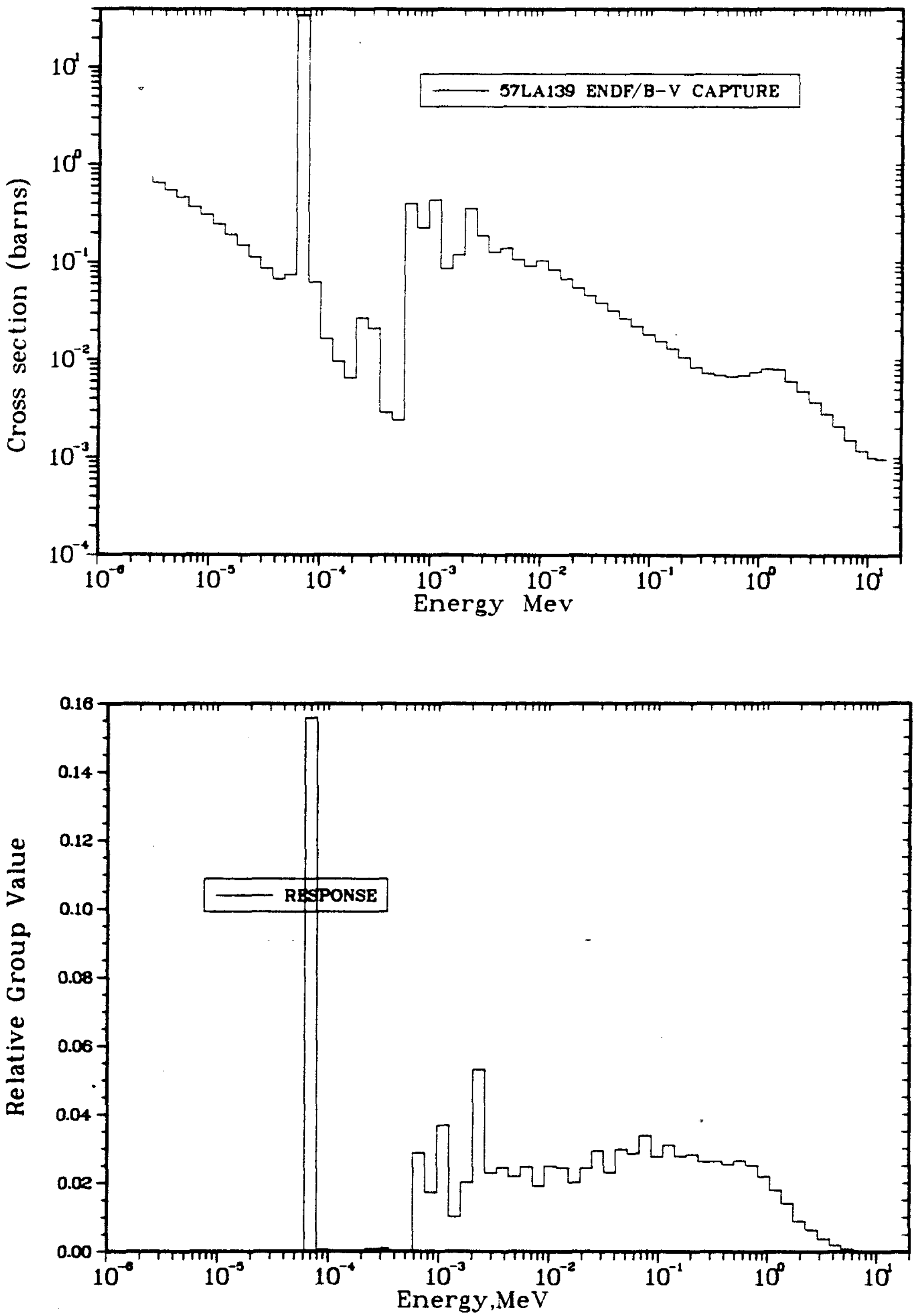

Figure B-18. ENDF/B-V cross section and response in CFRMF for $^{139}La(n,\gamma)$.

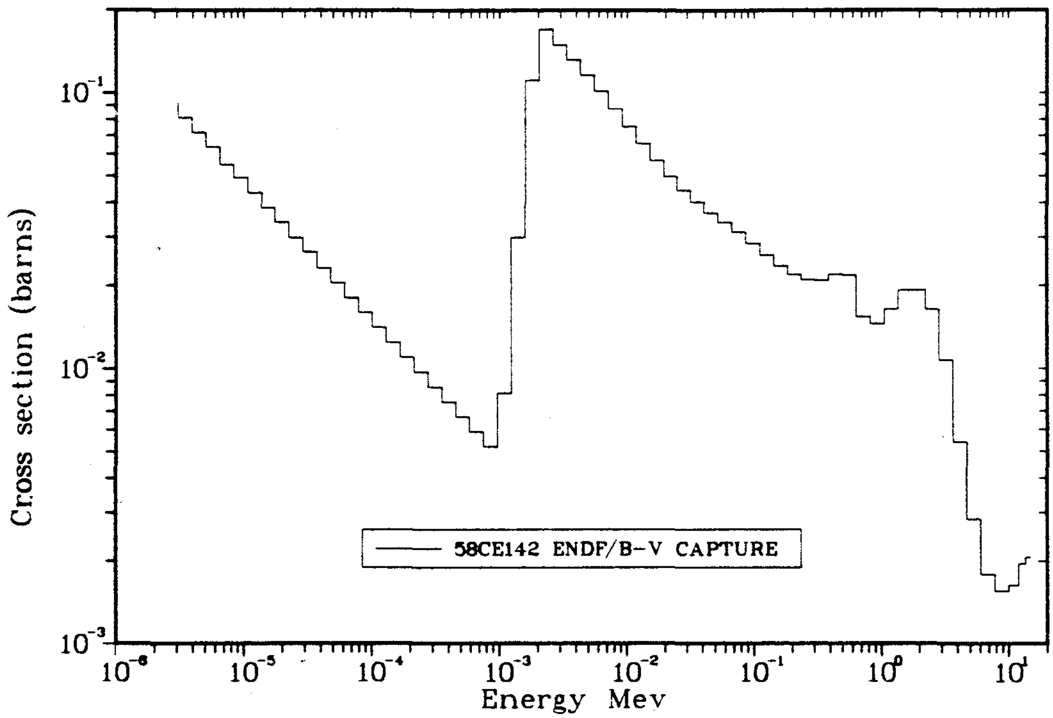

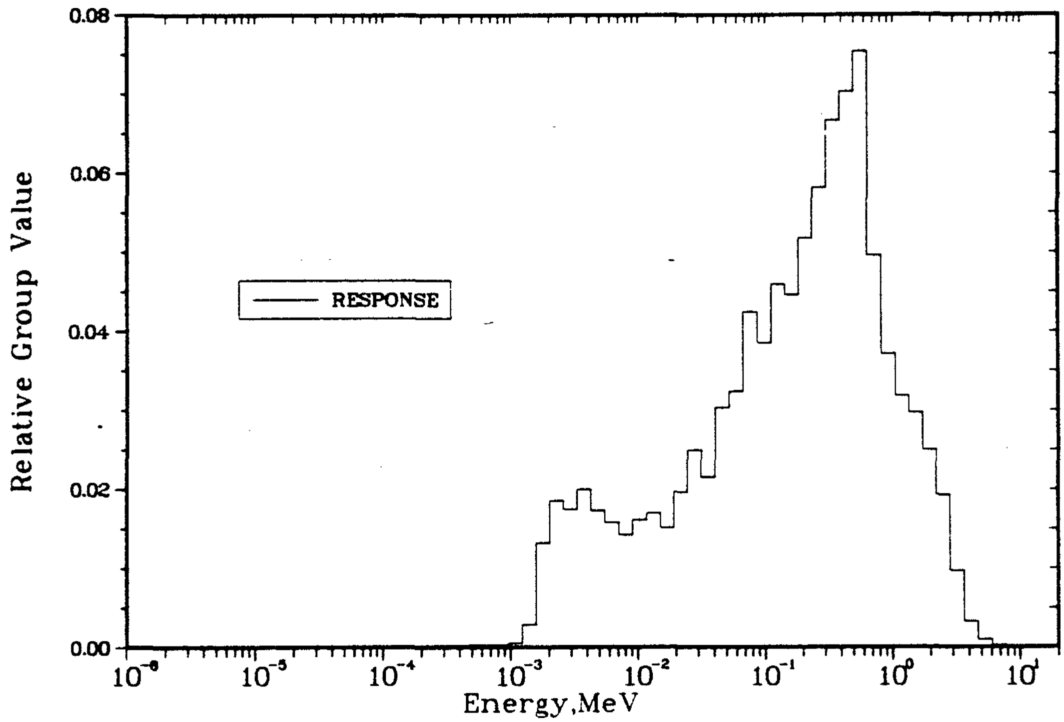

Figure B-19. ENDF/B-V cross section and response in CFRMF for $^{142}Ce(n,\gamma)$.

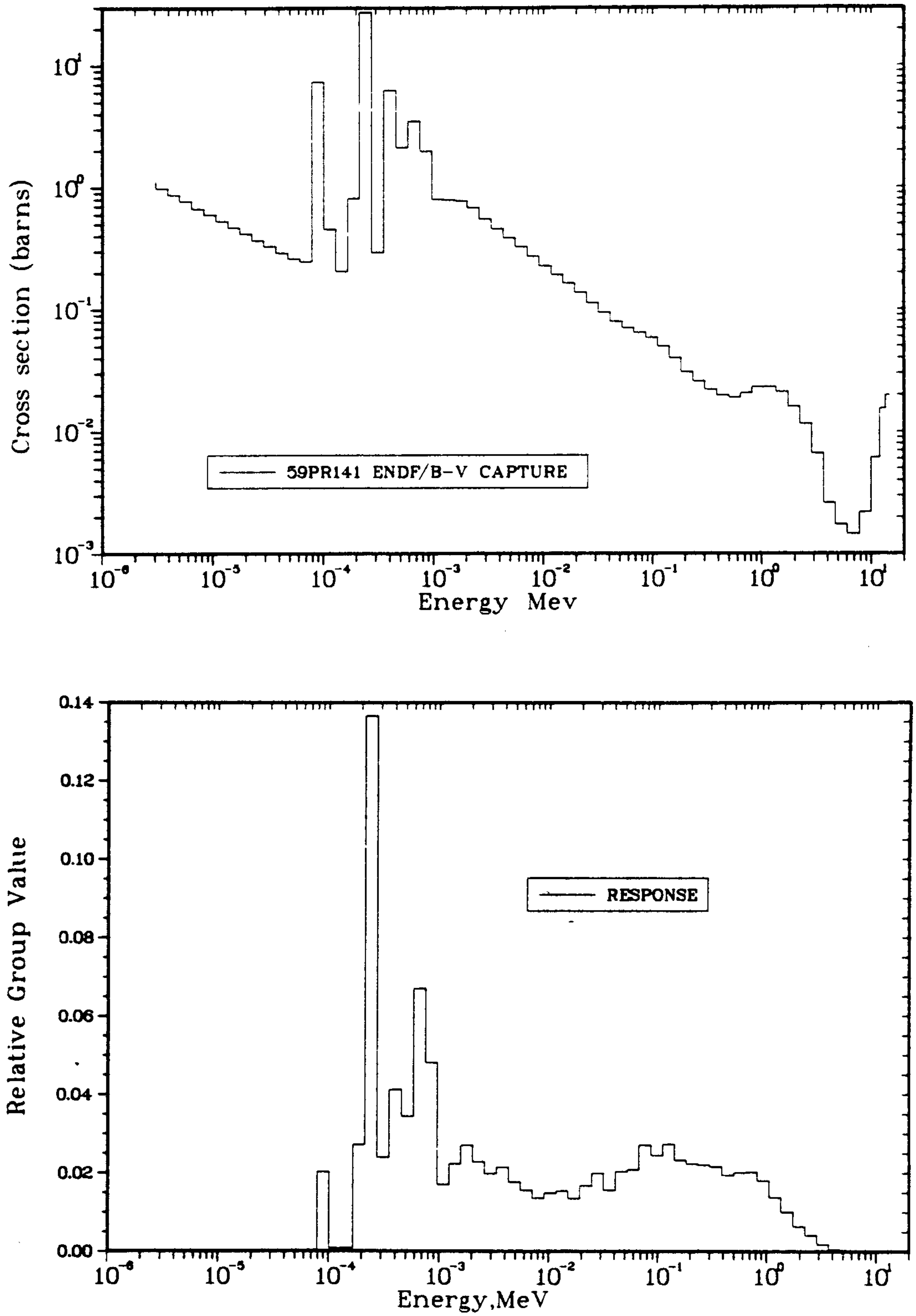

Figure B-20. ENDF/B-V cross section and response in CFRMF for $^{141}Pr(n,\gamma)$.

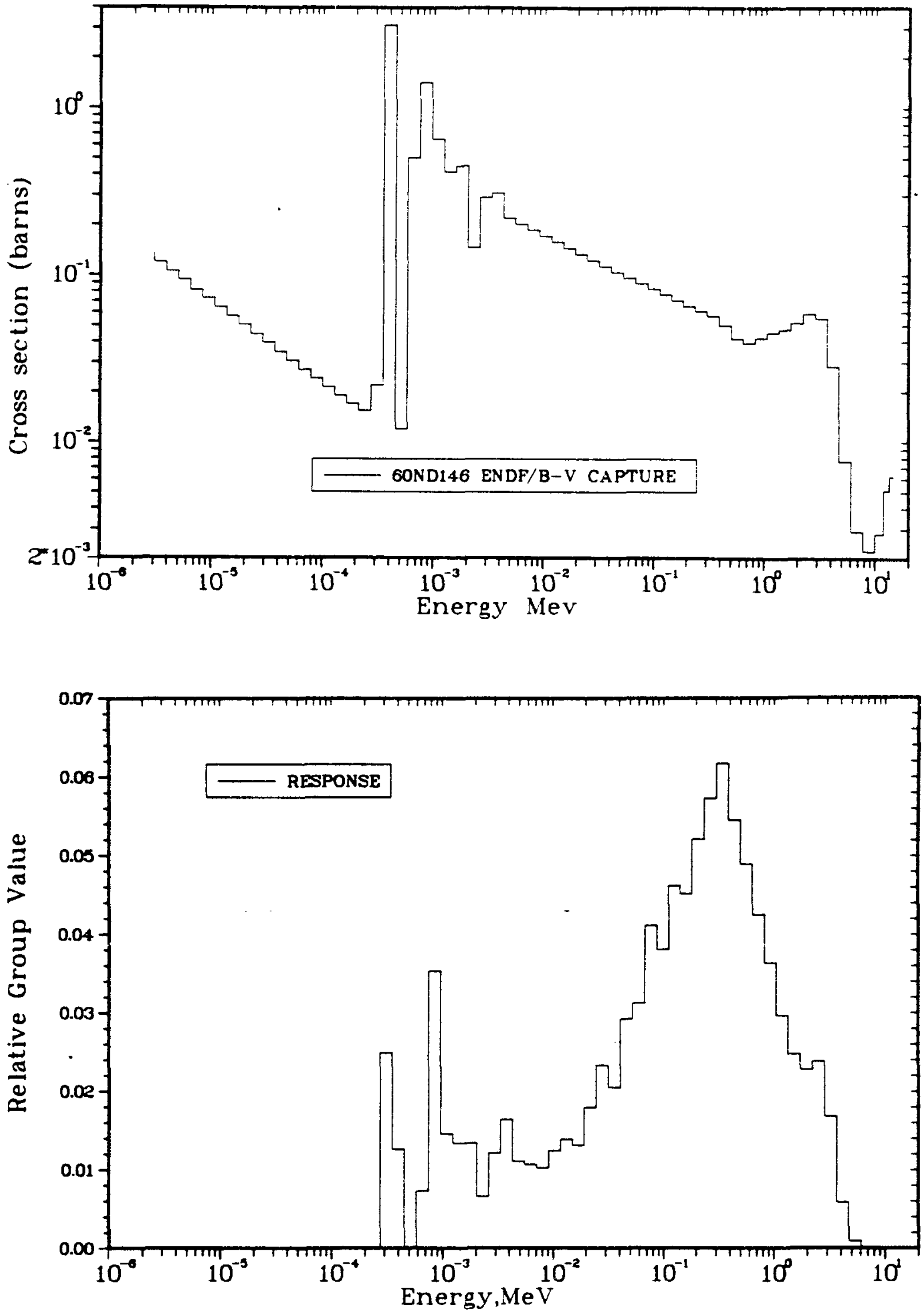

Figure B-21. ENDF/B-V cross section and response in CFRMF for $^{146}Nd(n,\gamma)$.

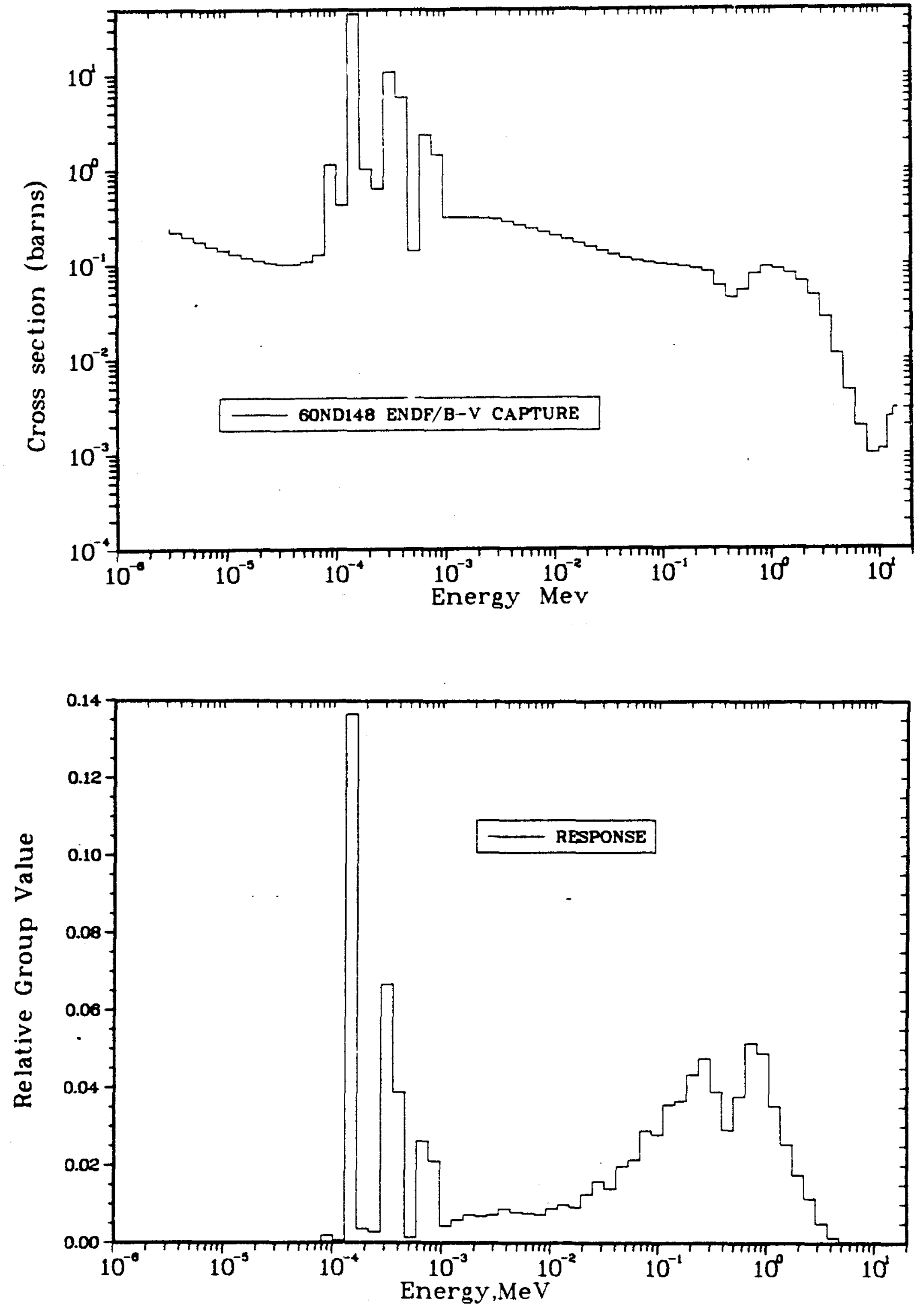

Figure B-22. ENDF/B-V cross section and response in CFRMF for $^{148}Nd(n,\gamma)$.

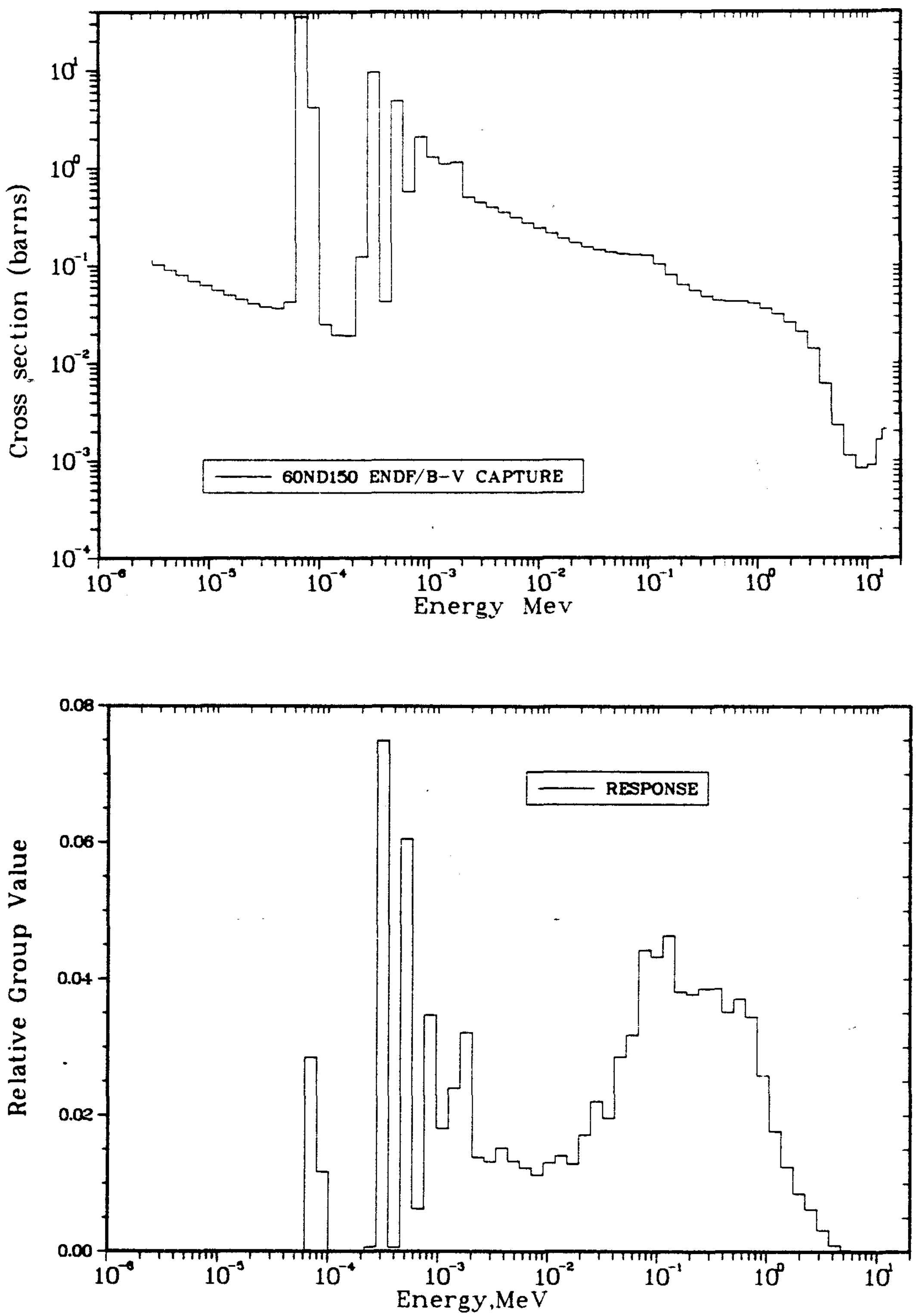

Figure B-23. ENDF/B-V cross section and response in CFRMF for $^{150}Nd(n,\gamma)$.

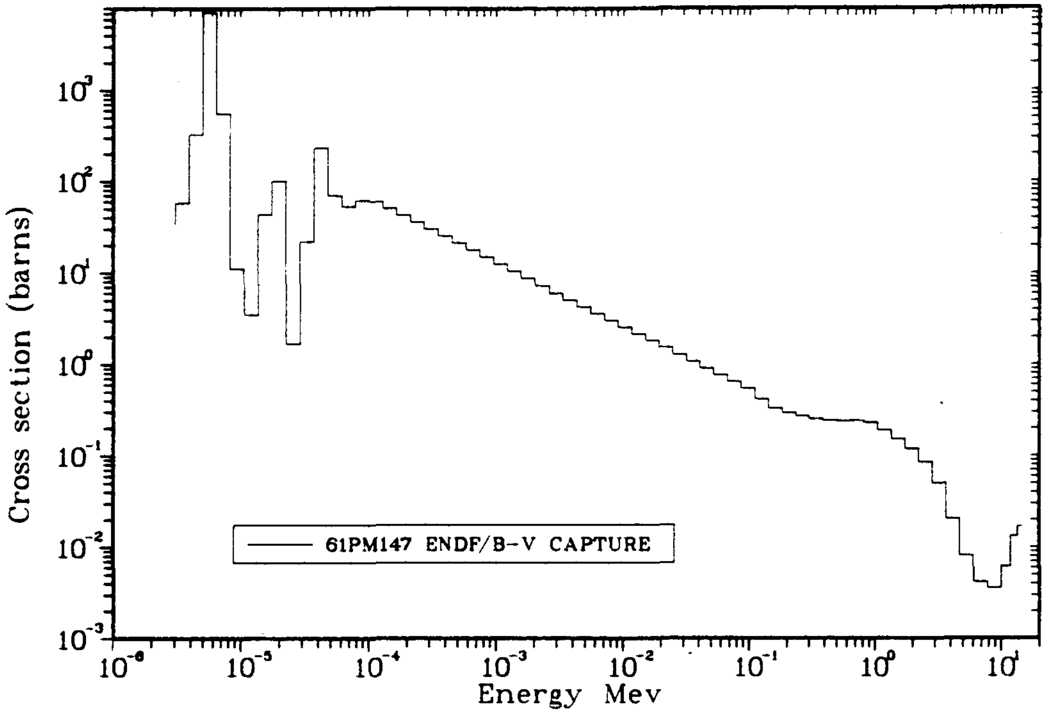

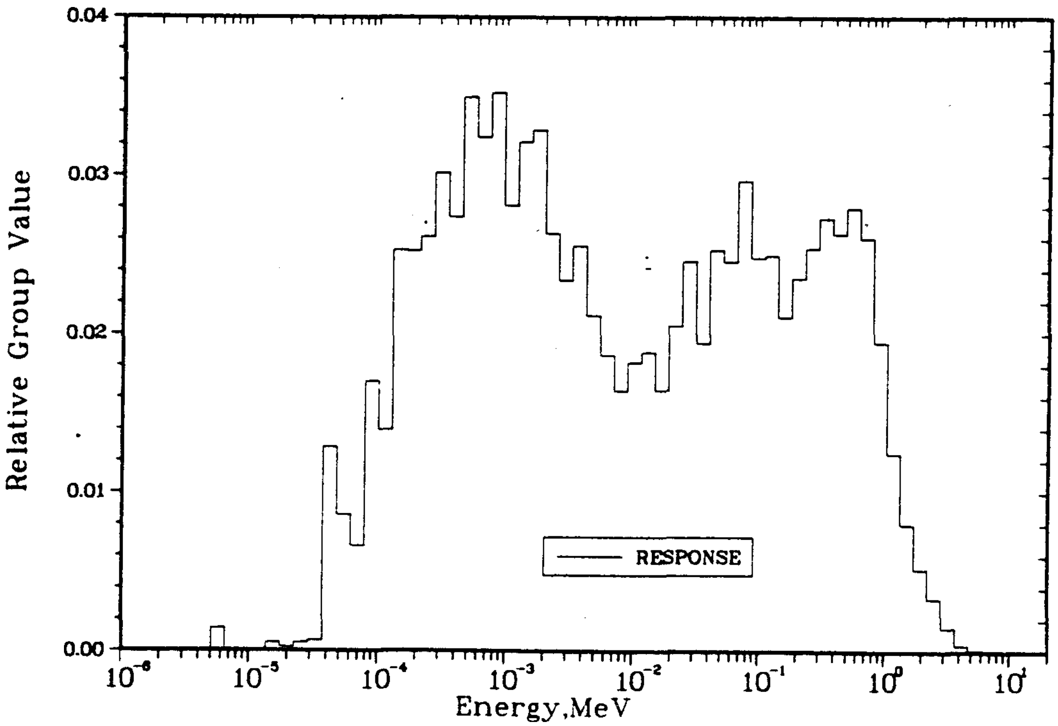

Figure B-24. ENDF/B-V cross section and response in CFRMF for $^{147}Pm(n,\gamma)$.

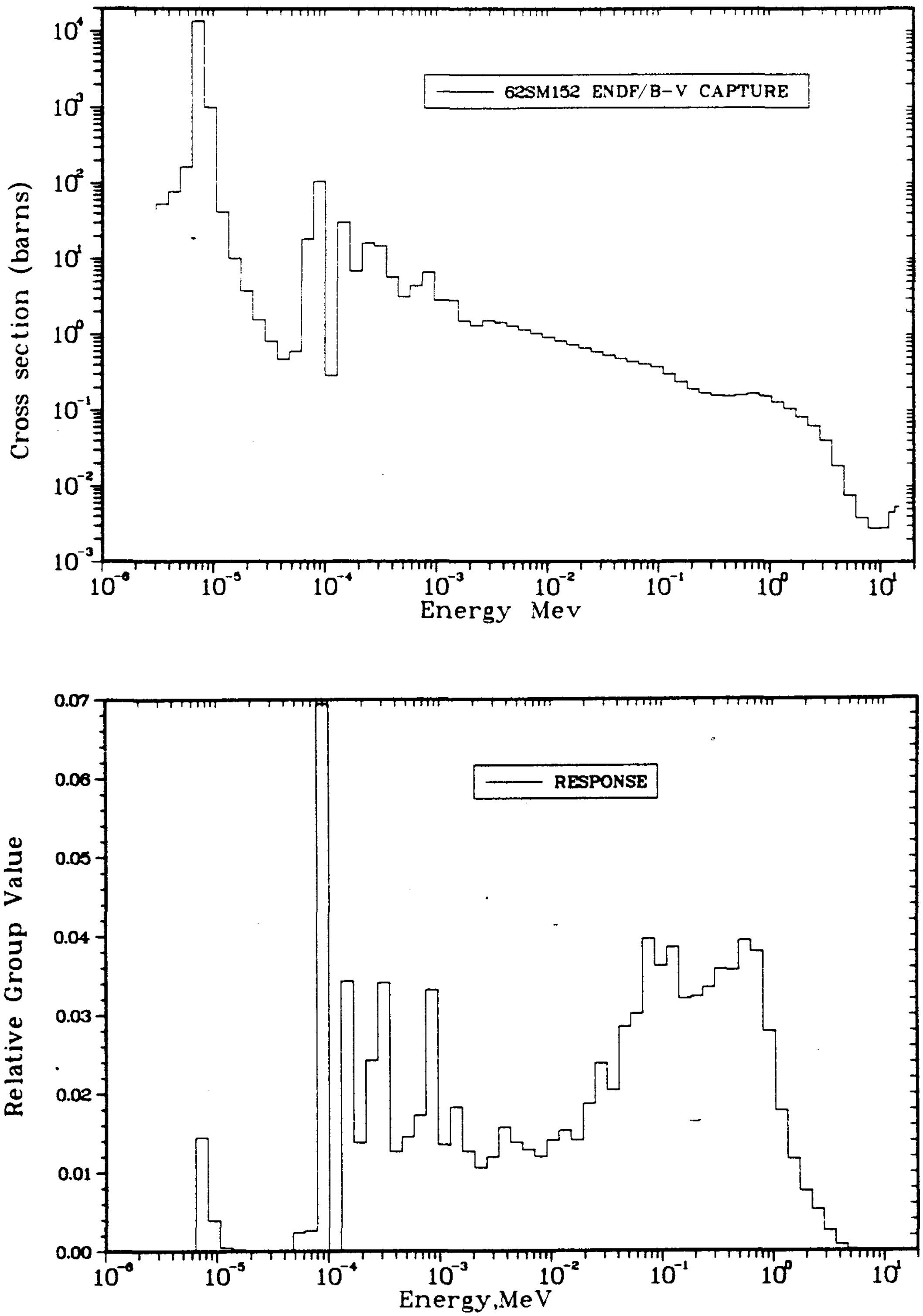

Figure B-25. ENDF/B-V cross section and response in CFRMF for $^{152}Sm(n,\gamma)$.

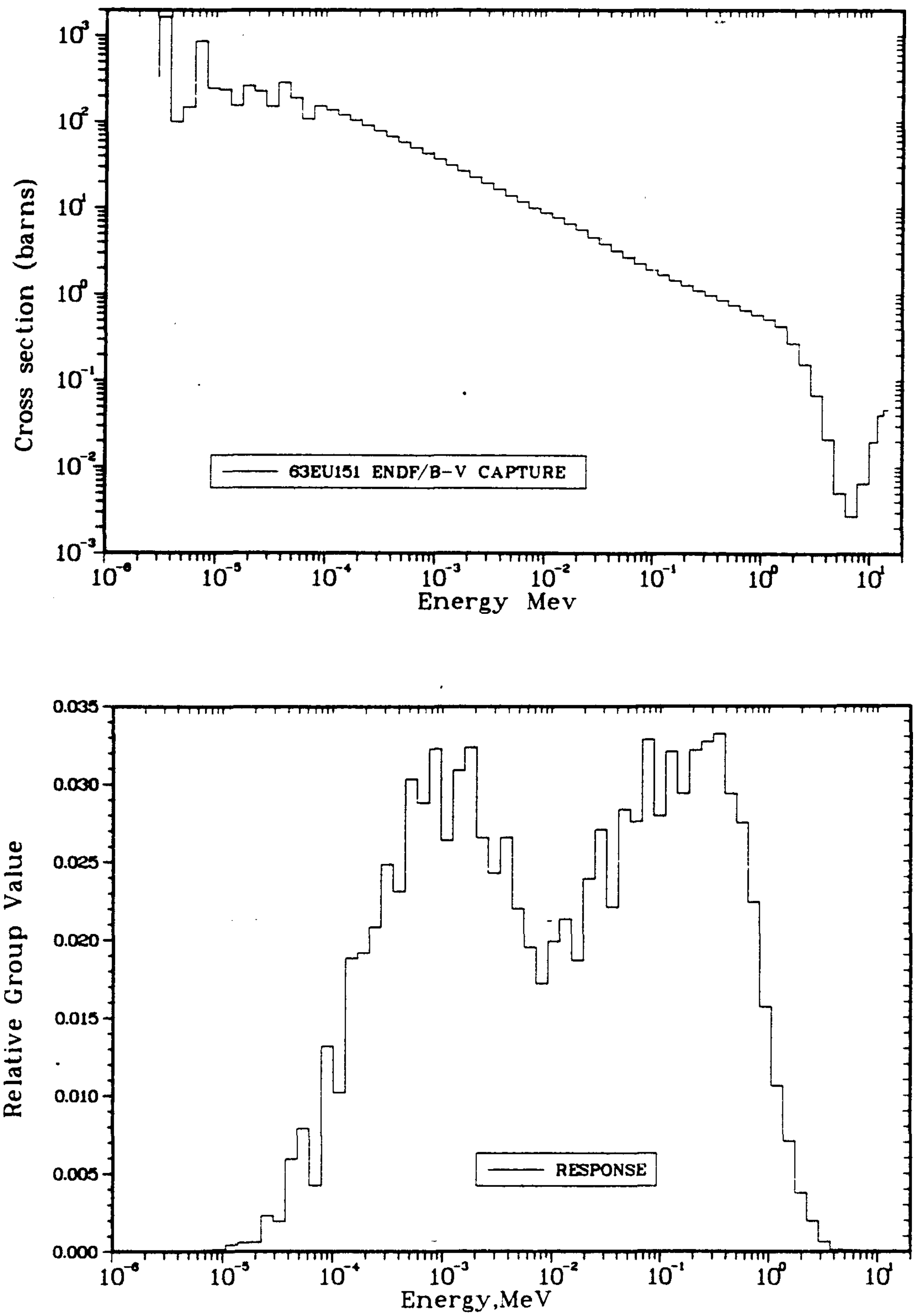

Figure B-26. ENDF/B-V cross section and response in CFRMF for $^{151}Eu(n,\gamma)$.

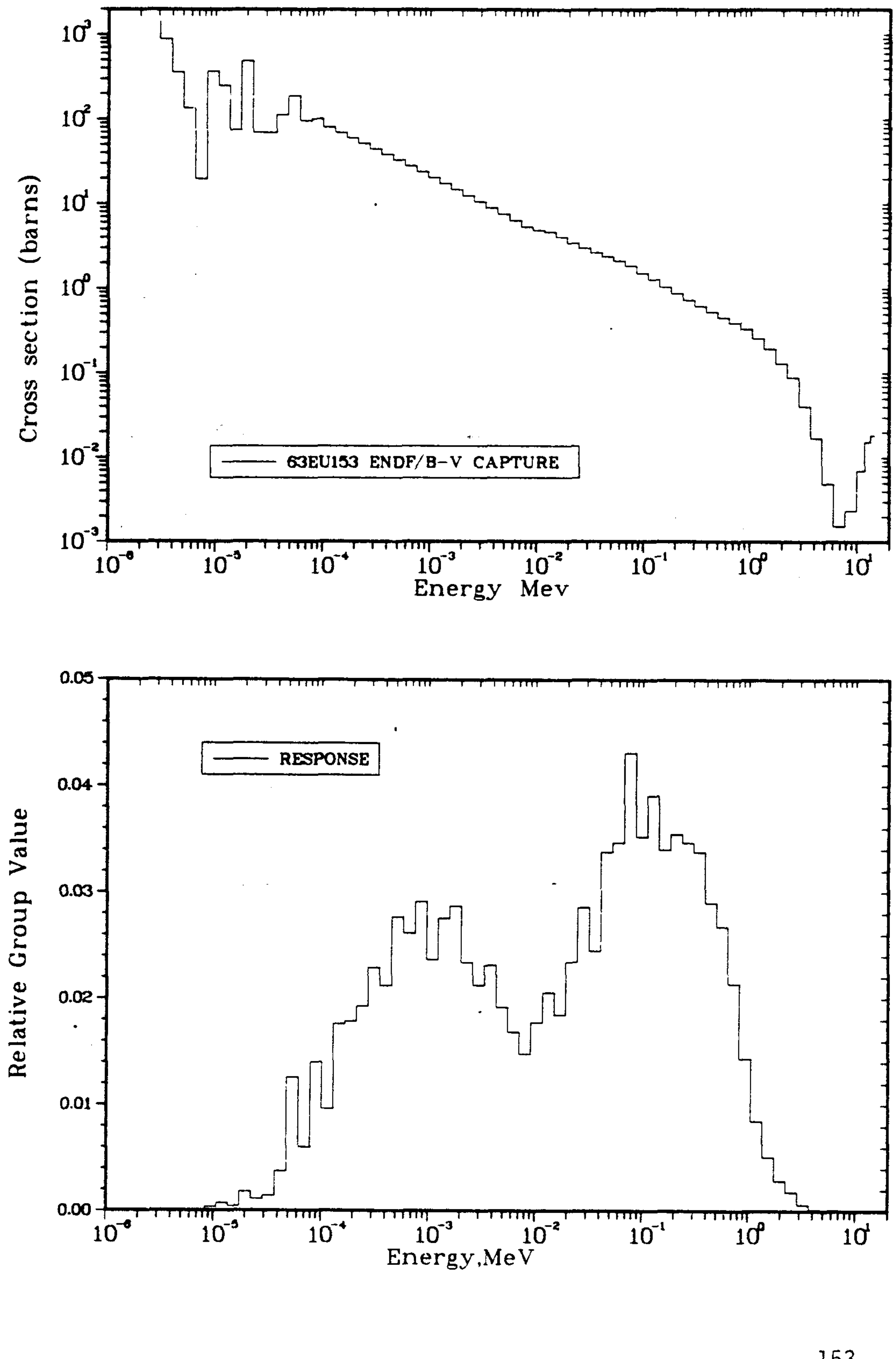

Figure B-27. ENDF/B-V cross section and response in CFRMF for $^{153}Eu(n,\gamma)$.

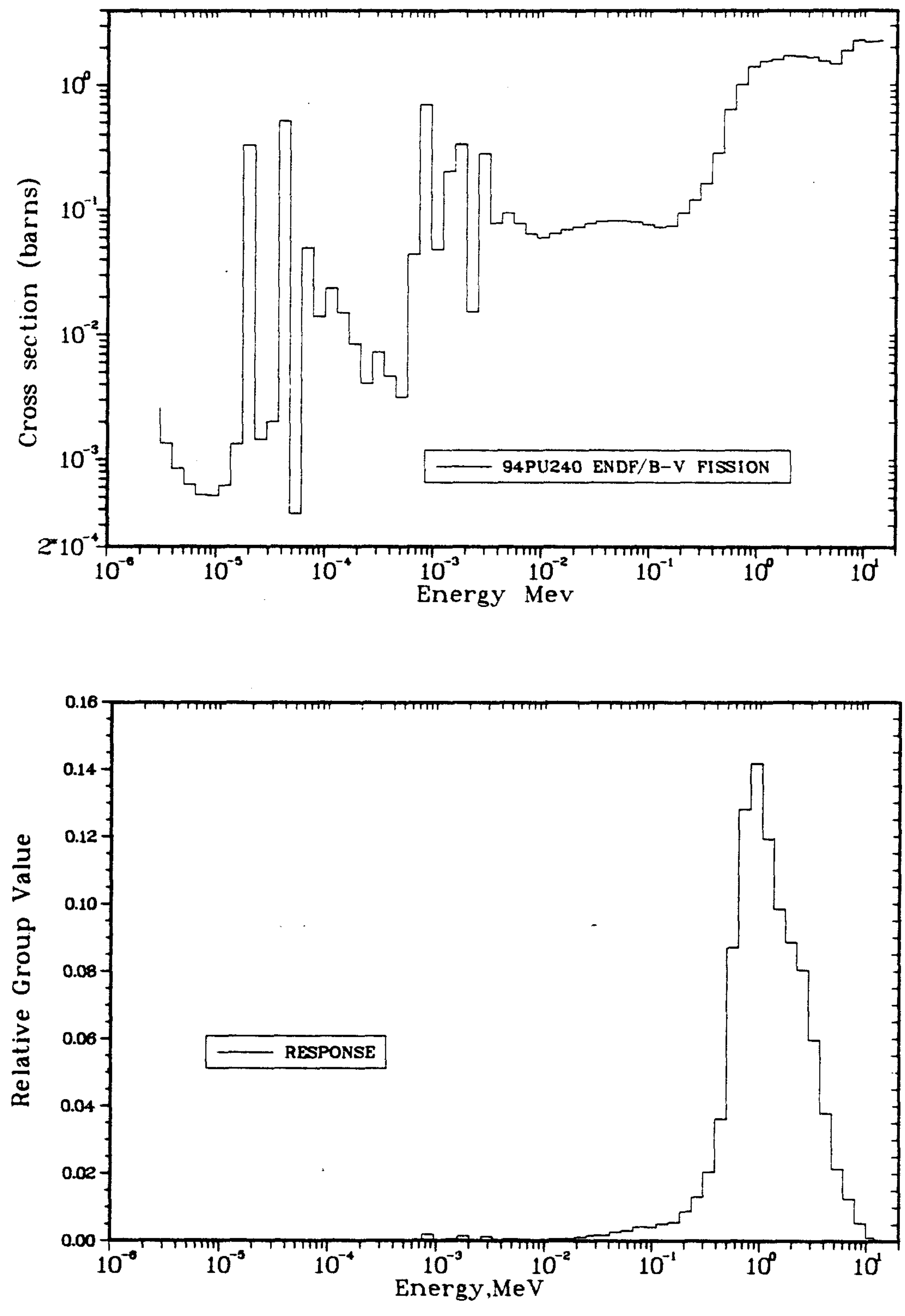

Figure B-28. ENDF/B-V cross section and response in CFRMF for $^{240}Pu(n,f)$.

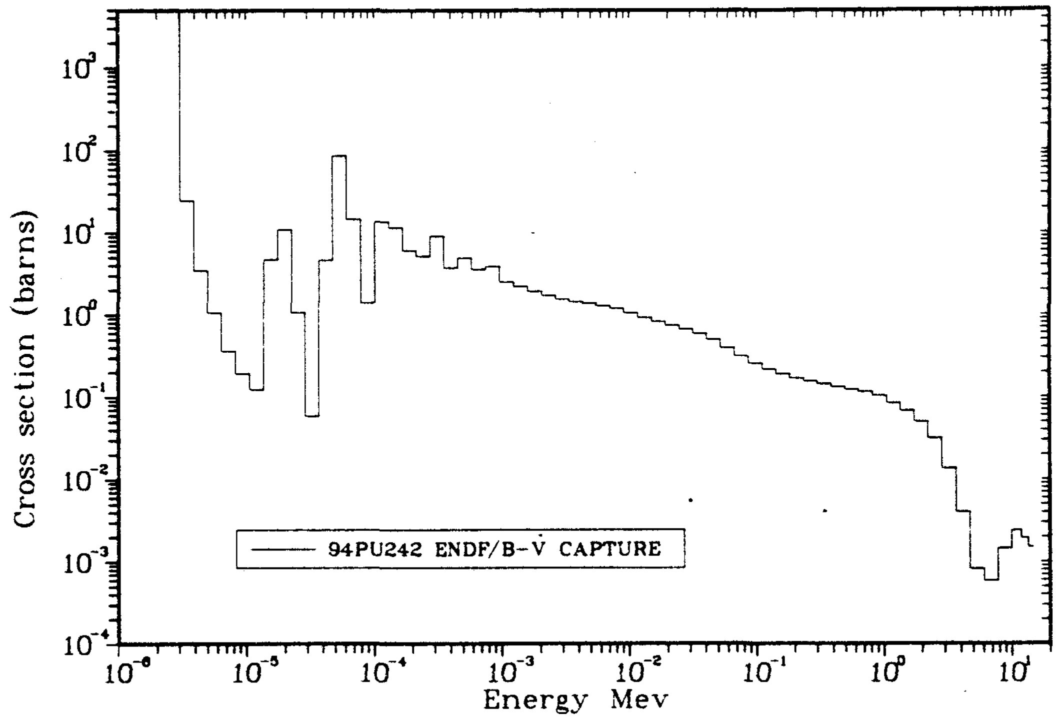

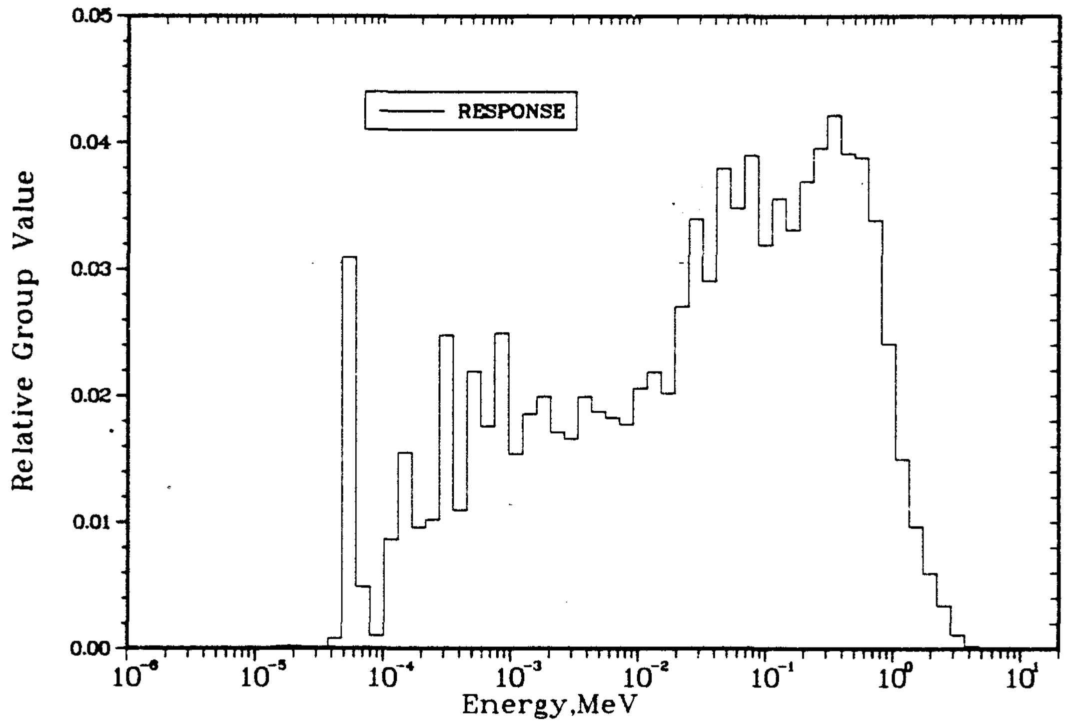

Figure B-29. ENDF/B-V cross section and response in CFRMF for $^{242}Pu(n,\gamma)$.

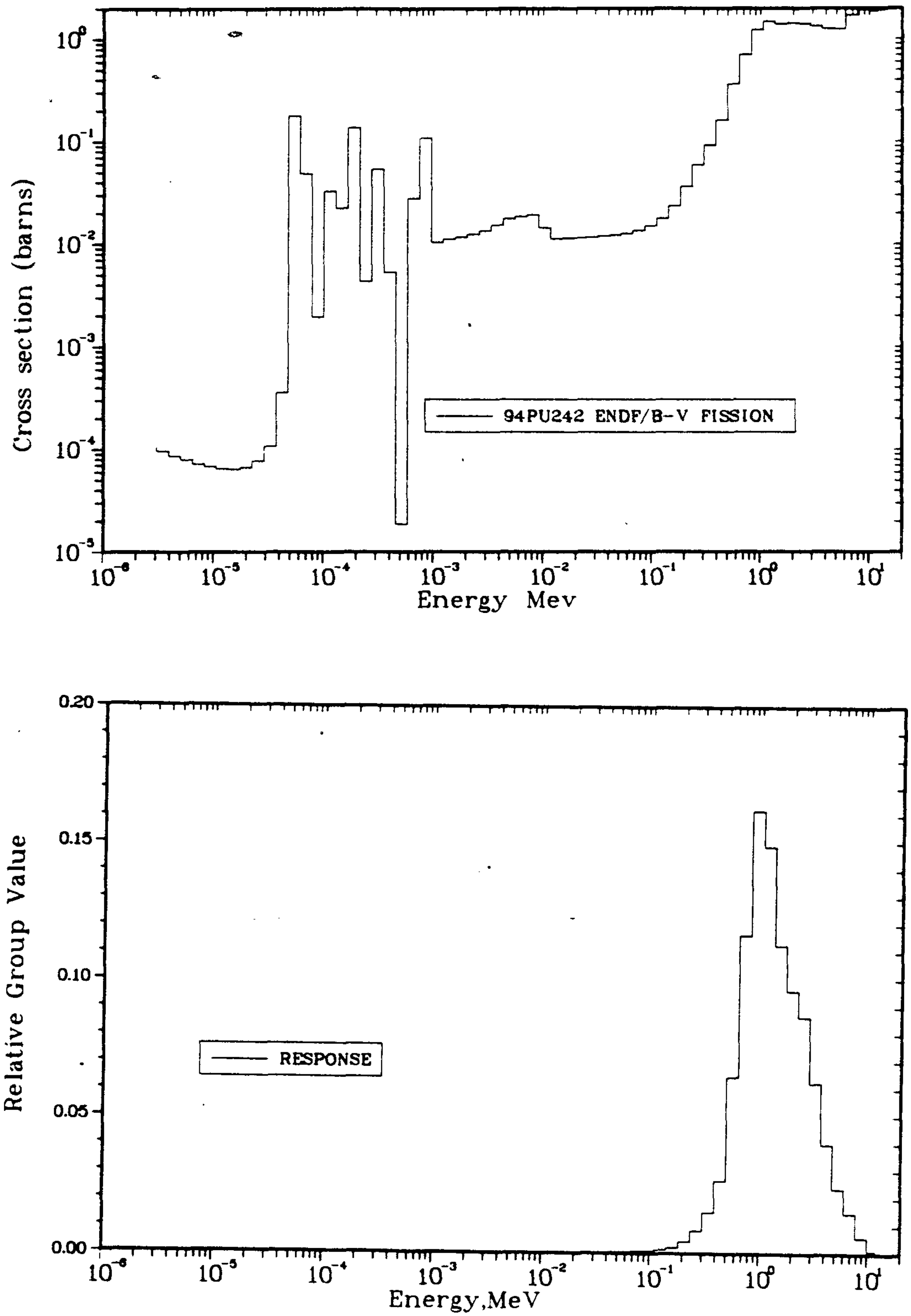

Figure B-30. ENDF/B-V cross section and response in CFRMF for $^{242}Pu(n,f)$.

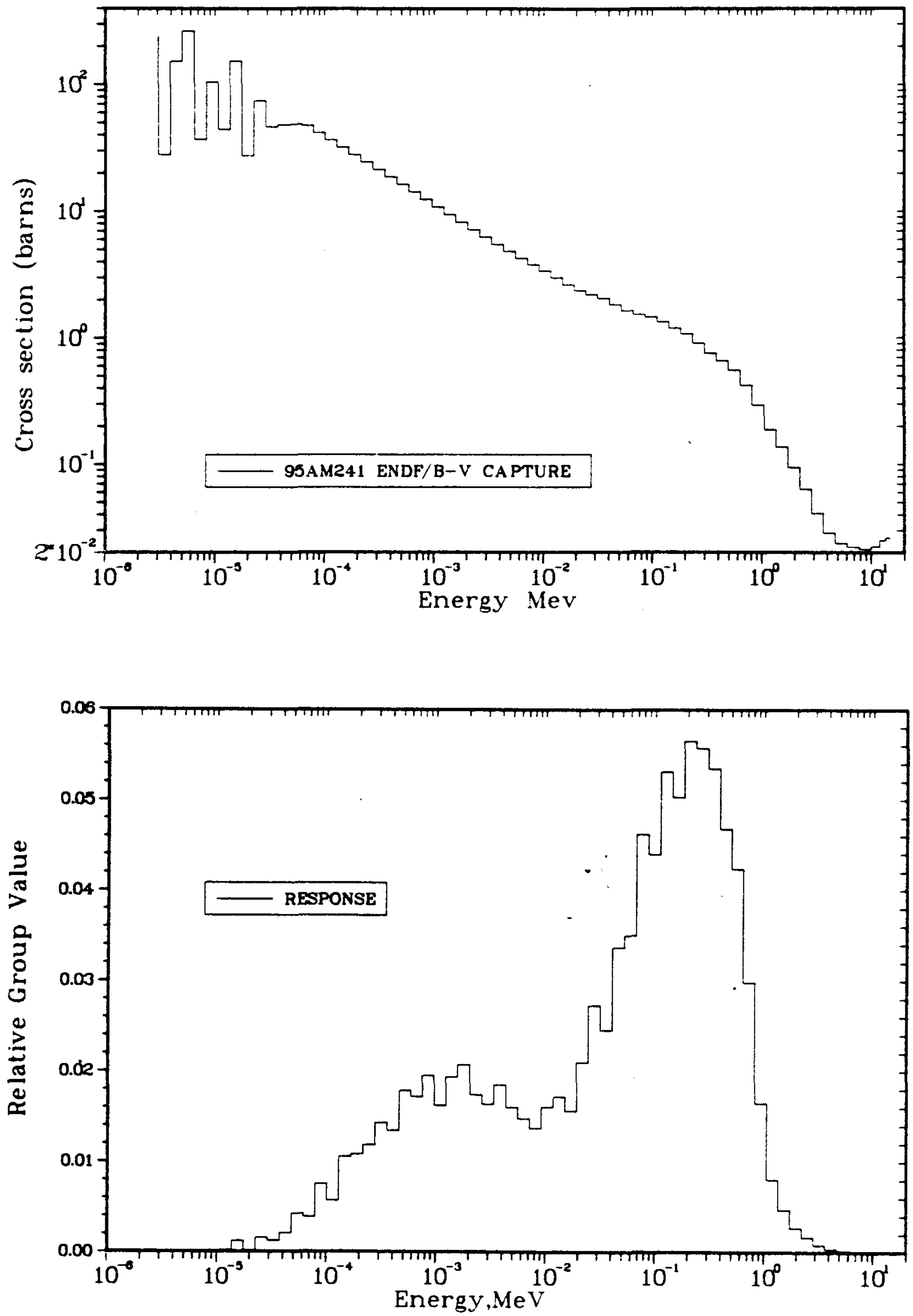

Figure B-31. ENDF/B-V cross section and response in CFRMF for $^{241}Am(n,\gamma)$.

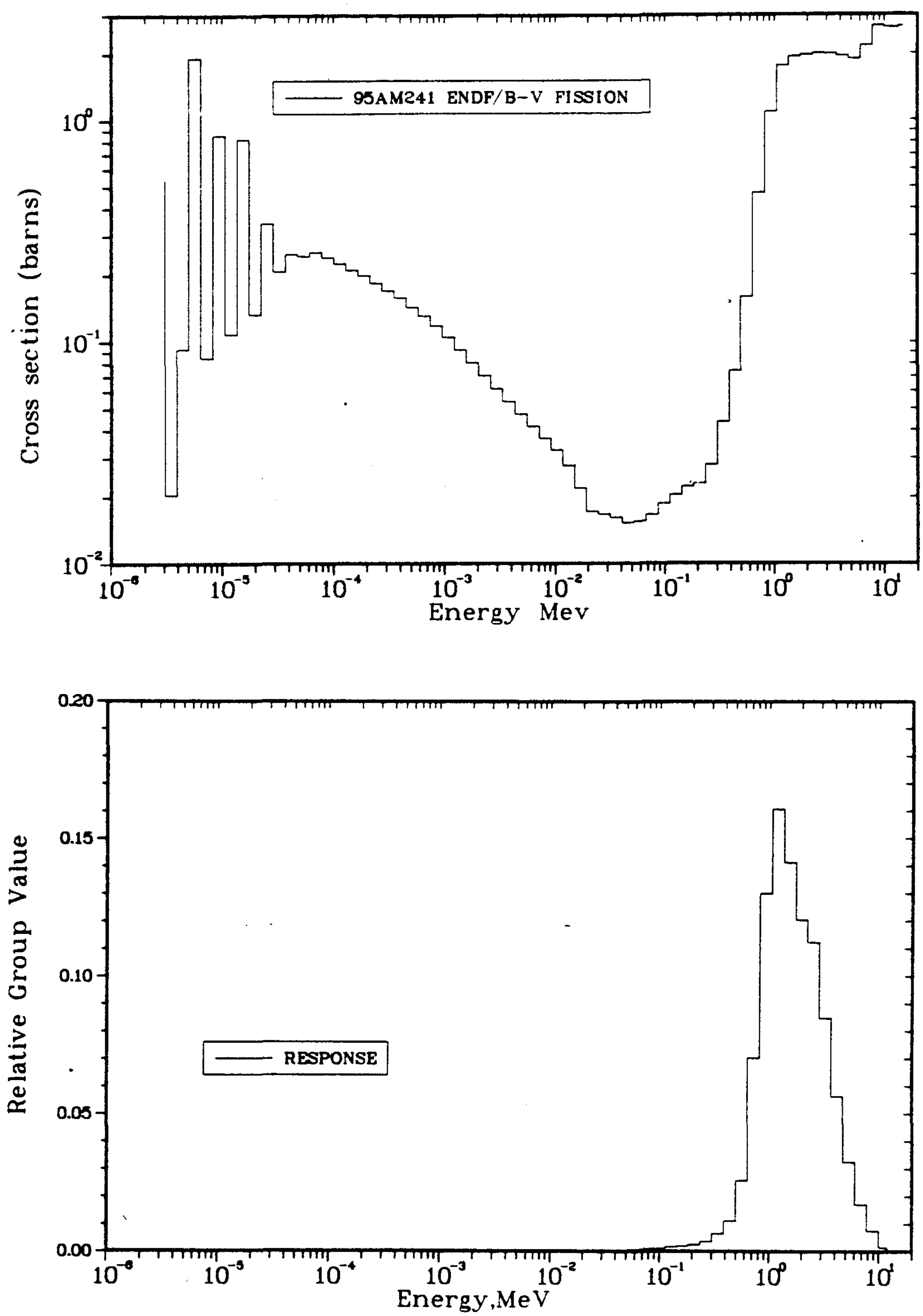

Figure B-32. ENDF/B-V cross section and response in CFRMF for ^{241}Am(n,f).

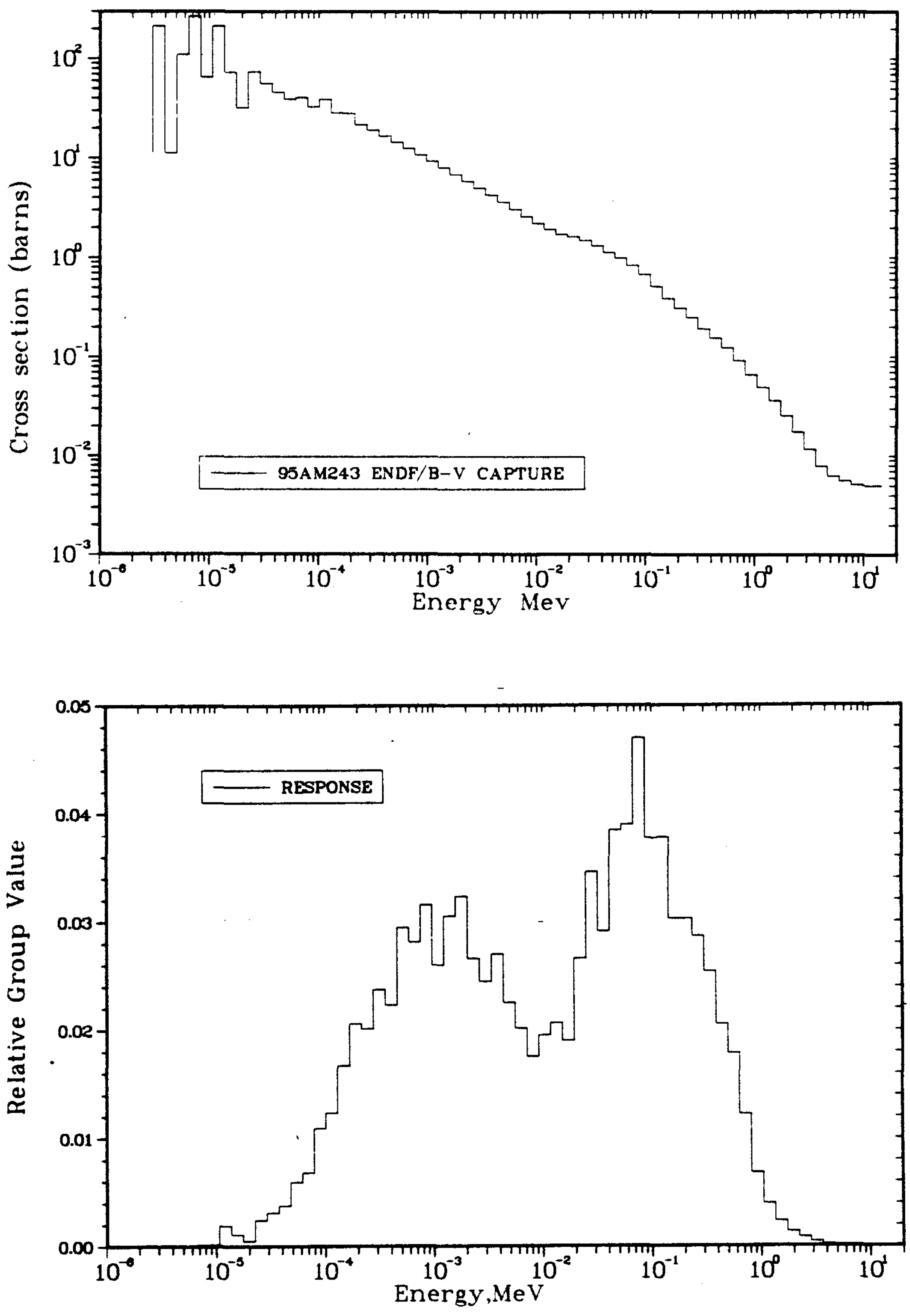

Figure B-33. ENDF/B-V cross section and response in CFRMF for $^{243}Am(n,\gamma)$.

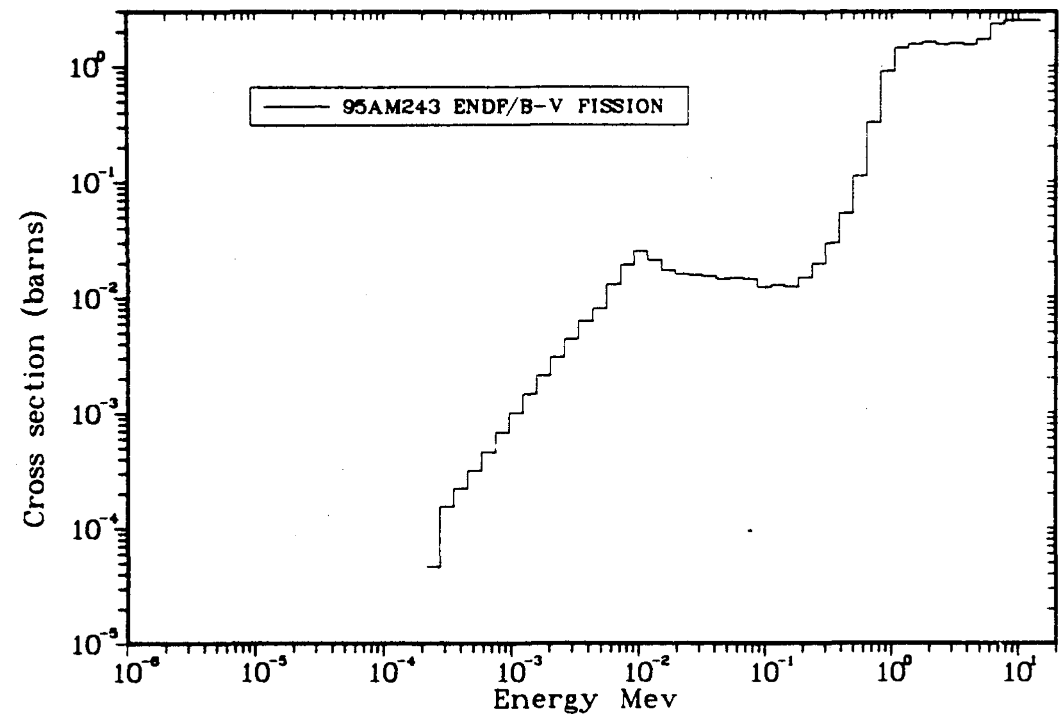

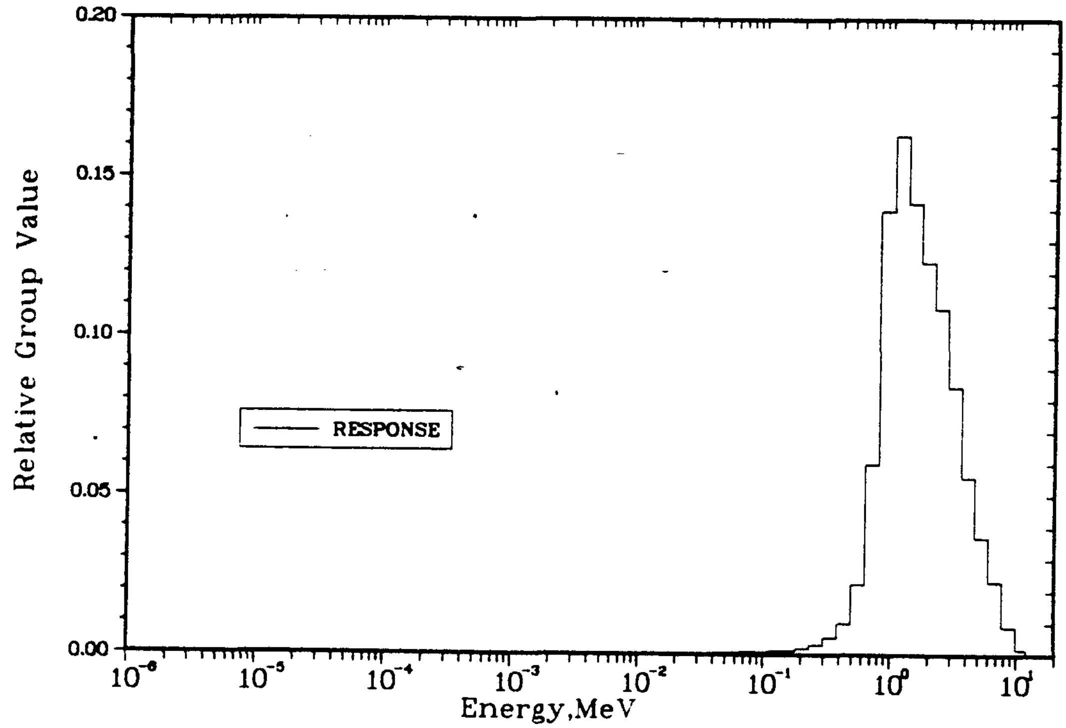

Figure B-34. ENDF/B-V cross section and response in CFRMF for $^{243}Am(n,f)$.

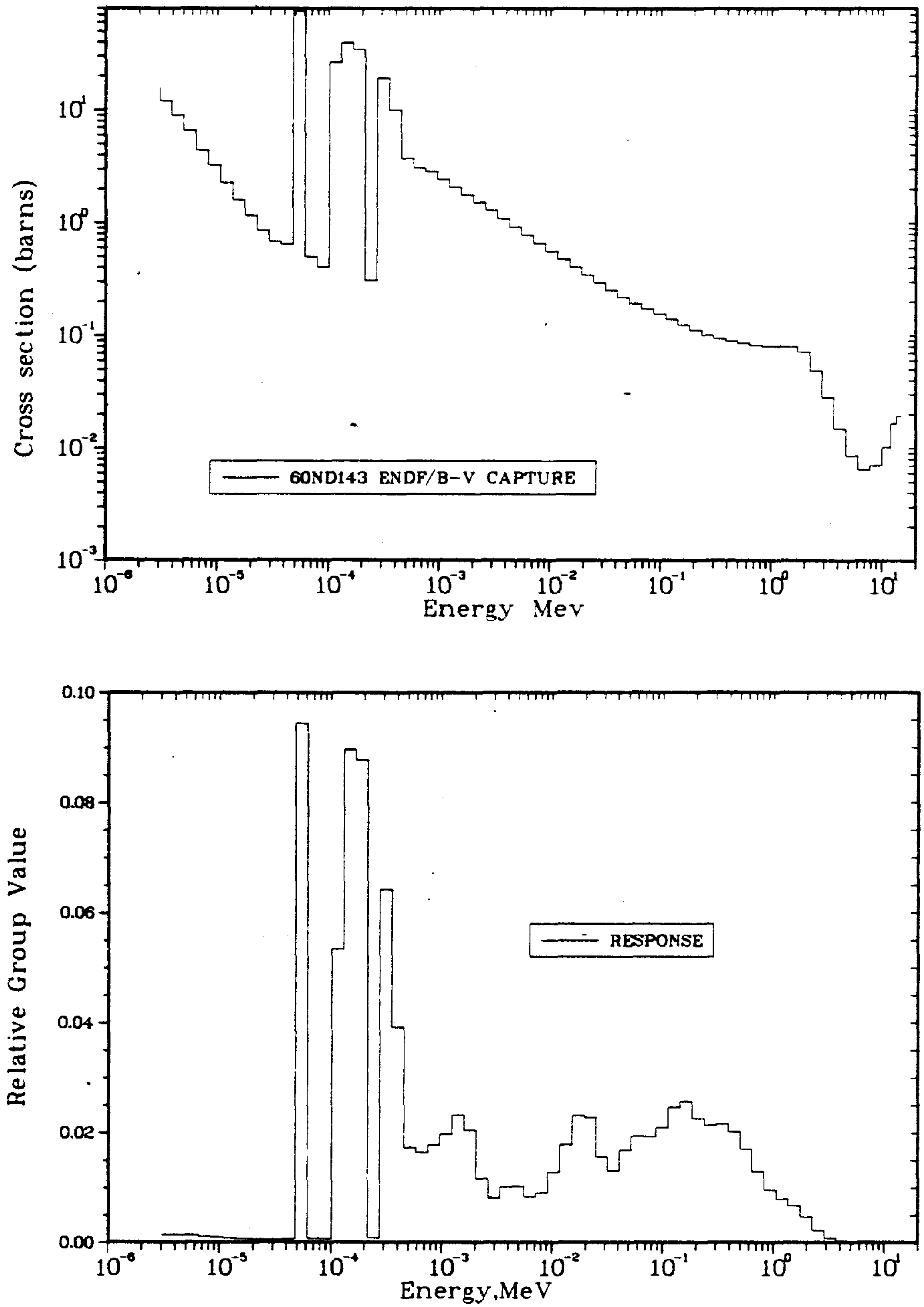

Figure B-35. ENDF/B-V cross section and response in EBR-II midplane for $^{143}Nd(n,\gamma)$.

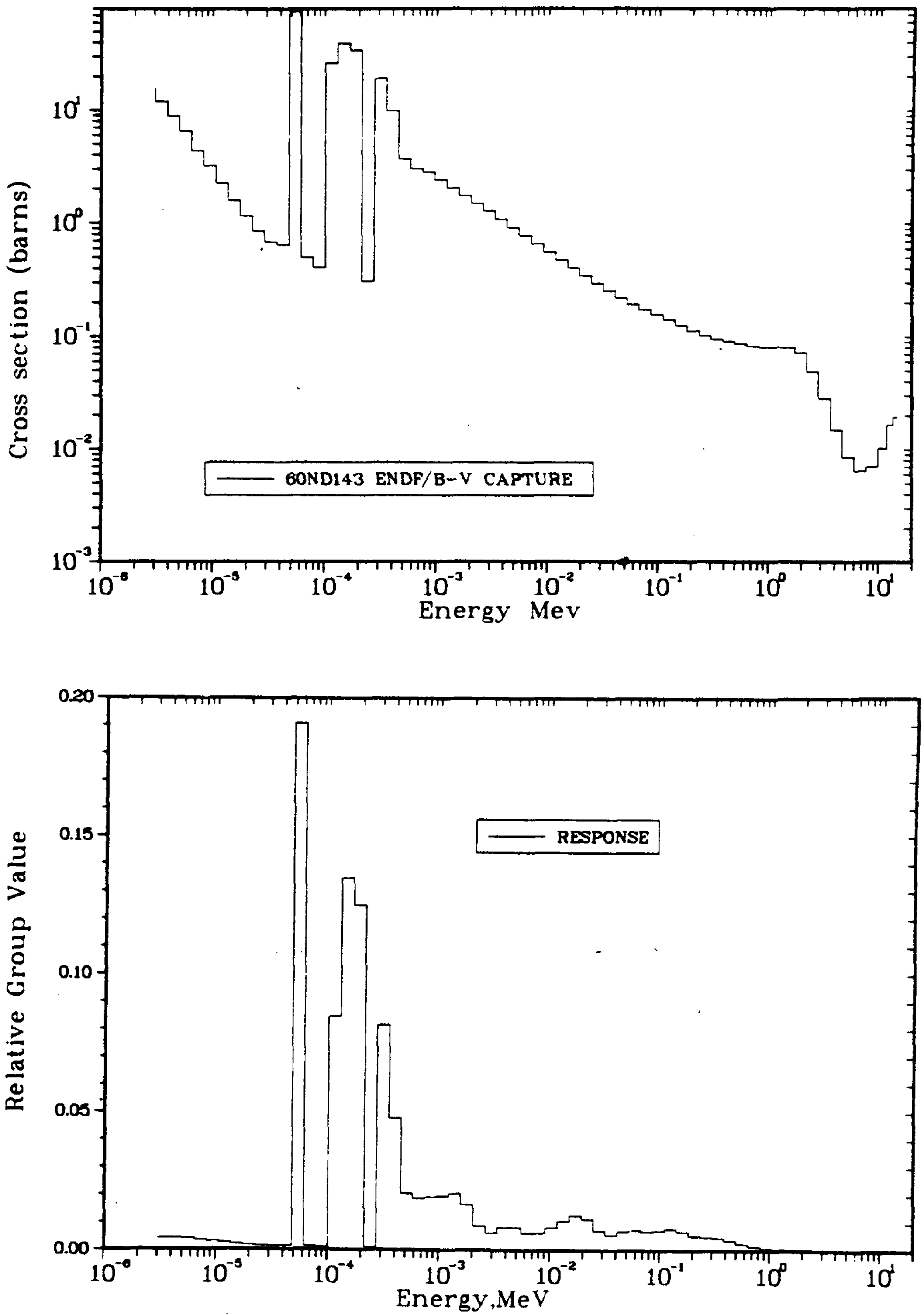

Figure B-36. ENDF/B-V cross section and response in EBR-II reflector for $^{143}Nd(n,\gamma)$.

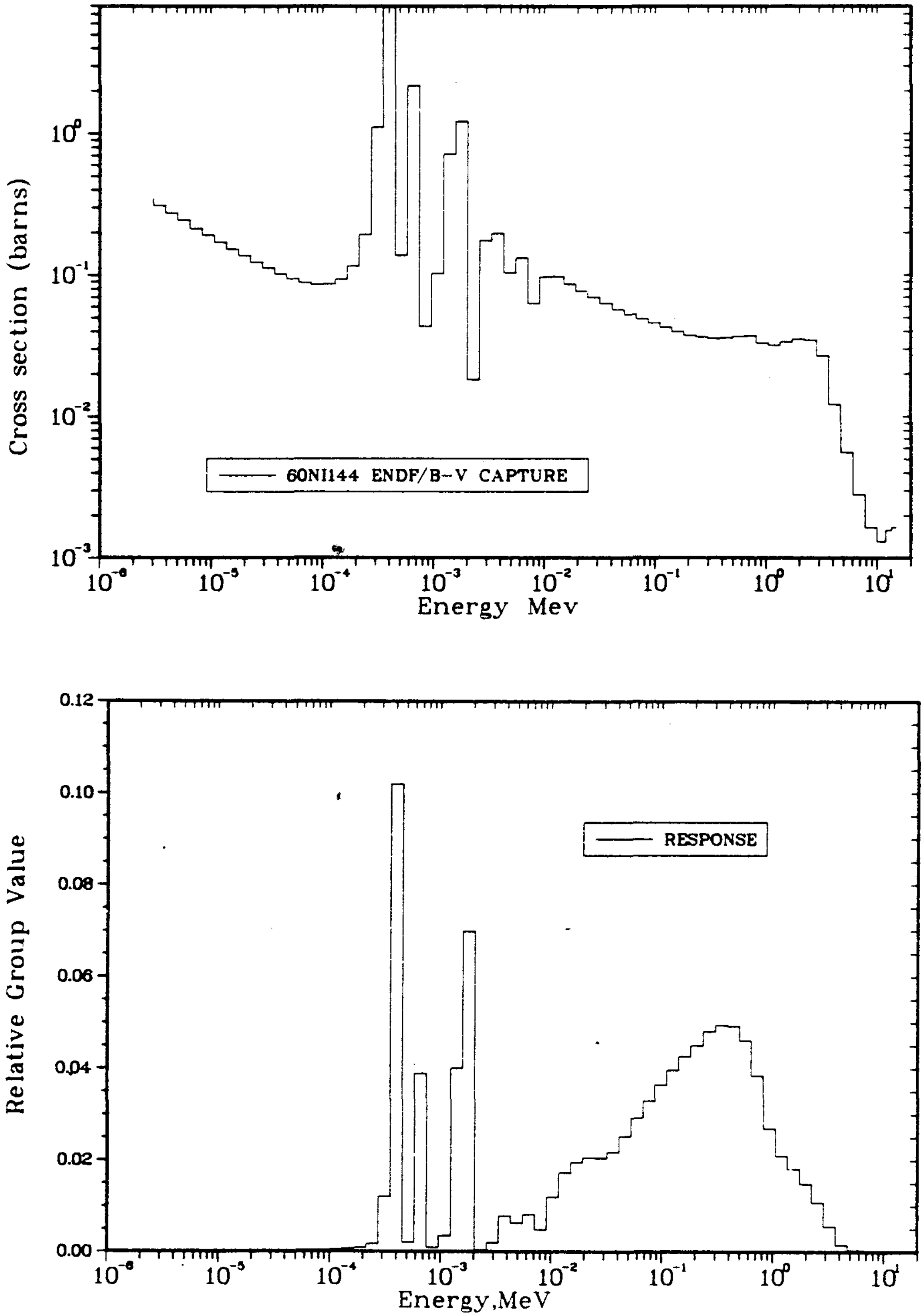

Figure B-37. ENDF/B-V cross section and response in EBR-II midplane for $^{144}Nd(n,\gamma)$.

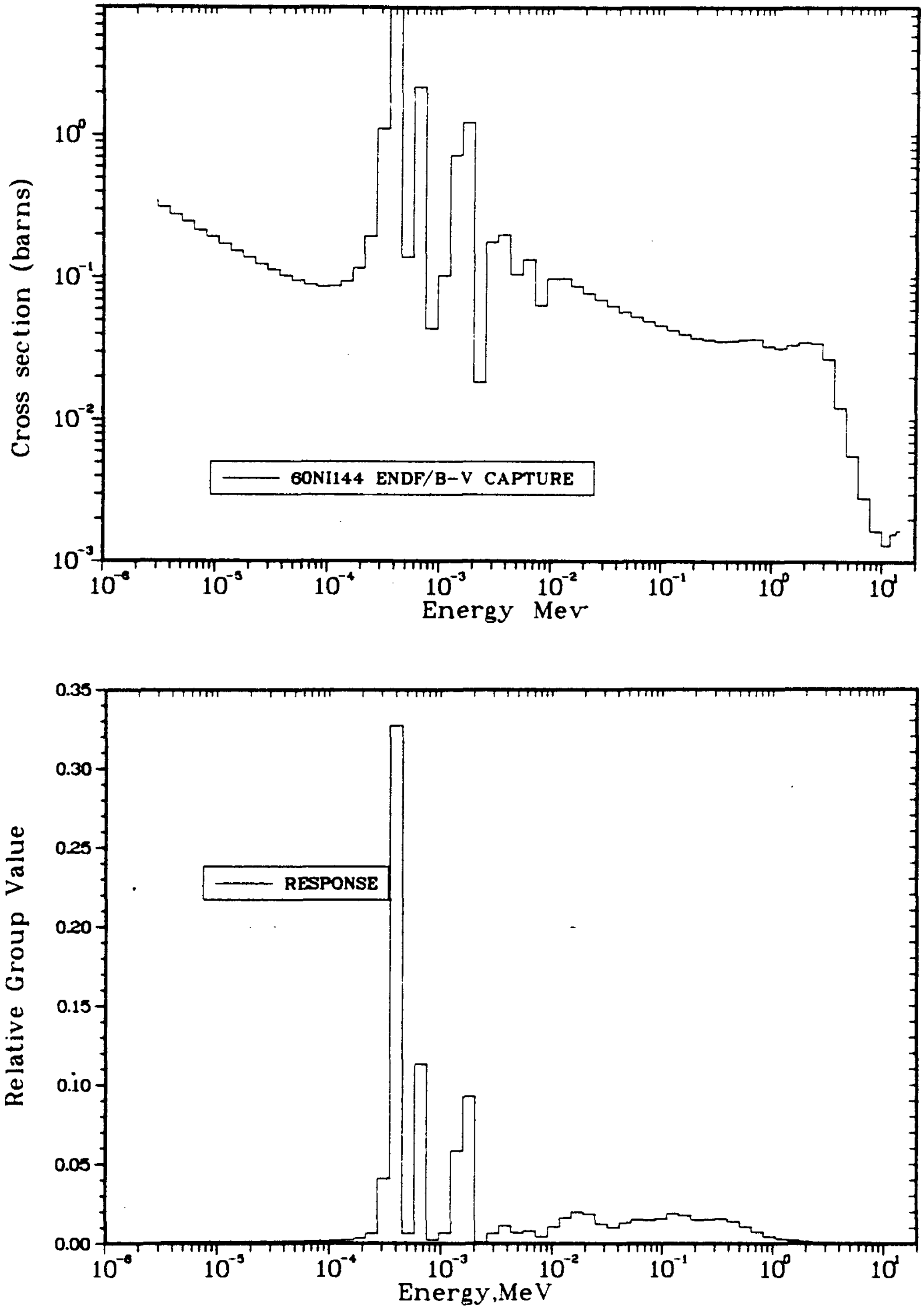

Figure B-38. ENDF/B-V cross section and response in EBR-II reflector for $^{144}Nd(n,\gamma)$.

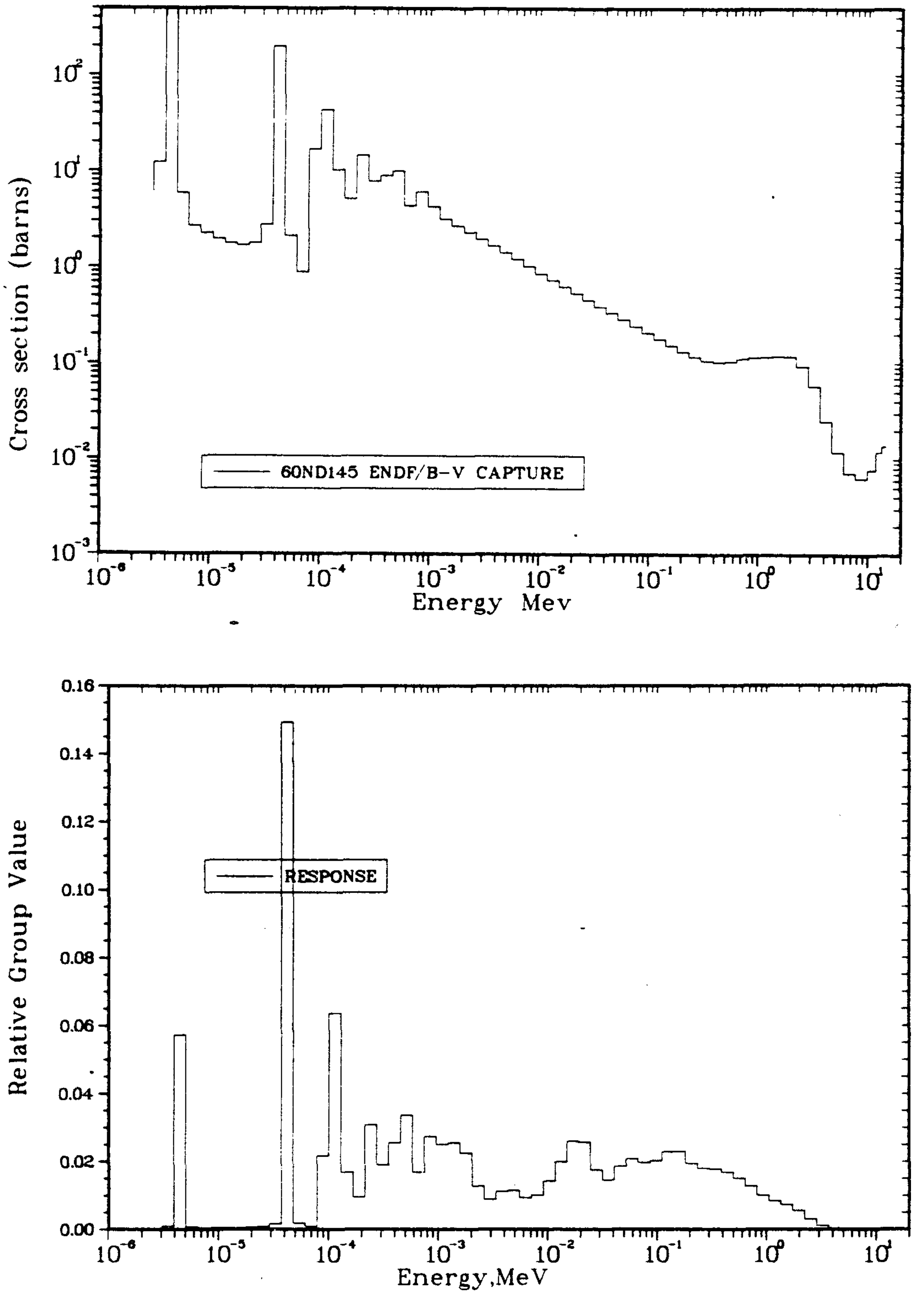

Figure B-39. ENDF/B-V cross section and response in EBR-II midplane for $^{145}Nd(n,\gamma)$.

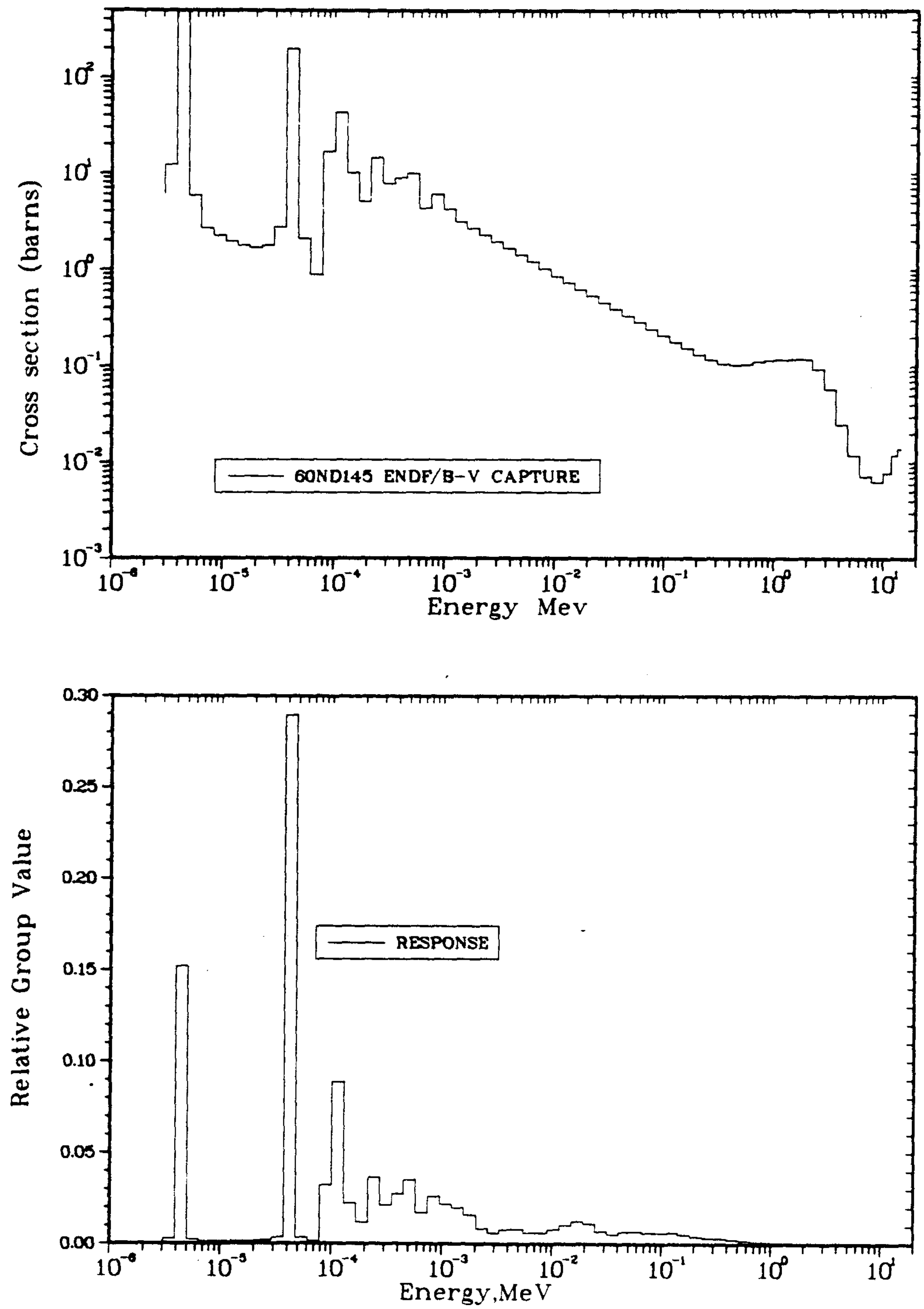

Figure B-40. ENDF/B-V cross section and response in EBR-II reflector for $^{145}Nd(n,\gamma)$.

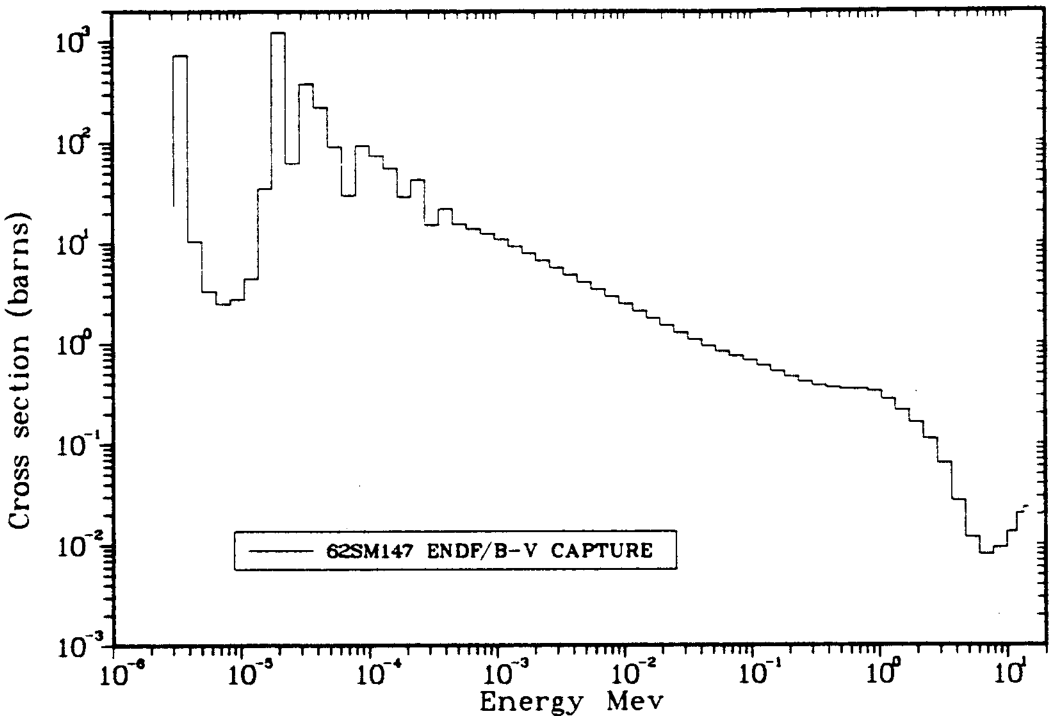

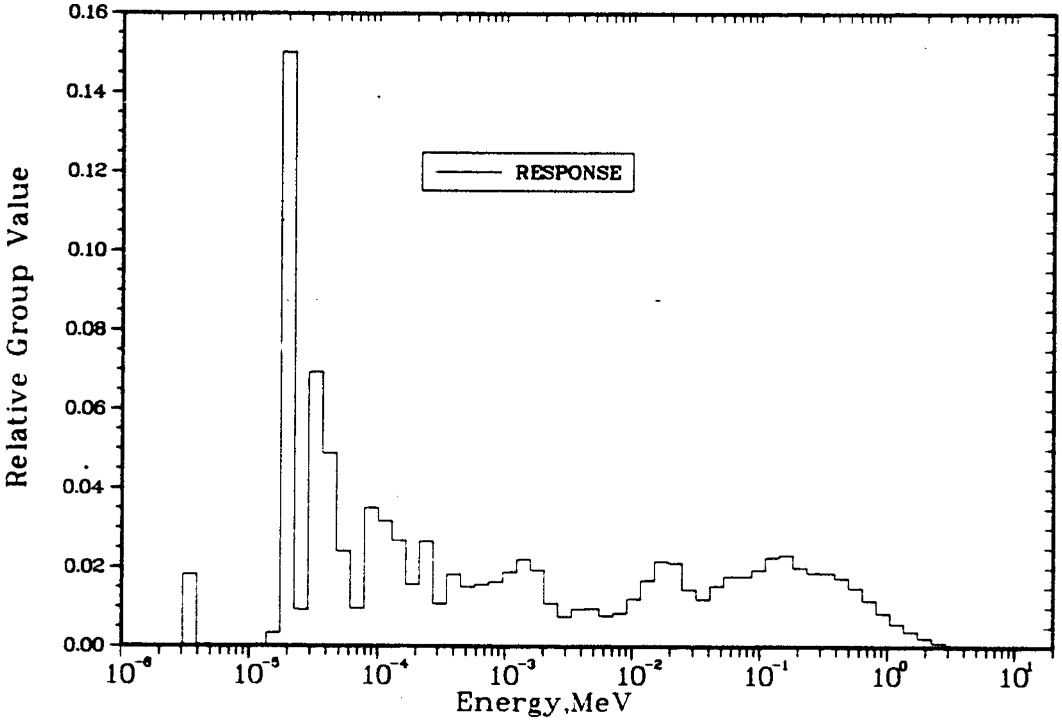

Figure B-41. ENDF/B-V cross section and response in EBR-II midplane for $^{147}Sm(n,\gamma)$.

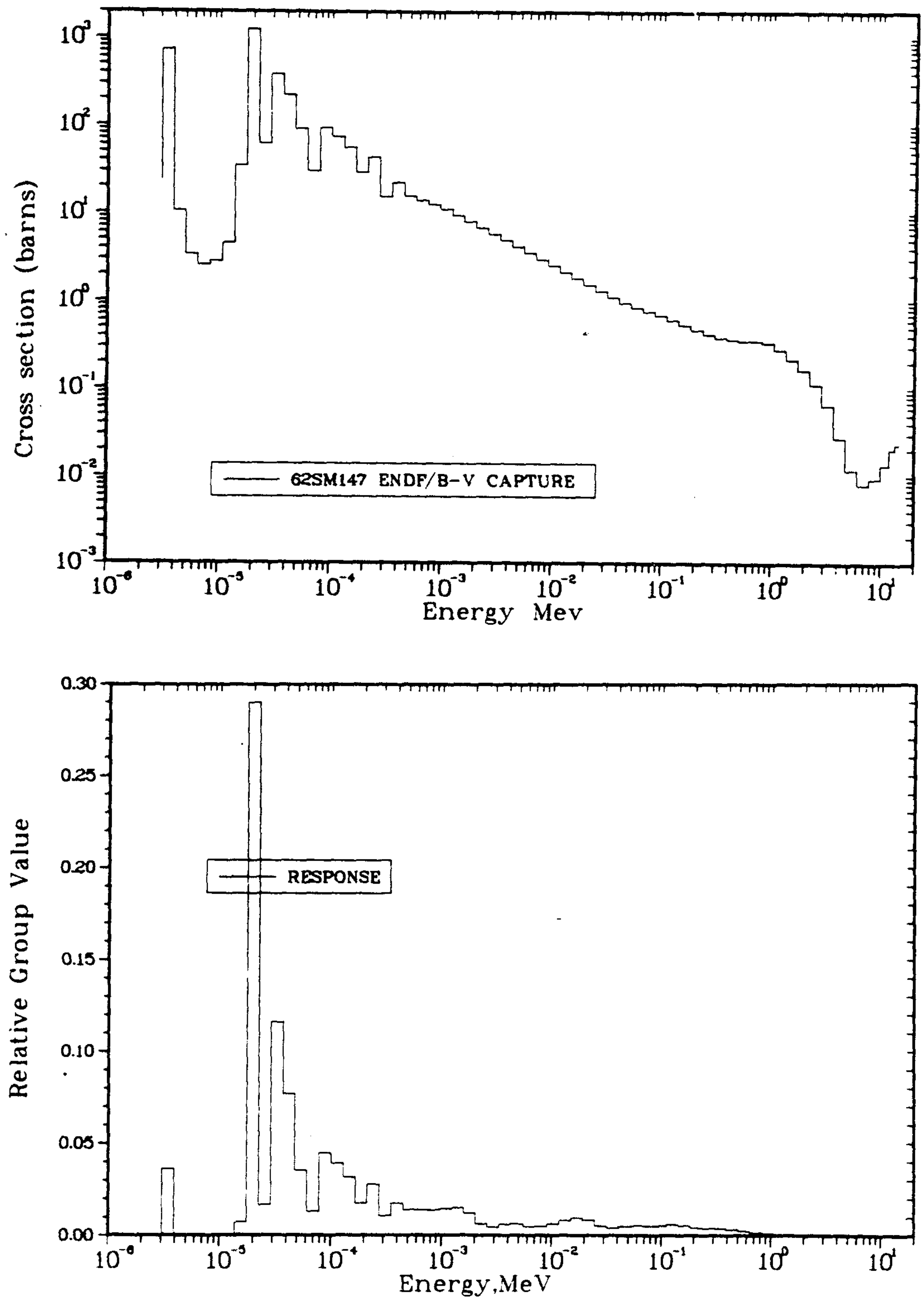

Figure B-42. ENDF/B-V cross section and response in EBR-II reflector for $^{147}Sm(n,\gamma)$.

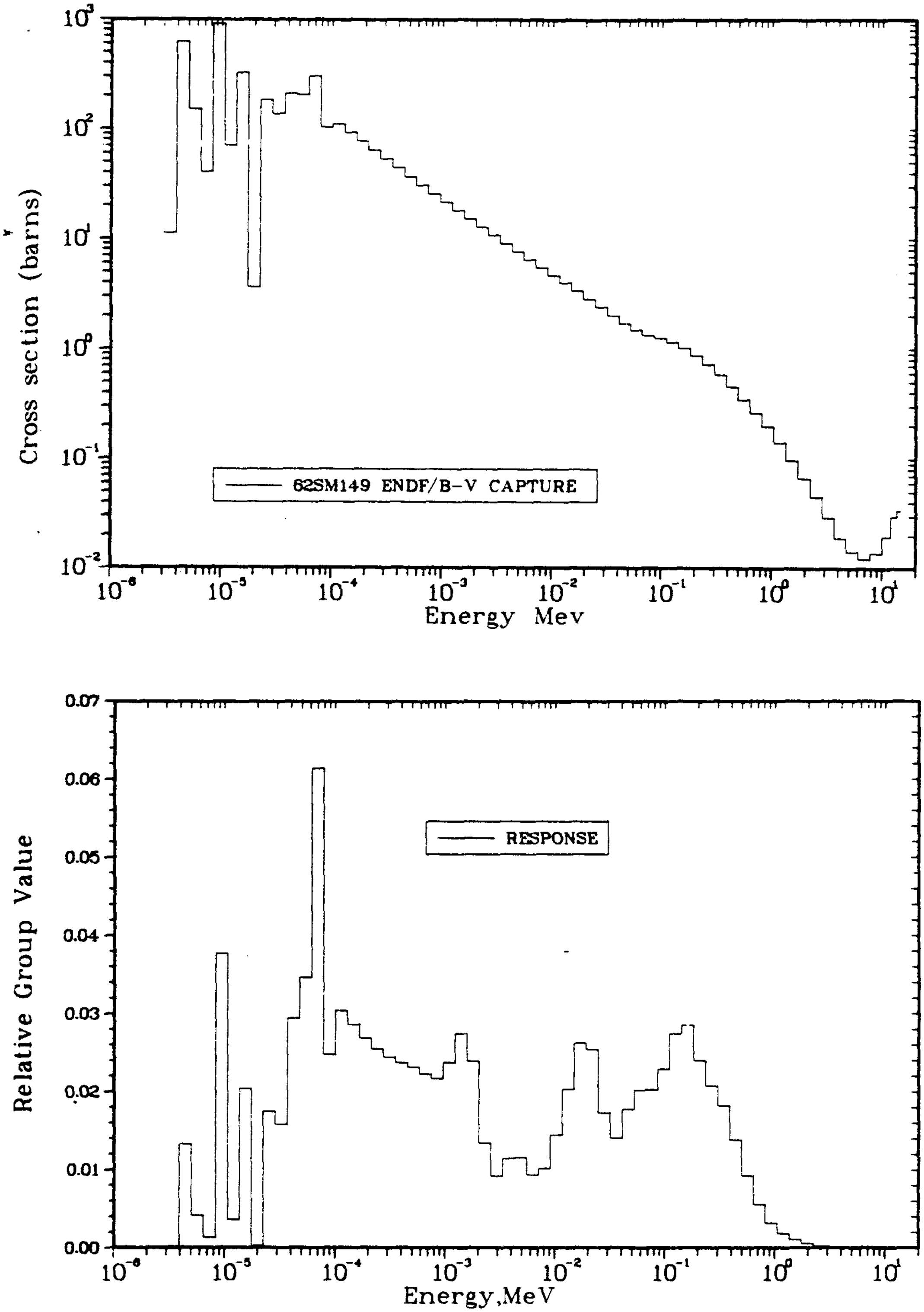

Figure B-43. ENDF/B-V cross section and response in EBR-II midplane for $^{149}Sm(n,\gamma)$.

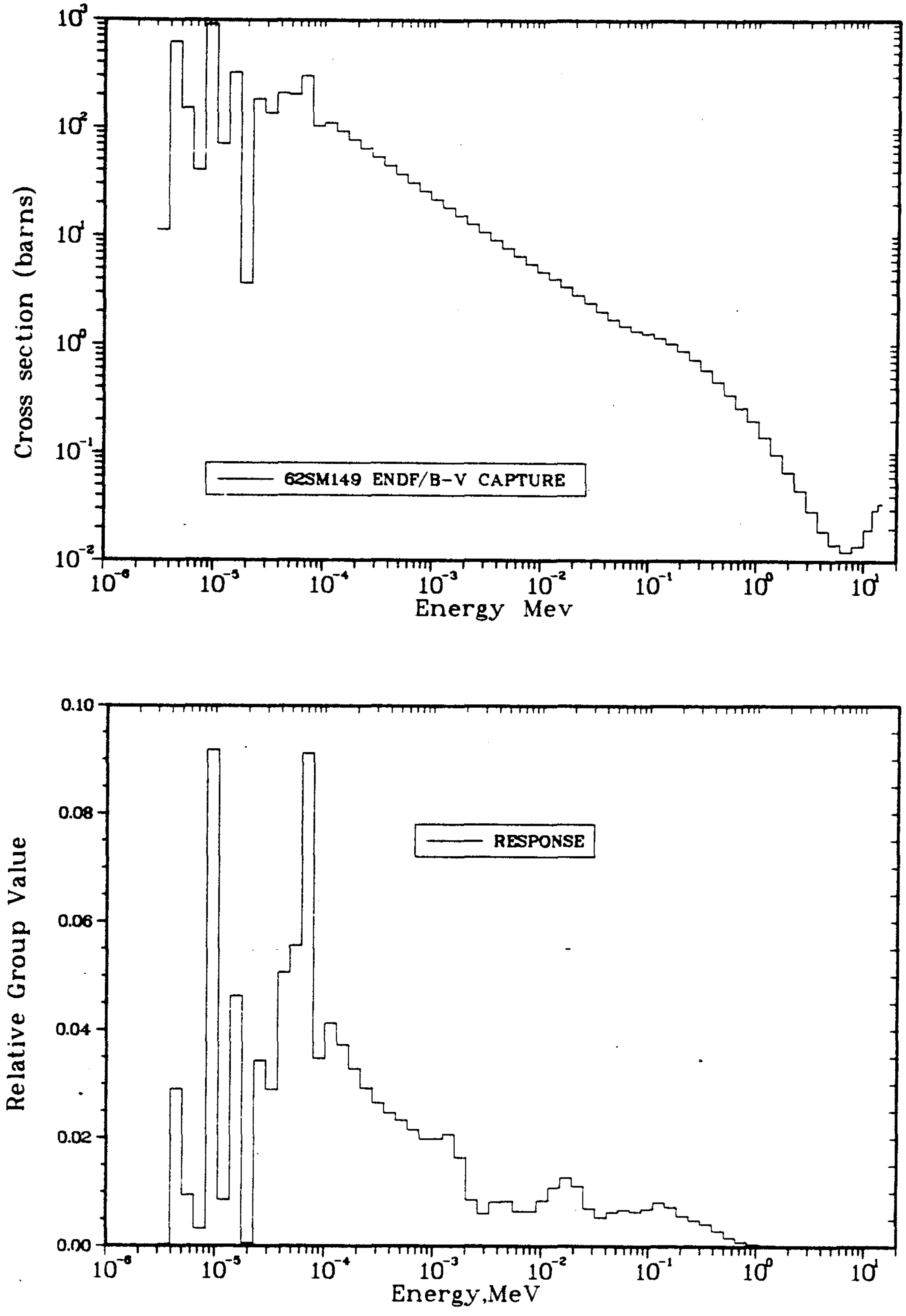

Figure B-44. ENDF/B-V cross section and response in EBR-II reflector for $^{149}Sm(n,\gamma)$.

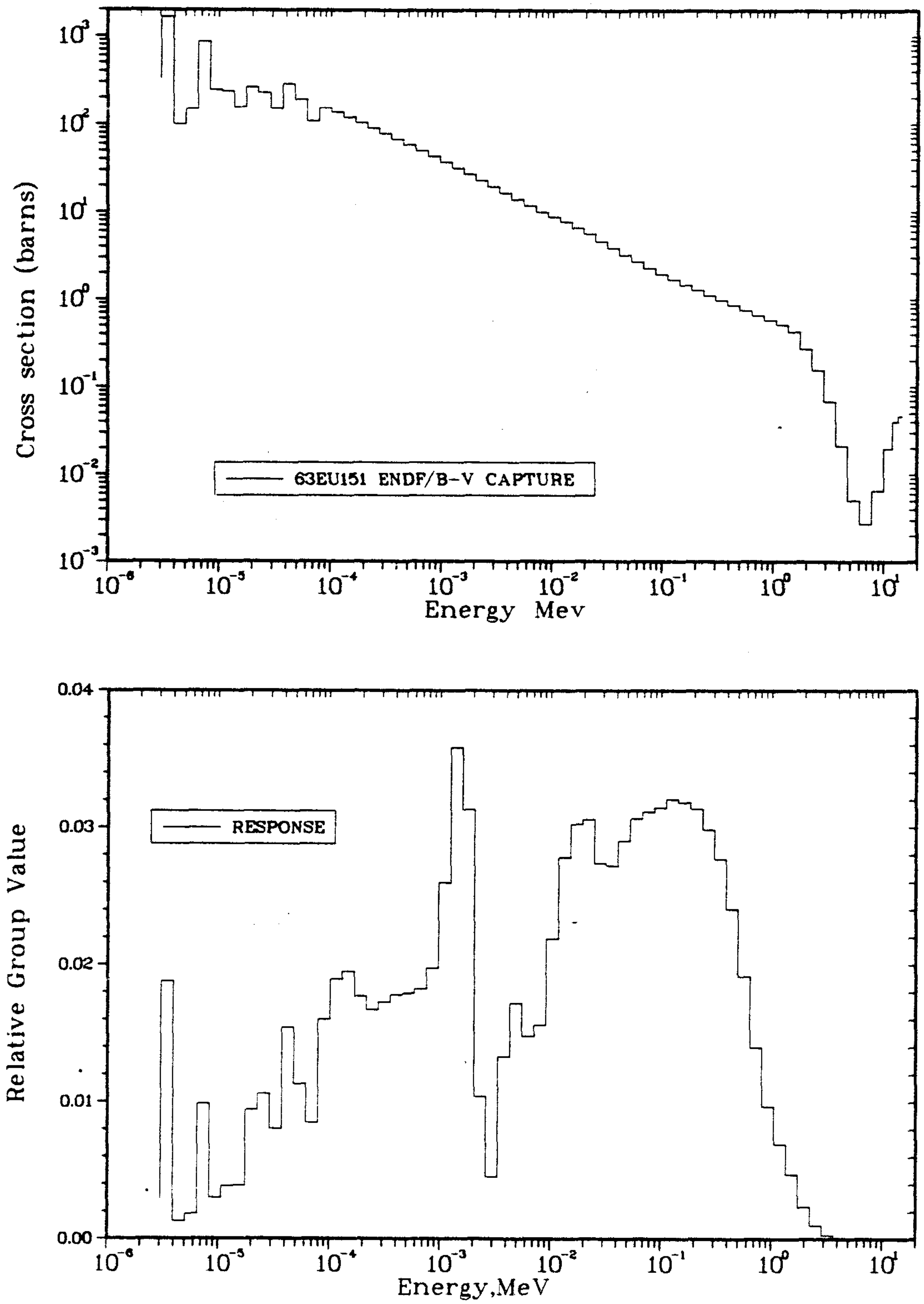

Figure B-45. ENDF/B-V cross section and response in EBR-II midplane for $^{151}Eu(n,\gamma)$.

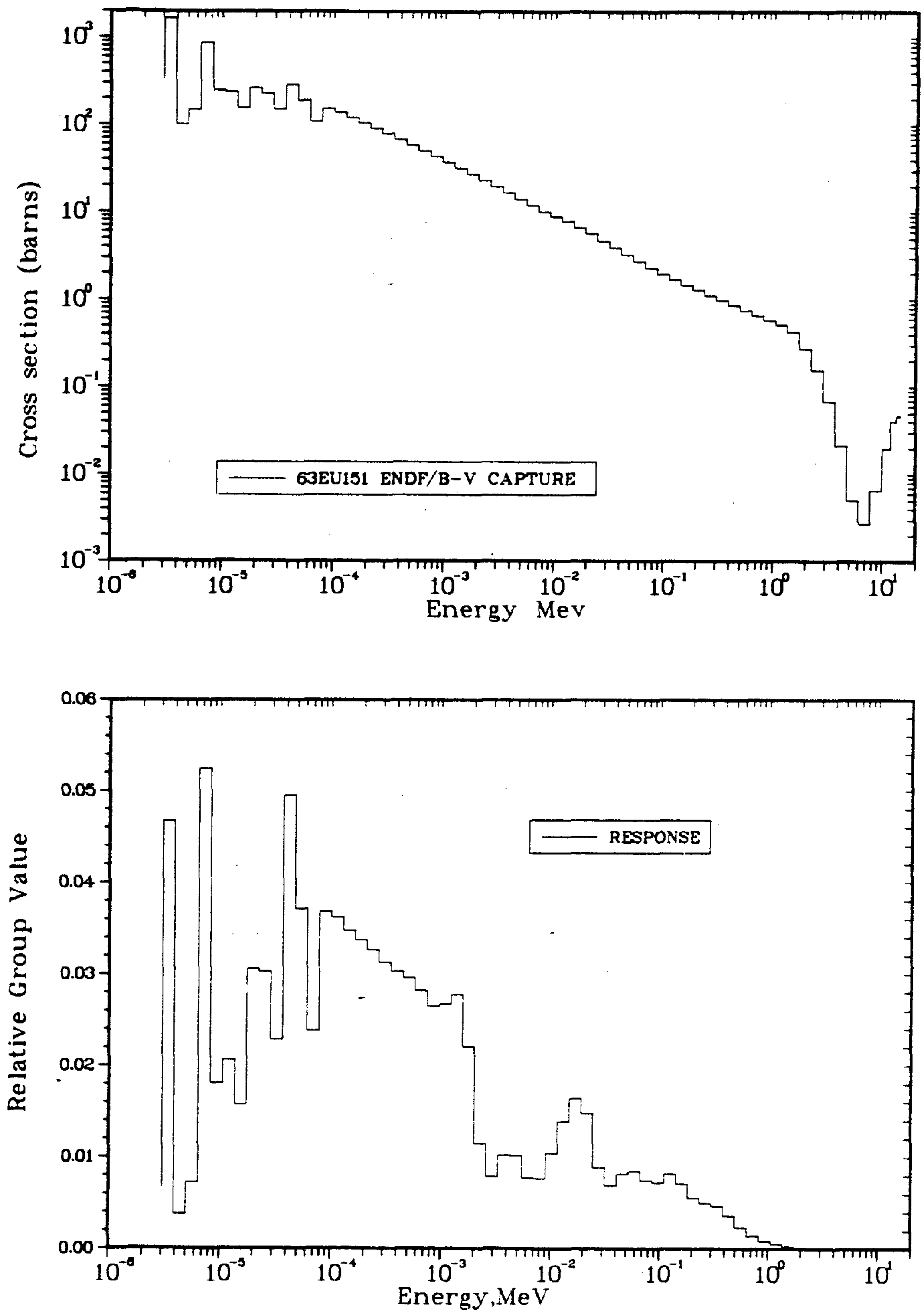

Figure B-46. ENDF/B-V cross section and response in EBR-II reflector for $^{151}Eu(n,\gamma)$.

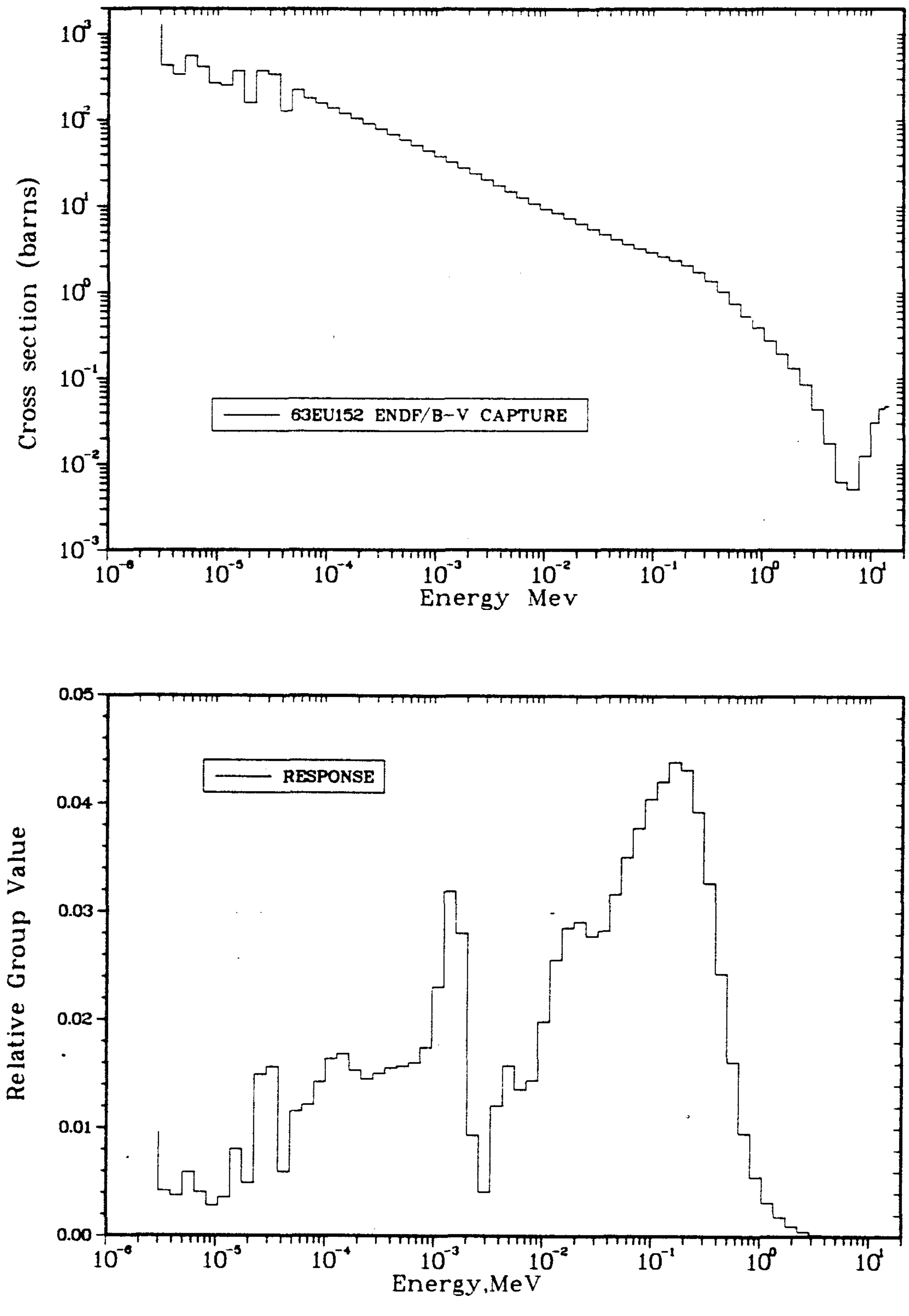

Figure B-47. ENDF/B-V cross section and response in EBR-II midplane for $^{152}Eu(n,\gamma)$.

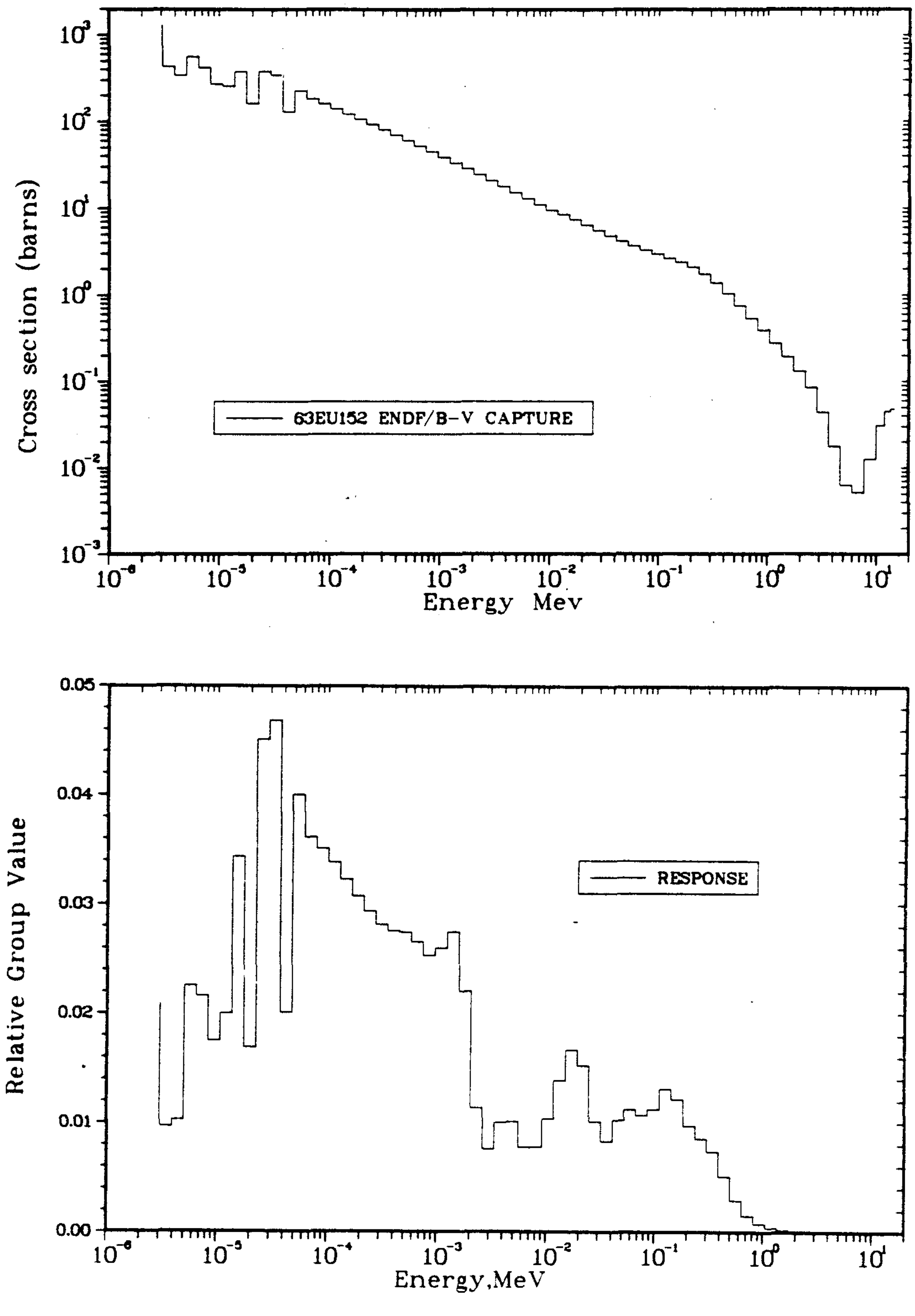

Figure B-48. ENDF/B-V cross section and response in EBR-II reflector for $^{152}Eu(n,\gamma)$.

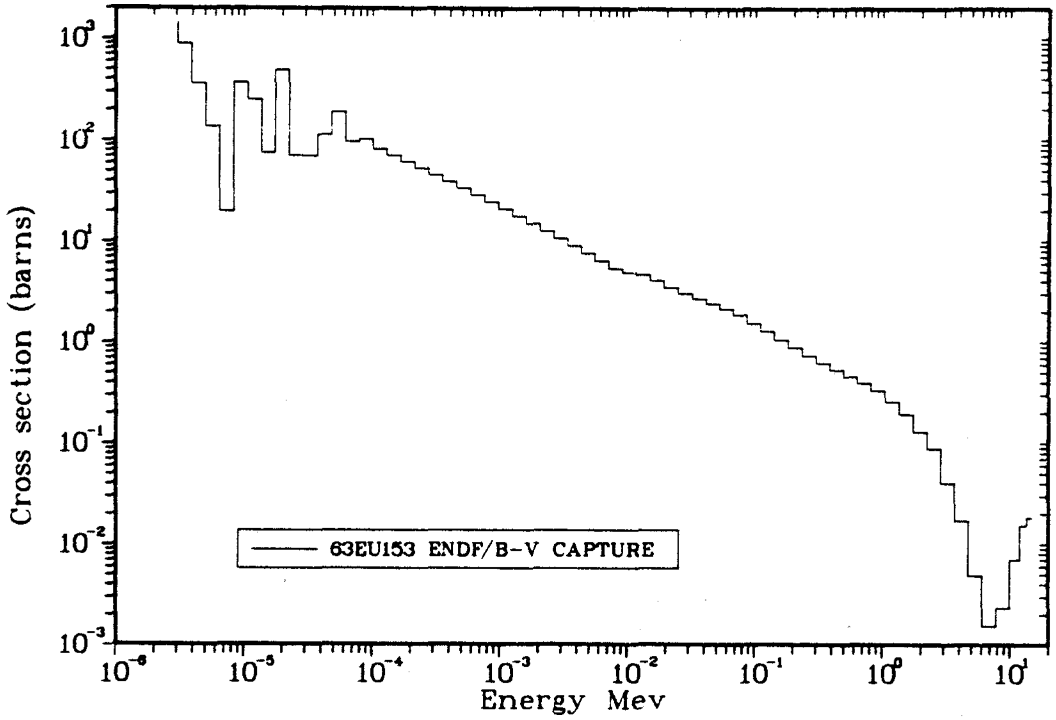

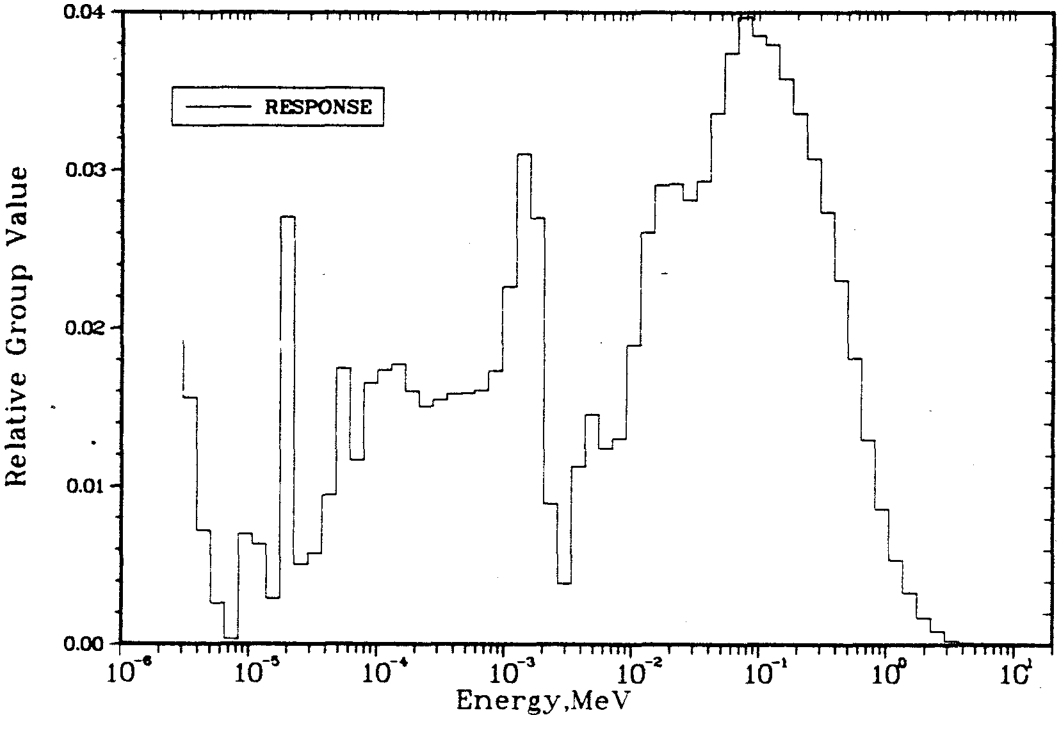

Figure B-49. ENDF/B-V cross section and response in EBR-II midplane for $^{153}Eu(n,\gamma)$.

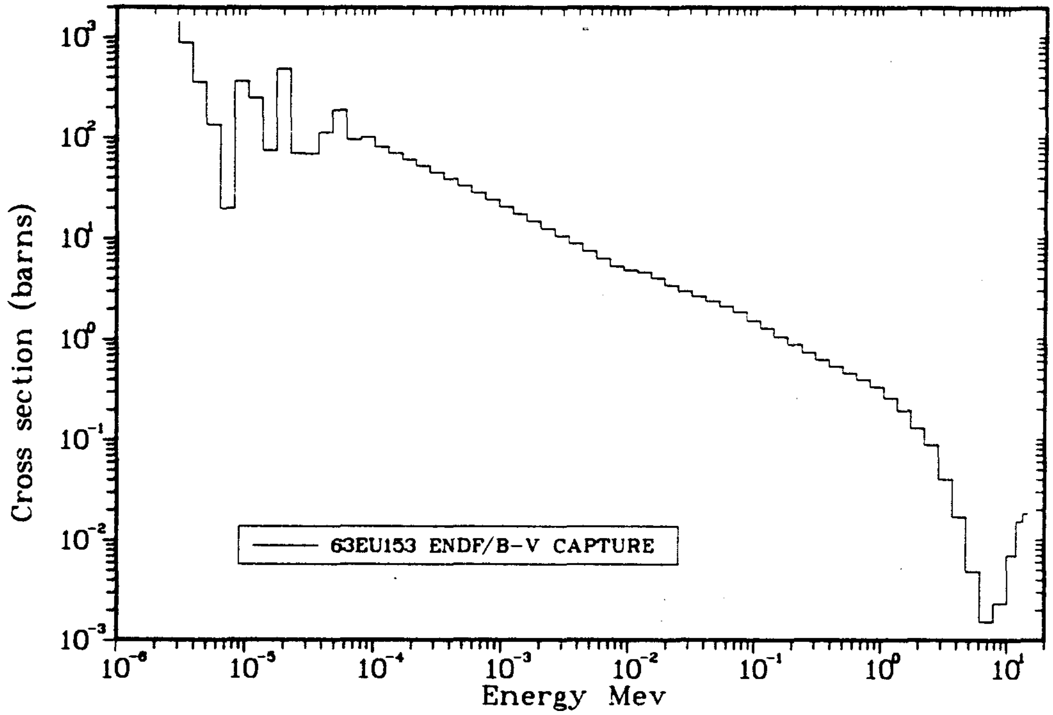

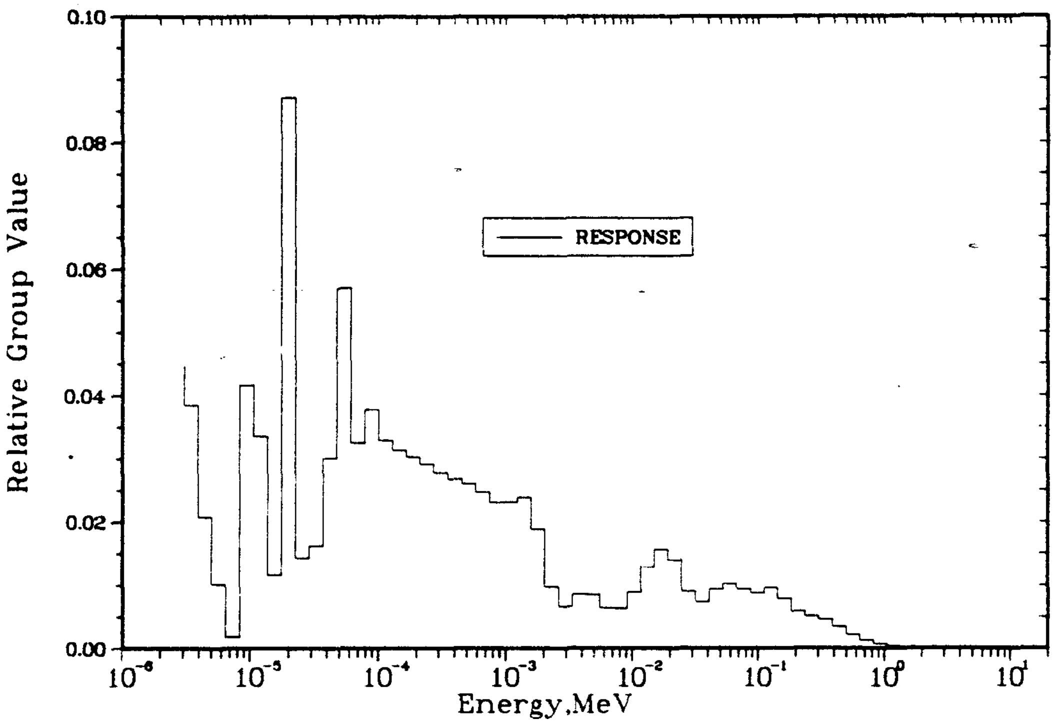

Figure B-50. ENDF/B-V cross section and response in EBR-II reflector for $^{153}Eu(n,\gamma)$.

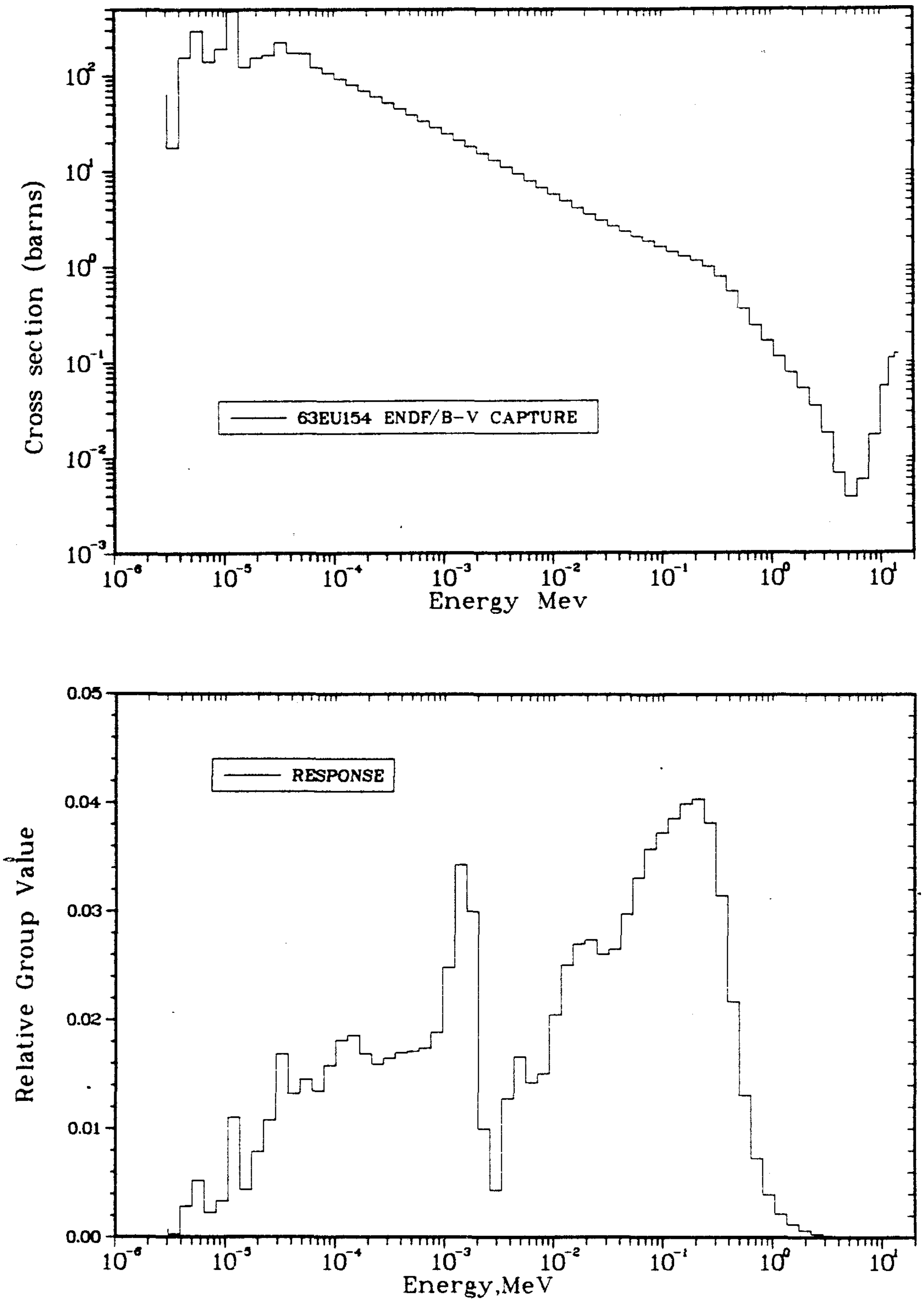

Figure B-51. ENDF/B-V cross section and response in EBR-II midplane for $^{154}Eu(n,\gamma)$.

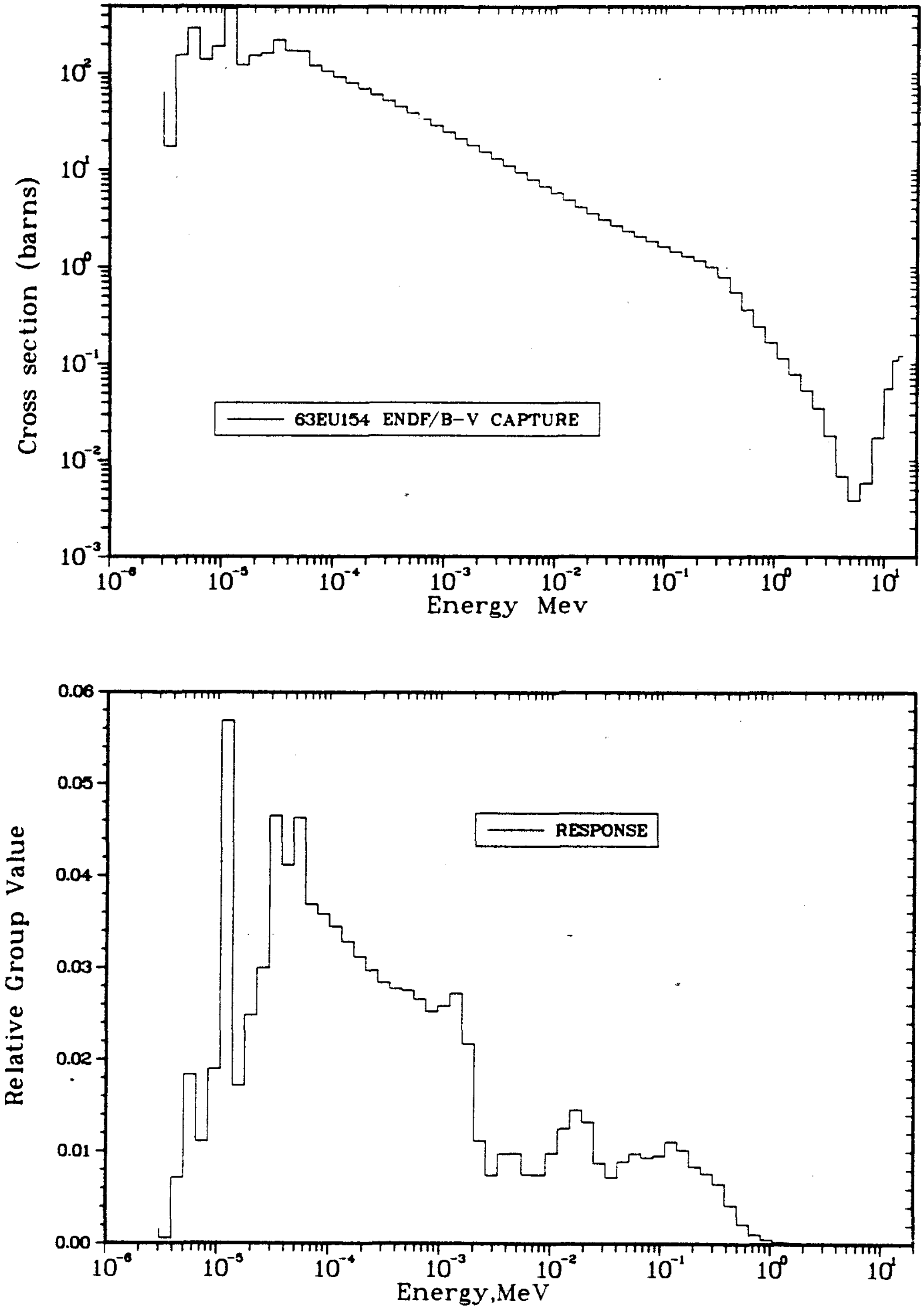

Figure B-52. ENDF/B-V cross section and response in EBR-II reflector for $^{154}Eu(n,\gamma)$.